Measurement of High Frequency Dielectric Constant and Conductivity of Fluids and Fluid-Saturated Rocks at High Pressure

by

David J. Yuen

Submitted to the
Department of Electrical Engineering and Computer Science
in Partial Fulfillment of the Requirements for the Degree of

Master of Science
in Electrical Engineering and Computer Science

at the

Massachusetts Institute of Technology

January 1990

© David J. Yuen, 1990

The author hereby grants to M.I.T. permission to reproduce and to distribute copies of this thesis document in whole or in part.

Signature of Author _____
Department of Electrical Engineering and Computer Science

Certified by _____
Professor Jin Au Kong
Thesis Supervisor

Certified by _____
Dr. M. Reza Taherian
Schlumberger-Doll Research
Company Supervisor

Certified by _____
Dr. Tarek M. Habashy
Schlumberger-Doll Research
Company Supervisor

Accepted by _____
Professor Arthur C. Smith, Chairman
Committee on Graduate Students

ARCHIVES

MASSACHUSETTS INSTITUTE
OF TECHNOLOGY

AUG 10 1990

LIBRARIES

MIT Libraries
Document Services

Room 14-0551
77 Massachusetts Avenue
Cambridge, MA 02139
Ph: 617.253.2800
Email: docs@mit.edu
http://libraries.mit.edu/docs

DISCLAIMER OF QUALITY

Due to the condition of the original material, there are unavoidable flaws in this reproduction. We have made every effort possible to provide you with the best copy available. If you are dissatisfied with this product and find it unusable, please contact Document Services as soon as possible.

Thank you.

The images contained in this document are of the best quality available.

Measurement of High Frequency Dielectric Constant and Conductivity of Fluids and Fluid-Saturated Rocks at High Pressure

by

David J. Yuen

Submitted to the Department of Electrical Engineering and Computer Science
on January 31, 1990 in partial fulfillment of the
requirements for the degree of
Master of Science in Electrical Engineering
at Massachusetts Institute of Technology

Abstract

A two-port coaxial cell was designed and manufactured to operate under pressures of up to 20,000 psi. The cell can be used for measuring scattering parameters of fluids and fluid-saturated solids at high frequencies. Inversion models were developed to retrieve the complex dielectric constant from the measured scattering parameters.

Using this cell, we studied the complex dielectric constant of pure water and .6 Ω-m waters in the pressure range of 14 - 20,000 psi. Also two rock samples, Berea and Massilon, saturated with .1 Ω-m water, were measured under pore pressures in the range of 14 - 20,000 psi. At atmospheric pressure, Berea has a porosity of 19% and Massilon has a porosity of 24%. The effect of pressure on their high frequency dieletric constant and conductivity was determined. The frequency dependence of this pressure effect is also investigated.

The dielectric constant of the two water solutions was found to increase as pressure is applied. The conductivity of the .6 Ω-m water was also found to increase as pressure is applied. The conductivity of the pure water, on the other hand, changed in such small

amount, that the measurement noise overshadowed the data. The frequency dependence of the pressure effect on the dielectric constant is to increase the dielectric constant as frequency is increased. The pressure effect on the conductivity of the .6 Ω-m water also increases as frequency is increased. The high frequency dielectric constant of pure water was extrapolated to determine the DC dielectric constant for selected pressures. The DC values were then compared to the data from Srinivasan and Kay. The data from these experiments and the literature values showed good agreement. The overall behavior of the conductivity of the two waters is similar to what Adam and Hall observed in their conductivity data.

The effect of pore pressure on the dielectric parameters of Berea and Massilon at high frequency was also studied. The dielectric constant of Massilon increased as pressure is applied. The conductivity of both Berea and Massilon increased as pressure is applied. There seems to be no apparent frequency dependence of this increase in all cases. However, it is interesting to note that the overall effect of pressure on the conductivity of Massilon is greater than that of Berea.

Schlumberger-Doll Research Supervisors: Dr. M. Reza Taherian
Dr. Tarek M. Habashy

M.I.T. Thesis Supervisor: Professor Jin A. Kong

Acknowledgements

I thank my two company supervisors, M. Reza Taherian and Tarek M. Habashy, for their valuable mentorship and friendship. I admire and respect these men for their scientific and personal accomplishments and for the depth of their personal involvement with me during the entire research.. They set exceptionally high standards for their peers, and I am honored by their confidence in me.

I am very grateful to my thesis supervisor, Professor Jin Au Kong, for his guidance and encouragement.

I thank Ray White for sharing his expertise in design work. I also thank him for the tennis lessons and for making my stay at Schlumberger very pleasant. You are a great guy.

I thank Lisa Louie and M. Relton for helping me with the mechanical analysis in the design of the cell.

I thank Andy, Larry, Joe, Ken, Dave, Jeff, and Yupai for their friendship and warmth; you have given me new confidence that intellectual brilliance and personality are not mutually exclusive.

To my Parents and Grandparents
with Love

Table of Contents

List of Figures

List of Tables

Chapter 1

INTRODUCTION

High frequency dielectric constant and conductivity of rock formations are used for borehole geophysical applications. Dielectric logging is an established technique in oil exploration. These dielectric constants and conductivities are usually used to determine geophysically important quantities, such as water-filled porosity. When compared with total porosity, the water-filled porosity is used to calculate water saturation of earth formation. In the oil bearing zones, this is an indication of the mobility of the hydrocarbons. Therefore, accurate quantitative determination of these parameters is of great interest in oil-well logging.

Although the dielectric and conductivity measurement of reservoir rock formations is important, many geophysical factors, such as pressure, affect the measurements. The effect of pressure on the complex dielectric constant of the reservoir rock formations has been ignored in laboratory measurements due to the technical difficulty in simulating borehole conditions. With the rising demand for more accurate determination of dielectric information in dielectric logging, it is imperative that we take this factor into account. To my knowledge, no high-pressure, high-frequency dielectric measurement has been reported in literature.

Measurements of the dielectric constant and conductivity of aqueous electrolyte solutions and brine-saturated rocks under high pressure have been the subject of several investigations in the past. However, all these measurements were carried out with DC excitation. The permittivity of electrolyte solutions and brine-saturated rocks have been measured at high frequency for many years, but there is no study of their permittivity at high pressures.

In studying the behavior of rock formations under pressure, it is important to distinguish between pore pressure and confining pressure. Pore pressure originates from the fluid inside the rock. Confining pressure is the pressure imposed on the rock matrix. In an oil well, these two pressures are functions of rock type, depth, and temperature. In order to determine accurate dielectric information for dielectric logging, it is important to understand their respective roles in different conditions.

In this study, we have devised a laboratory method to measure the dielectric constant and conductivity of electrolyte solutions under high pressure and brine-saturated rocks under high pore pressure at frequencies up to 3 GHz. This method employs a high-pressure coaxial cell. A hollow-cylindrical sample is placed inside the cell. A TEM wave propagates through the cell and the scattered intensities are measured with a network analyzer. From the scattering parameters, we are able to invert for the complex dielectric constant of the sample of interest at the pressure of the experiment.

In the next section the work of several pioneers in the field of high pressure dielectric and conductivity measurements is reviewed. Although these measurements were at DC, we will later use some of them to compare with our results. The next section is a description of the proposed permittivity measuring cell. We then briefly describe the theoretical background needed to develop the forward model and the inversion algorithm. Finally, we discuss the results obtained from measuring several fluids and fluid-saturated rock samples.

Chapter 2

LITERATURE REVIEW

Measurements of the dielectric constant and conductivity of liquids under high pressure have been made as early as the late 1800s. Roentgen, Ratz, Barus, and Lussana are among the first researchers to investigate the effect of high pressure on the dielectric constant and conductivity of the liquids. But the pressures considered were comparatively low, due to the limited availability of equipments. It is also important to note that all the early experiments were carried out with DC excitation.

In the early part of this century, fewer efforts are made to understand the high pressure effect on liquids. The most interesting work was the study on the high pressure dependence of several polar organic liquids by Onsager and Kirkwood.

Adam and Hall studied the behavior of liquids under high pressure in 1931. They measured the conductivity of few strong electrolyte solutions and concluded that the pressure has no significant effect on the resistivity of the solutions except in very conductive solutions.

Quist and Marshal measured the conductivity variations of sodium chloride solutions as a function of both temperature and pressure in 1967. They descibed the temperature and pressure effects on dielectric constant in terms of density and viscosity of the solution.

Recently few more liquids have also been measured in a high pressure environment. The static dielectric constant of H_2O and D_2O were measured by Srinivasan and Kay in 1973. Vij studied the pressure and temperature dependence of the dielectric constant of 1,1-dimethoxy-2-propanol in 1973. Finally, Haynes measured the dielectric constant of normal butane, isobutane, and propane in 1983.

The experimental techniques used in all these studies involved a capacitor-type measurement. Although these studies were at DC, there are cases where frequencies in the audio and radio range were used. In 1956 Gilchrist, Earley, and Cole studied the effect of pressure on dielectric constant and loss tangent of 1-propanol and glycerol. They measured these samples at pressures of up to 1,000 kg/cm^2 (approximately 14,000 psi) and at room temperature. The increase in static dielectric constant was found to be less than the predicted value from density increase alone. They explained the difference in terms of molecular compression and liquid structure effects.

Although Archie was not involved in pressure dependence of the electrical properties of saturated rocks, he was the first to quantitatively relate the resistivity of the brine-saturated rocks to the resistivity of the brine in 1941. Although his experiments were carried out at atmospheric pressure, his work formed the basis on which all future analyses of pressure dependence of water-saturated rocks have been treated. He defined formation factor, **F**, by the following equation:

$$\mathbf{R_0 = FR_w} \tag{1}$$

where $\mathbf{R_0}$ is the resistivity of the brine-saturated rock and $\mathbf{R_w}$ is the resistivity of the brine. He then showed that this formation factor is related to the porosity of the rock by the following equation:

$$\mathbf{F = \Phi^{-m}} \tag{2}$$

where $\mathbf{\Phi}$ is the porosity of the rock and **m** is the porosity exponent or cementation factor. Archie's law was later generalized by W. Winsauer in 1952. The generalized relationship has the following form:

$$\mathbf{F = C\Phi^{-m}} \tag{3}$$

where C is determined experimentally from measurements of rocks with different $\mathbf{\Phi}$ or different $\mathbf{R_w}$.

In the next few paragraphs, we review the work done on the measurement of the DC resistivity of rocks. The first attempt was by I. Fatt in 1957. He studied 21 brine-saturated rock samples and determined that the resistance, and therefore the formation factor,

increases as the pressure is increased. He also found that the exponents and coefficients in the Archie's law are functions of the pressure.

In 1958 Wyble measured the conductivity variations of three sandstones as a function of pressure up to 5,000 psi. He observed a similar trend of decrease in conductivity, porosity, and permeability with pressures of up to a 3,500 psi. From this data, the increase of formation factor over the same range was calculated. His results showed that Archie's cementation exponent increases with pressure.

Brace, Orange, and Madden in 1965 reported the effect of pressure on the resistivity of eight igneous rocks and two crystalline limestones. The rocks were saturated with tap water or brine solution. They observed that the resisitivity increases as pressure increases. On the other hand, surface conduction (conduction due to the presence of solids, such as clay or shale, along the network of pores, cracks, and passages) decreases with increasing pressure. They explained the phenomenon in terms of closure of some flow passages as a result of an increase in confining pressure.

In 1987 Johnston studied the resisitivity of three shales at pressures of up to 800 bars (approximately 12,000 psi) and temperature of up to 100°C. He realized that the resistivity of the shales increases rapidly at lower pressures and levels off at higher pressures due to the closure of microcracks in the rock matrix. He also noted that shales in general are less sensitive to pressure changes than sandstones with similar porosity.

Although these studies have attempted to determine the effect of pressure on the dielectric constant and conductivity of rocks, none has been carried out at high frequency. These measurements are relevant to resistivity logging, but the frequencies of measurement are not high enough for dielectric logging. We feel that high pressure permittivity measurements at high frequencies will provide new information to better relate the laboratory dielectric measurements with downhole logs.

We have devised a new cell to determine the dielectric constant and conductivity of fluids and fluid-saturated rocks under high pressure and at high frequencies. This cell is described in section 3.1.1.

Chapter 3

METHODS OF INVESTIGATION

3.1 Experimental Approach

In this study, a high-pressure system is designed to operate at pressures of up to 20,000 psi. A photograph of the overall system is shown in Figure 3.1.1.

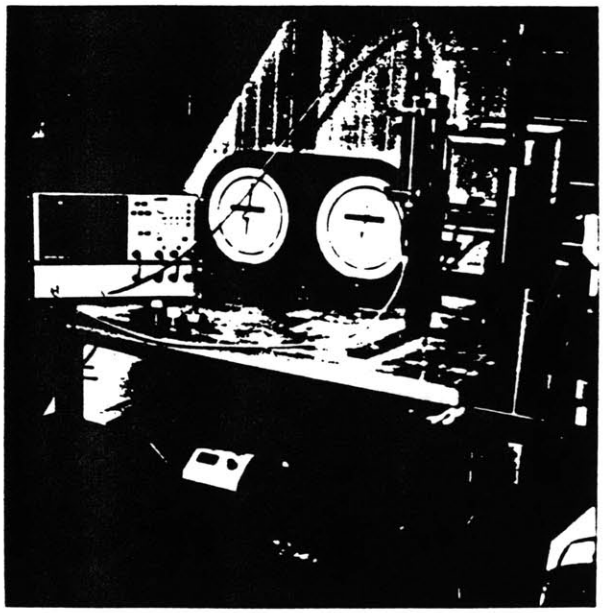

Figure 3.1.1: Overall High-Pressure System

For the sake of this discussion, the overall system is divided into three sub-units. These sub-units are the high-pressure cell, the data acquisition/processing unit, and pressurizing

unit. In the next three sections, we will describe in detail the design, implementation, and function of each of the three sub-units.

3.1.1 High-pressure cell

The high-pressure cell is essentially a two-port symmetrical coaxial line with sections filled with different materials. The advantage of two-port cells is that a full set of scattering parameters can be measured. In designing this cell, there are two options available. The first option involves making a lossless 50-Ω coaxial line up to the sample chamber. This structure requires calculation of only one reflection coefficient at the interface between the lossless 50-Ω section and the sample. However, this would cause abrupt jumps in either the inner or the outer conductor. Consequently, TM modes have to be taken into consideration. The second option involves making a continuous coaxial line with non 50-Ω sections. Local reflection coefficients at the different junctions have be to calculated, but there is only TEM mode in this case. We chose to use the second option, because it is simpler in terms of theoretical modeling of the coaxial line. Once we have decided on using the second option, the following criteria must be observed.

a. It should simulate a coaxial line with no discontinuities or abrupt junps in the dimensions of either inner or outer conductor.
b. It is preferable to have end configuration which is compatible with the GR900 connectors.
c. There should be provisions to allow additional fluid to enter the sample chamber to attain the desired pressure.
d. It should withstand pressure up to at least 28,000 psi. This is precaution to make the high-pressure cell man-safe.
e. The inner and outer conductors should have minimal change in dimensions as a result of high pressure.

With these criteria in mind, now we will discuss the design of the high-pressure cell. A photograph of the disassembled cell is shown in Figure 3.1.1.1. An overall cross-section of the assembled cell is shown in Figure 3.1.1.2.

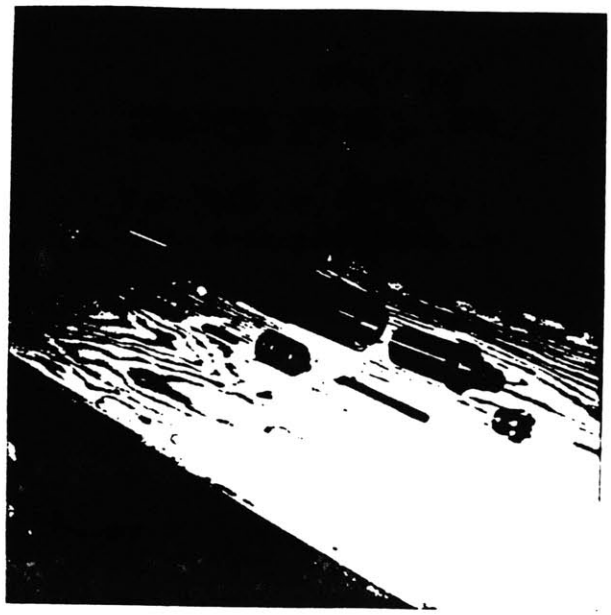

Figure 3.1.1.1: Disassembled High-Pressure Cell

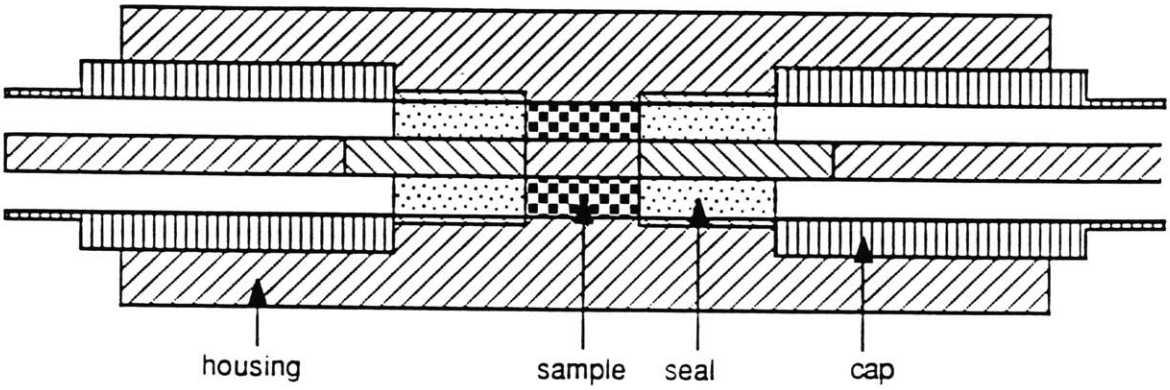

Figure 3.1.1.2: Cross Section of the High-Pressure Cell

The cell consists of a housing where the sample is placed in its center. The sample has the configuration of a hollow cylinder. High-pressure seals are placed on the two sides of the sample. These are followed by sections of airline which are attached to RF connector (GR900). The sample compartment is pressurized by the injection of a pressurized fluid (in the case of water-saturated rocks, this is the same as the saturating liquid) through a small bleedhole in the middle of the cell (not shown). The two high-pressure seals isolate the pressurized sample chamber from the atmospheric pressure air sections in the caps. The caps provide the basic mechanism to hold the seals in place. Even though all the components have very different structures, when assembled there are no discontinuities or

abrupt jumps in either inner or outer conductors. This characteristic is crucial, since this eliminates the possibility of creating TM modes. However, this translates to the formation of sections with different characteristic impedances. In the following paragraphs, descriptions of the components are given.

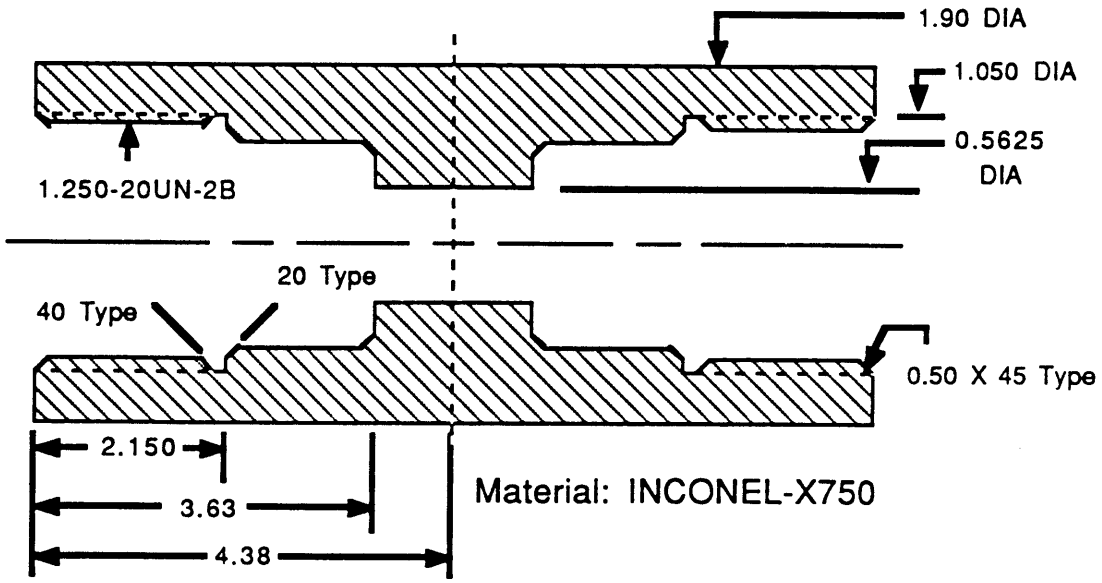

Figure 3.1.1.3: Housing Design

A cross sectional view of the housing is shown in Figure 3.1.1.3. Note that the inner diameter of the center section is the same as that for the GR900 connector. The housing is made from INCONEL-X750, a nickel-chromium alloy. We choose to use this material for its excellent corrosion and oxidation resistance. It also has high tensile strength which enables this material to maintain its shape under high pressure.

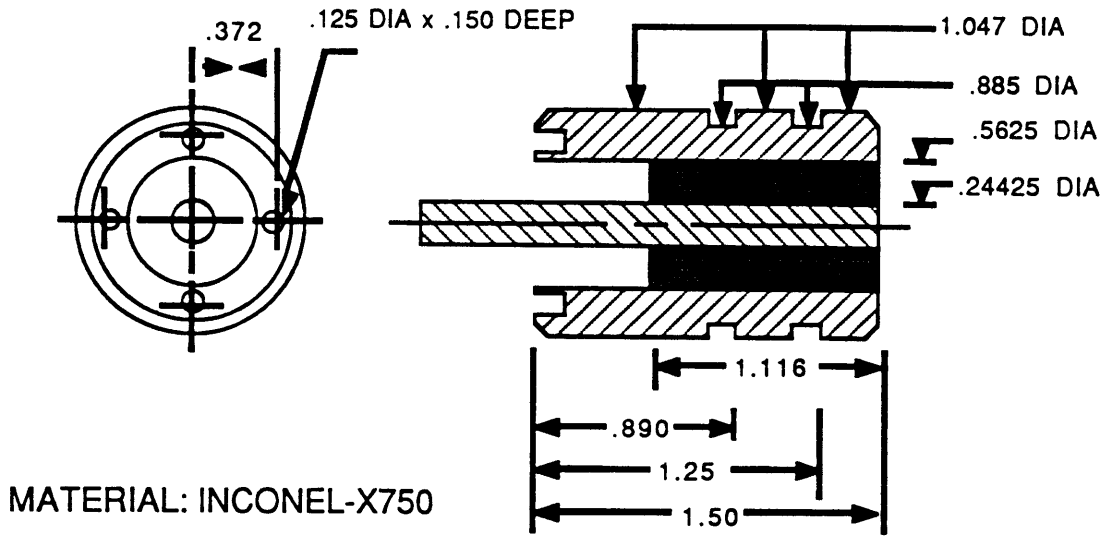

Figure 3.1.1.4: Seal Design

The high-pressure seal is shown in Figure 3.1.1.4. The inner diameter of the outer conductor corresponds to that of the GR900 connector. Similarly, the center rod has the same diameter as the inner conductor of the GR900 connector. The high-pressure seal conductors are also made of INCONEL. The space between the inner and outer conductors is filled with a yellowish ceramic called Kyro-flex 314. The metal parts and the ceramic parts are first heated to a temperature of 1100°F. Then in its liquid state, the ceramic is poured into a customized jig, where the outer and inner conductors are fitted precisely in a manner to achieve a high concentricity. The seal is then placed in an ambient temperature environment overnight to cool down. After the ceramic solidified in place, a grinding machine is used to shave off the .003" menicus formed as the result of the cooling process. The finished seal has a width of 1.116". The seals have been designed to withstand high pressures. They are manufactured by Kyle Technology Corporation. One major reason for using INCONEL in the design of the pressure seals is that Kyro-flex binds only to INCONEL. On the outer surface of the seal two grooves are machined for the installation of two VITON 95 durometer O-rings. These O-rings prevent any leakage of liquid from the sample chamber to the air sections.

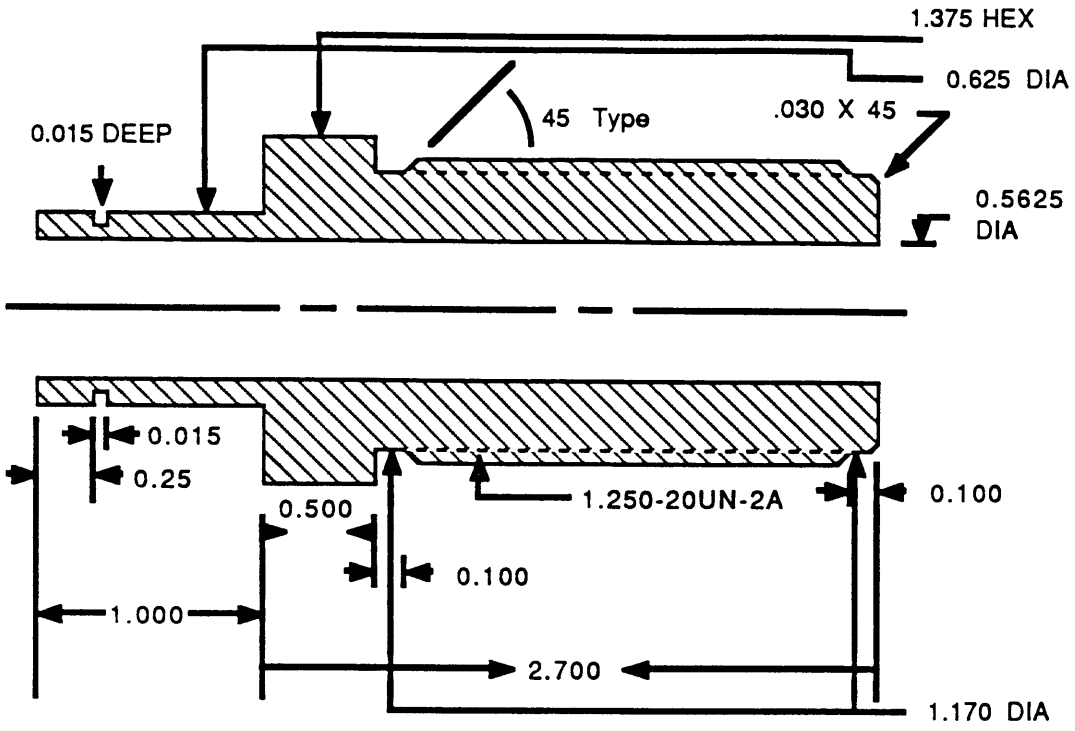

Material: MONEL-K500

Figure 3.1.1.5: Cap Design

The end cap is shown in Figure 3.1.1.5 and is made of MONEL-K500, a nickel-copper alloy. This metal also exhibits excellent corrosion and oxidation resistance characteristics. The use of a different metal from INCONEL for manufacturing the end caps reduces the possibility of galling between the cap and the housing. Galling is a phenomenon where similar metal parts fuse together as a result of pressure. The cap has a thread length of two inches. This length is chosen to ensure that the high pressure seals will stay in place when the pressure is applied in the sample chamber. The connector side of the cap was machined to specific outer diameter and groove dimensions to match the fitting on the GR900 connector. The inner conductor is made of five pieces of 0.24425" diameter stock. The inner conductor sections, except for the sections in the pressure seals, are also made of MONEL. The reason for using different materials is to prevent galling between different sections.

So far we have discussed the physical construction of the cell to meet the criteria mentioned earlier. Now we will discuss the mechanical issues to ensure that the cell can indeed operate

with pressures of up to 20,000 psi in its sample chamber. Dimensions of the different components of the cell were calculated to ensure the safe operation of the system.

In order to avoid any possibility of metal rupture under 20,000 psi, we have determined the maximum pressure that the cell can withstand with the given dimensions. The high-pressure seals have been tested by Kyle Technology Corporation and shown to withstand the pressure. We neglect the inner conductor, since its presence does not effect the pressure rating of the sample region. The high-pressure region then simply becomes the hollow-cylindrical structure shown in Figure 3.1.1.6.

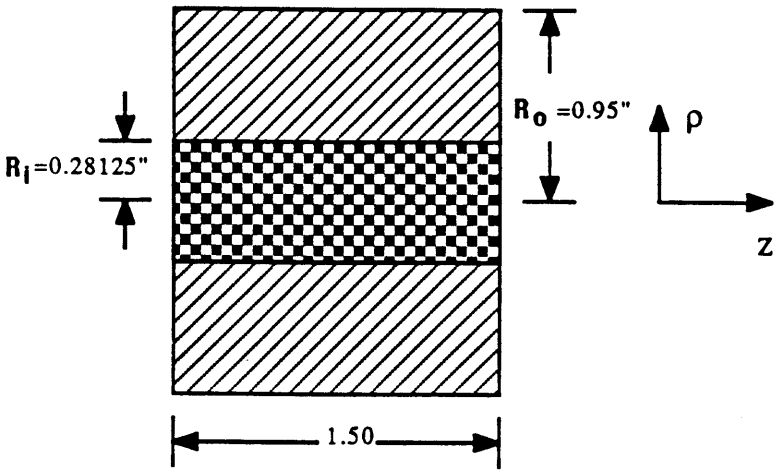

Figure 3.1.1.6: High-Pressure Region without Ends

Note that in this analysis cylindrical coordinate system is employed. Since the following condition holds, thick wall analysis is assumed for the sample chamber.

$$\frac{2(R_o - R_i)}{(R_o + R_i)} = \frac{0.66875}{0.615625} \rangle\rangle .1 \qquad (4)$$

In this analysis, we can neglect the radial stress experienced by the cylinder, since calculations based on the radial stress analysis will provide us with only the upper limit for the sustainable pressure in the sample chamber, we are interested in the lower limit. We now consider tangential and axial stress components for the cylinder. The fundamental stress equations can be found in most modern textbooks. The tangential stress equation is given below. (M.I.T., 2.30 Mechanical Behavior of Materials, Handout 3, Spring 1989)

$$\sigma_{\theta\theta}(r) = \frac{1}{\left(\frac{b}{a}\right)^2 - 1}\left\{\left[p_i - p_o\left(\frac{b}{a}\right)^2\right] + (p_i - p_o)\left(\frac{b}{r}\right)^2\right\} \tag{5}$$

where $\sigma_{\theta\theta}$ is the tangential stress, p_o is the pressure outside the cylinder, p_i is the pressure inside the cylinder, a is the inner radius of the hollow cylinder, b is the outer radius of the hollow cylinder, and r is the radial coordinate from the center of cylinder where the stress analysis is carried out.

The highest point of stress is on the inner wall of the cylinder, where the pressure is directly applied. Therefore, by setting r to R_i in eqs. (5), we obtained the following equation:

$$\sigma_{\theta\theta}(r) = \frac{1}{\left(\frac{R_o}{R_i}\right)^2 - 1}\left\{\left[p_i - p_o\left(\frac{R_o}{R_i}\right)^2\right] + (p_i - p_o)\left(\frac{R_o}{R_i}\right)^2\right\} \tag{6}$$

Making appropriate substitution of variables and rewriting the tangential stress equation, we obtained the following relationship:

$$p_i = \frac{\sigma_{\theta\theta}\left[\left(\frac{R_o}{R_i}\right)^2 - 1\right] + 2p_o\left(\frac{R_o}{R_i}\right)^2}{1 + \left(\frac{R_o}{R_i}\right)^2} \tag{7}$$

In this analysis, p_o is atmosperic pressure, approximately 14.7 psi. In order to determine the maximum pressure which can be sustained in the tangential direction, the yield strength for the cylinder must be known. From a table of mechanical properties for INCONEL-X750 (Alcan Corporation's Metalog), we obtained a yield strength of 100,000 psi. This value can be substituted for $\sigma_{\theta\theta}$. Subtituting the appropriate values in eq. (7), we get p_i=83,856 psi. This means that the sample chamber can withstand pressures of up to 83,856 psi in the tangential direction. Since the sample chamber is pressured to only 20,000 psi, there is no problem in the tangential direction.

Now we will consider the axial stress component and carry out a capped cylinder analysis. Can the end caps hold the seals in place under pressure? In order to analyze this issue, the force, generated from the pressurized fluid in the sample chamber, on the seal must first be determined. This force is calculated using the following equation:

$$F = (p_i - p_o)(a^2 - b^2) \tag{8}$$

Since the pressure in the axial direction is actually applying directly on the seals, the inner and outer radii, a and b, are those for the high-pressure seals shown in Figure 3.1.1.4. a=.28125" and b=.5235". From eq. (8), we get F=3,896 lbs at p_i of 20,000 psi. Therefore, the clamping force of the pressure cap must be at least 3,896 lbs. to prevent the seals from shooting outward. Two inches of thread, 1.250-20UN-2A, is machined onto the pressure caps for this application. In order to ensure that the two inches of thread can provide a clamping force of at least 3,896 lbs., empirical data is obtained for a similar thread configuration. This data is included in Appendix B.1. (Draper Laboratory intralab memorandum on graphs to determine screw tightening torques) On the graphs, clamping force is given as a function of thread friction coefficient at different torques. Since the threads on the pressure cap are well lubricated, a thread friction coefficient of 0.12 is used. A torque of approximately 100 lb-in is used in securing the pressure cap in place. Since available data only covers torques of up to 13 lb-in, a linear interpolation scheme is utilized to calculate the clamping force when the applied torque is 100 lb-in. From this scheme, a clamping force of 4940 lbs. is obtained for the pressure cap. This indicate that the high-pressure seals can indeed operate properly with pressures of up to 20,000 psi in the sample chamber. Actually, the end caps can operate to pressures of as high as 25,354 psi.

Finally, the issue of changing dimensions in both inner and outer conductors of the sample chamber as a result of high pressure is addressed. The change in dimensions of the inner and outer conductors can create problems with RF propagation in the cell and it is very important to keep this change at minimum. To calculate the actual change in the outer conductor, the strain equation for the coaxial line must be utilized. (M.I.T., 2.30 Mechanical Behavior of Materials, Handout 3, Spring 1989)

$$\varepsilon_r = \frac{u_r}{r} = \frac{(1+\nu)}{E\left[\left(\frac{b}{a}\right)^2 - 1\right]}\left\{(1-2\nu)\left[p_i - p_o\left(\frac{b}{a}\right)^2\right] + (p_i - p_o)\left(\frac{b}{r}\right)^2\right\} - \nu r\varepsilon_o \tag{9}$$

where ε_r is the strain, u_r is the actual displacement, ν is the poisson's ratio, E is the young's modulus, and ε_o is initial strain.

In this analysis, there is no initial strain on the outer conductor, therefore, $\varepsilon_o=0$. The actual change in the outer conductor can be calculated by setting r in the above equation to R_i. Substituting in the appropriate variables, the following equation is obtained.

$$u_r = \frac{(1+\nu)R_i}{E\left[\left(\frac{R_o}{R_i}\right)^2 - 1\right]}\left\{(1-2\nu)\left[p_i - p_o\left(\frac{R_o}{R_i}\right)^2\right] + (p_i - p_o)\left(\frac{R_o}{R_i}\right)^2\right\} \tag{10}$$

From a table of mechanical properties for INCONEL-X750, ν equals 0.29 and E equals 31,000,000 psi. (Alcan Corporation's Metalog) Now substituting the appropriate values in the above equation, we obtain u_r=0.00027023 in. We can neglect the effect of this change, since it amounts to only 0.05% of the undisplaced dimension.

Now the effect of pressure on the inner conductor is considered. The strain equation has the following form for a solid stock.

$$\varepsilon_r = \frac{u_r}{r} = \frac{\sigma_{rr}}{E} \tag{11}$$

The inner conductor is made from MONEL-K500. From a table of mechanical properties for MONEL-K500, a value of 26,000,000 psi is obtained for its young's modulus. (Alcan Corporation's Metalog) Assuming maximum stress on the inner conductor is 20,000 psi, we calculate the strain, ε_r, to be 0.00076923. Consequently, the actual displacement, u_r, equals 0.00009394". The percentage change under a pressure of 20,000 psi is only .077%. We can also neglect the effect of pressure on the inner conductor. In the next section the acquisition and processing units are described.

3.1.2 Acquisition and processing units

The acquisition and processing system consists of the HP network analyzer/S-parameter test set, desktop computer, mainframe processor, and a laser printer. A schematic of the system is shown in Figure 3.1.2.1.

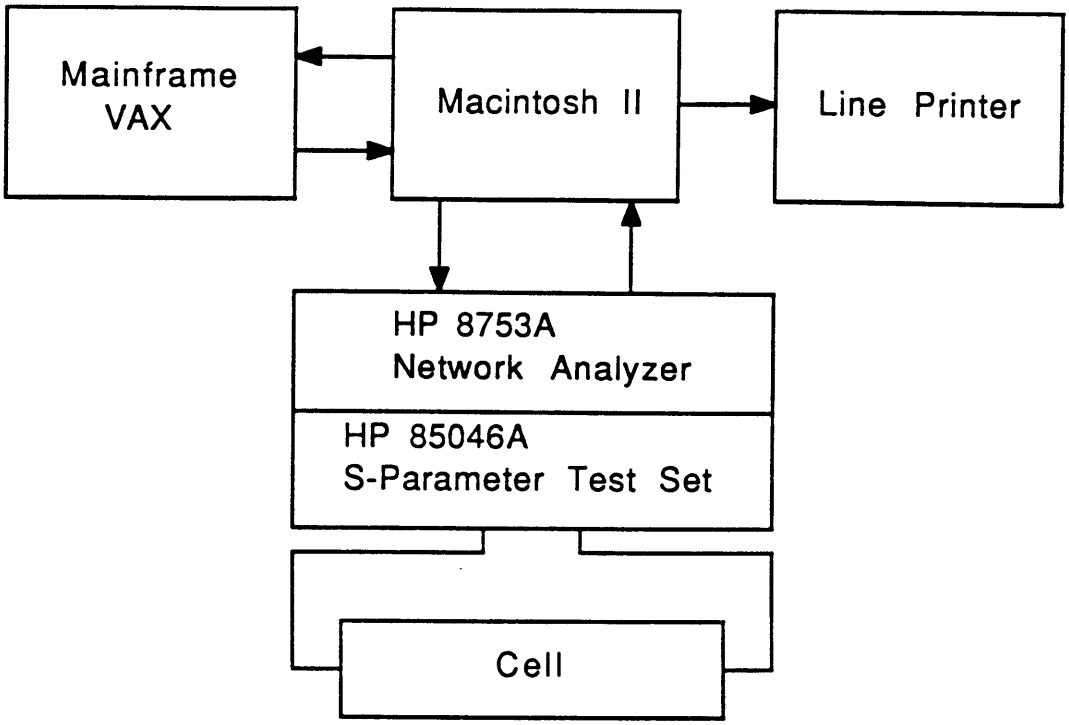

Figure 3.1.2.1: Simplified View of the Acquisition/Processing System

The network analyzer (Hewlett-Packard 8753A) and S-parameter test set (Hewlett-Packard 85046A) are the basic components which measure the scattering parameters for the high-pressure cell. They are connected to the cell by flexible 4-foot coaxial cables. These cables are the test port extension cables of the TS7878 Series by Quality Microwave Interconnects Inc. Their operation range is from DC to 6 GHz and they are phased matched to 2° at 1.3 GHz to ensure repeatable, low-loss RF connections to the cell. The HP measurement system is designed to measure the reflection and transmission characteristics of devices, a high-pressure cell in this case, by applying a known signal and measuring the response of the test device. The signal transmitted through the device or reflected from its input is compared with the incident signal.

The HP 8753A network analyzer integrates a high resolution synthesized source and a dual channal three-input receiver to measure and display magnitude, phase, and a group delay of transmitted and reflected power. The built-in synthesized source produces a RF signal in the range of 300 KHz to 3 GHz. The RF output power is leveled by an internal automatic leveling control circuit. To achieve frequency accuracy and phase measuring capability, the network analyzer is phase locked to a highly stable crystal oscillator. For this purpose, a portion of the output signal is routed via the test set or other external coupling to the input of the receiver, where it is sampled by the phase detection loop and fed back to the source.

The HP 85046A S-parameter test set contains the hardware required to make simultaneous transmission and reflection measurements in both the forward and reverse directions. An RF path switch in the test set is controlled by the network analyzer so that reverse measurements can be made without changing the connections to the device under test.

The operation of the network analyzer is controlled with a Macintosh computer. The IOtech MacDriver488 controller card was installed on the Macintosh II computer to provide an IEEE interface to the HP measurement system. With this interface installed, a Microsoft BASIC code was developed to automate the entire data acquisition process. This code enables the user to access a number of functions, such as calibration of network analyzer with standard terminations, measurement of scattering parameters, saving of measurement data to internal memory device, retrieving data, printing data on a laser printer, and finally plotting data in various graphical forms. A copy of this code can be seen in Appendix C.1. The primary function for the Macintosh computer is to automate the data acquisition process. The secondary function is to send raw data to the mainframe processor where inversion of scattering parameters takes place.

The actual computation of the complex dielectric constant is performed on the VAX mainframe computer. Inversion codes are developed and stored on the VAX mainframe. The VAX receives raw measurement data from the Macintosh computer and perform different inversion schemes. As a result, a set of complex dielectric constant as a function of frequency is returned to the Macintosh computer where printing and plotting can be performed on the data.

3.1.3 Pressurizing unit

A pressure system capable of generating pressure of up to 20,000 psi is described. A schematic of this system can be seen in Figure 3.1.3.1.

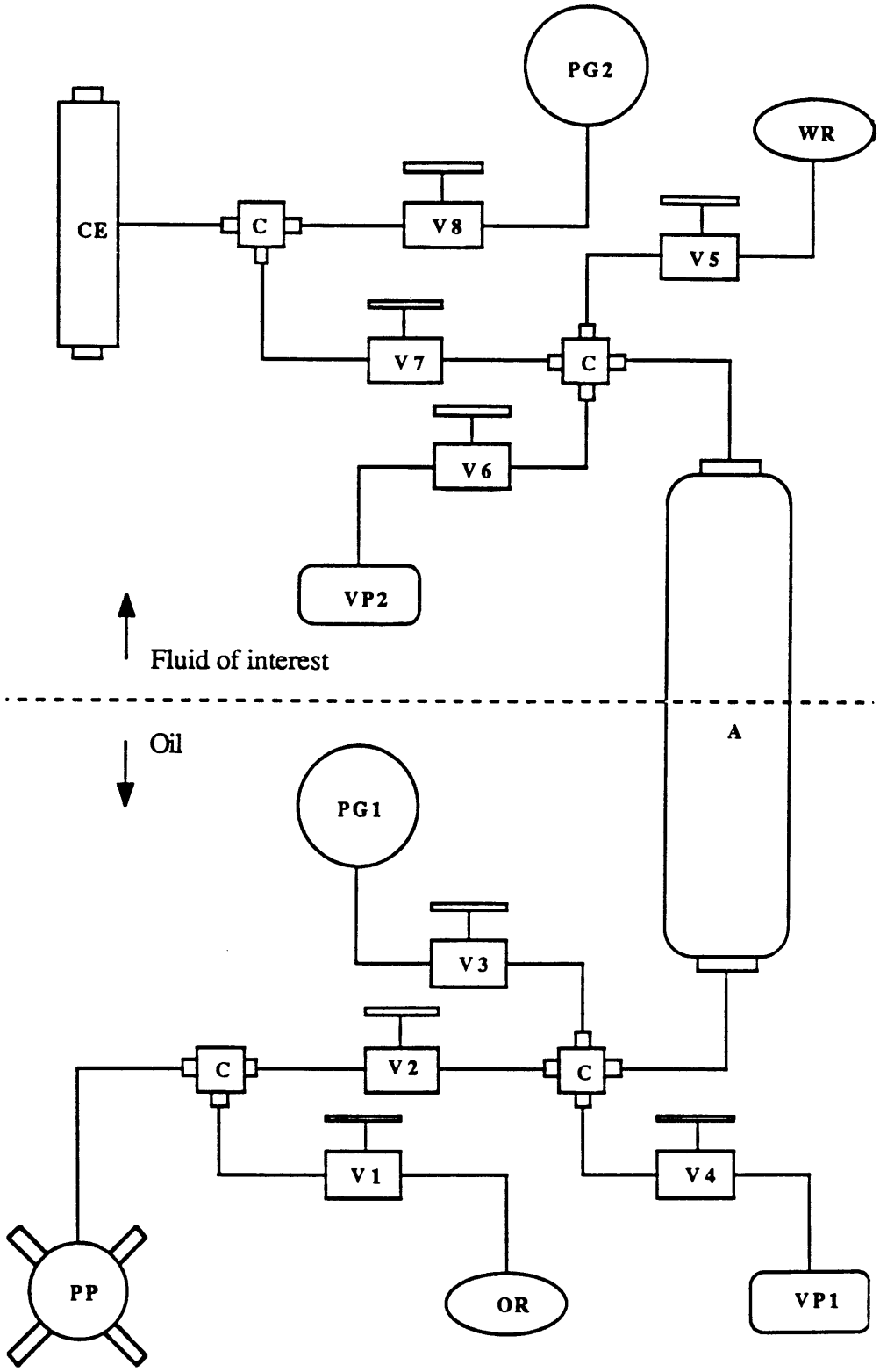

Figure 3.1.3.1: Pressurizing System

The notations used in Figure 3.1.3.1 are defined in the following:

PP - pressure pump
VP - vacuum pump (VP1,VP2)
PG - pressure gauge (PG1,PG2)
A - accumulator
OR - oil reservoir
WR - water reservoir
CE - cell
C - cross
V - valve (V1-V8)

A manually operated piston screw pump is used to generate pressures of up to 20,000 psi. This high-pressure pump is manufactured by High Pressure Equipment and is applicable to experiments where a fluid is to be compressed with a small volumn in order to develop the desired pressure. For this specific application, the 37-6-30 generator, pressure rated to 30,000 psi, is employed. However, this generator has a volumn of merely 11 cc. This small volumn can pressurized the system to only 1,200 psi. In order to generate pressures of up to 20,000 psi in this study, a procedure has been developed to allow more oil to enter the system. This procedure is presented in Appendix A.1.

An EPS Clamart accumulator, which is essentially a piston-type pressure transformer, is used to transfer pressure from oil region to fluid region. The primary reason for using two different liquids in this pressurizing system is that the pressure pump functions most effectively when the hydraulic fluid is viscous. The 200 cs. viscosity oil from Dow Corning is used in this study.

Two pressure gauges, made by Heise Plant Division of Dresser Industries, are installed to measure pressures in oil and fluid regions. They have large 1000 scale divisions over their 0-20000 psi range. It is possible to read to the smallest scale division used, or 20 psi. These gauges are calibrated with dead weigh tester, model 1277, by Harwood Engineering whose accuracy is traceable to the National Institute of Standards and Technology. The accuracy, as reported by the Heise Company was 0.1% of the full scale. Since the full scale reading of the two gauges is 20,000 psi, the maximum error is 20 psi. It is important to note that a maximum vacuum of 5μm of mercury can be drawn in the gauges. Precaution must be taken when drawing a vacuum in the two regions during the setup procedure. (refer to Appendix A.1)

Valves and crosses are fitted at various locations to accommodate the installation of vacuum pumps and inlet sources. A step-by-step setup procedure for the pressurizing system is given in Appendix A.1. In the following section, the theoretical modeling of the high-pressure cell is discussed.

3.2 Theory and Operation Principles

The problem of predicting the response of the cell, that is to determine its scattering parameters when the complex dielectric constant of the sample is known, is called the forward modeling. The reverse problem of solving for the complex dielectric constant with known set of scattering parameters is known as inversion. In order to fully understand these two processes, one must understand the boundary value problem associated with this coaxial cell. A simplified version of this cell is shown in Figure 3.2.1.

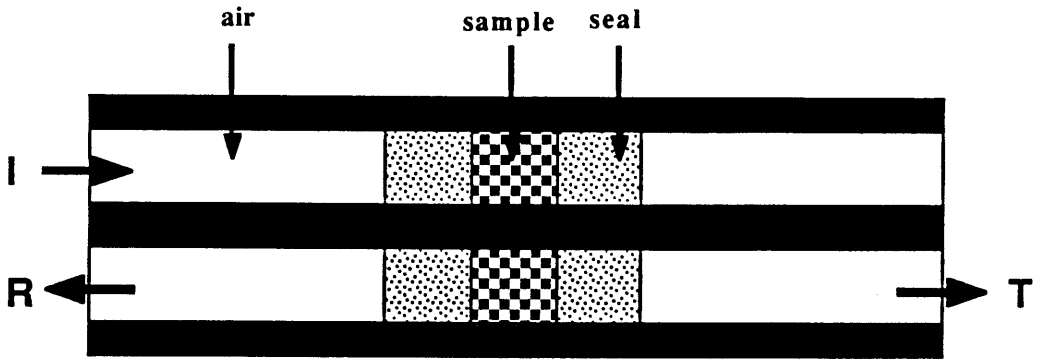

Figure 3.2.1: Coaxial Cell

The cell is basically a coaxial line with three different sections as discussed in the cell design in the last chapter. The white portions represents the air sections in the caps. The checker-patterned middle section represents the sample. The sparsely-dotted sections represents the high-pressure seals. In our design, each of the sections has a different characteristic impedance.

An incident TEM wave from a network analyzer, I, enters the cell from the left and propagates to the right. Because of the impedance mismatch at the boundaries separating

various sections, part of this incident wave is reflected back at each boundary and travels to the left, R. The remainder of the wave is attenuated through different sections and transmitted to the right end, T. In the steady state, and because of multiple reflections between the various boundaries, a standing wave is developed in the various sections of the cell. Since we are making a two-port measurement, four scattering parameters, namely, S_{11}, S_{12}, S_{21}, and S_{22} are obtained. They are defined in Figure 3.2.2.

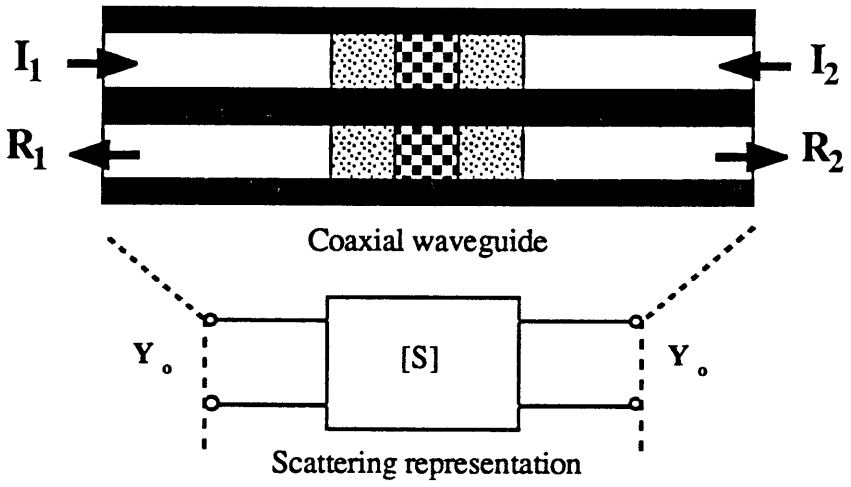

$$S_{11}=\frac{R_1}{I_1} \qquad I_2=0$$

$$S_{21}=\frac{R_2}{I_1} \qquad I_2=0$$

$$S_{12}=\frac{R_1}{I_2} \qquad I_1=0$$

$$S_{22}=\frac{R_2}{I_2} \qquad I_1=0$$

Figure 3.2.2: Definition of Scattering Parameters

From these scattering parameters, we can infer the complex dielectric constant for the sample.

The original boundary value problem in Figure 3.2.1 can be simplied a great deal if one considers the following equivalent problem.

3.2.1 Equivalent model

The original configuration in Figure 3.2.1 can be made up from the superposition of two simpler configurations shown in Figure 3.2.1.1 and Figure 3.2.1.2. In Figure 3.2.1.1, one should note that the incident field on the opposite ends of the cell have the same amplitudes and orientations. On the other hand, the incident fields at the two ends of the cell in Figure 3.2.1.2 differ in orientations, but have the same amplitudes.

Case 1

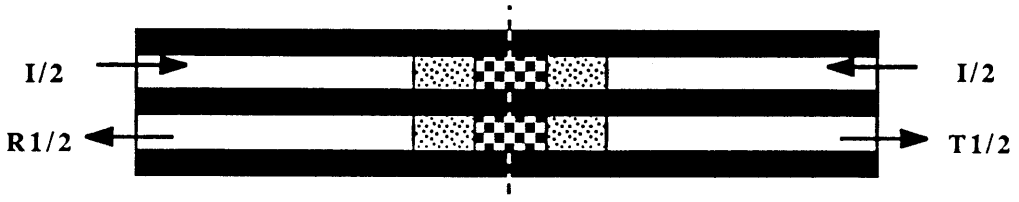

R1=T1

Figure 3.2.1.1: Same Orientation

Case 2

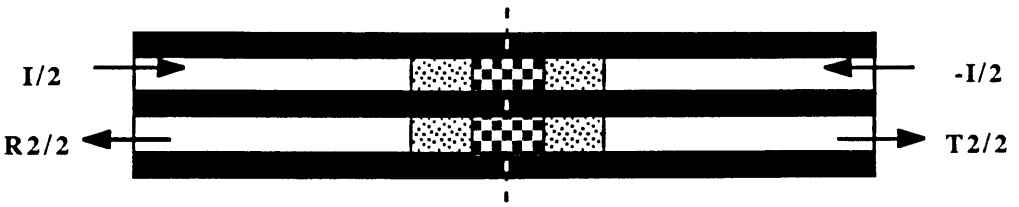

R2=-T2

Figure 3.2.1.2: Opposite Orientation

One can now exploit the symmetry in case 1 (configuration in Figure 3.2.1.1) to further simplify the problem. The incident waves, with an amplitude half that of the wave of the

original problem, enters the cell from the two ends and propagate towards the sample. Due to the mismatch at the different junctions, reflected waves are generated. From symmetry, the amplitudes of these reflected waves should be identical. Because the incident electric fields have similar orientations, they would reinforce each other at the center plane of the cell and the magnetic fields would cancel. Realizing that this is a characteristic of a perfect magnetic conductor (PMC), one can replace the two-port cell of Figure 3.2.1.1 with the simpler structure of a one-port cell with PMC termination as shown in Figure 3.2.1.3.

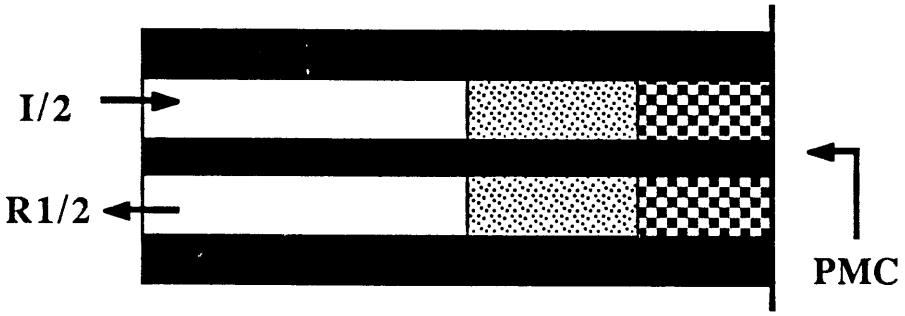

Figure 3.2.1.3: Half-Cell with a PMC Termination

The analysis for case 2 (the configuration in Figure 3.2.1.2) is very similar to that for case 1. The incident fields now have opposite orientations, but with the same amplitudes. Consequently, the reflected and transmitted waves generated also have opposite orientations and with the same amplitudes. The opposite orientations of the electric fields would cause a cancellation of fields at the center plane of the cell. This phenomenon is a characteristic of a perfect electric conductor (PEC). Therefore, the configuration in Figure 3.2.1.2 can be replaced with the one in Figure 3.2.1.4.

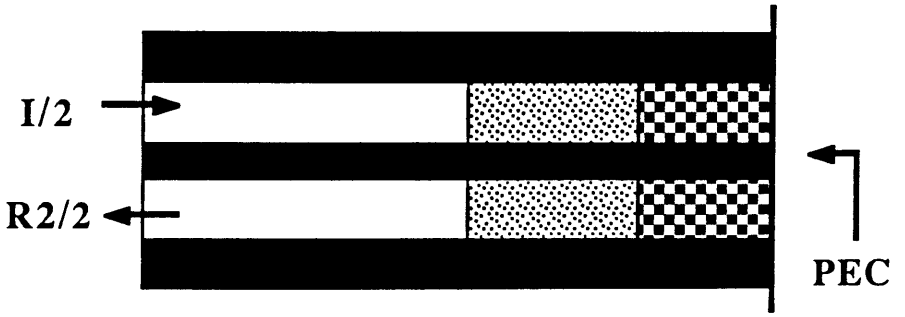

Figure 3.2.1.4: Half-Cell with a PEC Termination

The complete transformation process is summarized in Figure 3.2.1.5.

Complete Transformation Process

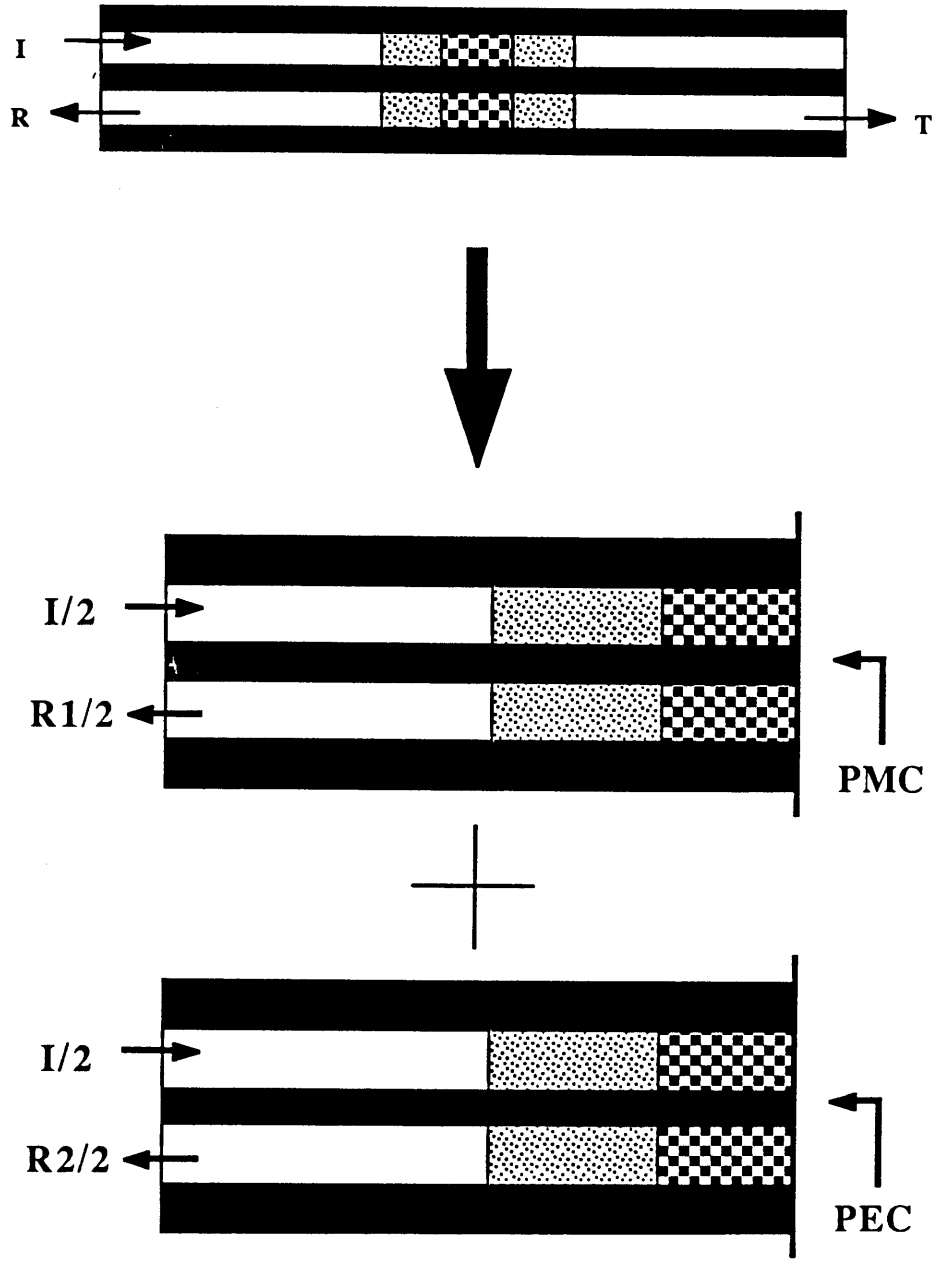

$$R = \frac{R1 + R2}{2} \qquad T = \frac{R1 - R2}{2}$$

Figure 3.2.1.5: Complete Transformation Process

Therefore, the two-port problem of Figure 3.2.1 is reduced to two one-port problems of Figure 3.2.1.3 and Figure 3.2.1.4. In the next section, we will describe the forward model.

3.2.2 Forward model

We first consider a half-cell with three different sections as shown in Figure 3.2.2.1, terminated by either PMC or PEC. This cell has an air section (section 1), a kyro-flex ceramic (section 2), and a sample of interest (section 3). Note that the length of the sample in Figure 3.2.2.1 is one-half the length of the original sample.

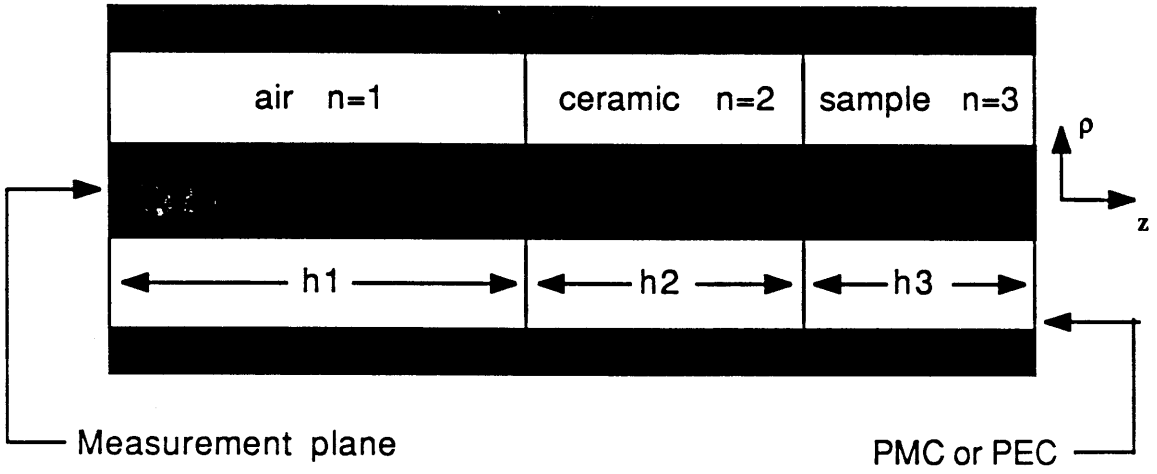

Figure 3.2.2.1: Schematic of a Half-Cell

Note that the above notations are applicable to half-cell with PMC or PEC termination. The measurement plane, which is the plane where calibration is performed for the network analyzer, is located on the leftmost plane of Figure 3.2.2.1.

The cell is excited by TEM waves and since there are no abrupt dimensional changes, both incident and reflected waves are TEM. Any mode conversion is small and is not included in the following derivation. The electric field in the n-th section of Figure 3.2.2.1 can be represented as the linear combination of incident and reflected TEM waves.

$$E_{n\rho}(\rho,z) = A_n \Psi_0(\rho)\left[e^{ik_n z_n} + R_n e^{ik_n(2h_n - z_n)}\right] \tag{12}$$

where k_n is the propagation constant of section n and has a value of $\omega\sqrt{\mu_0\varepsilon_n}$. ε_n is the complex dielectric constant of the material filling the space between the inner and outer conductors in section n. μ_0 is the magnetic permeability of the medium and is assumed to be the same as that of free space. R_n is the global reflection coefficient at the junction between section n and section n+1. z_n is the local axial distance. That is to say $z_1 = 0$ represents the measurement plane, $z_1 = h_1$ represents the end of the air section or the beginning of the ceramic section. Note that $z_1 = h_1$ is the same plane as $z_2 = 0$. Similarly, $z_2 = h_2$ is also the same plane as $z_3 = 0$. $\Psi_0(\rho)$ is the eigenfunction of the coaxial structure, corresponding to TEM mode. A_n are unknown amplitude coefficients, . $\Psi_0(\rho) = 1/\rho$.

The magnetic field of the n-th section can be derived as

$$H_{n\Phi}(\rho,z) = \frac{1}{i\omega\mu_n}\frac{\partial}{\partial z}E_{n\rho}(\rho,z) = \frac{1}{\eta_n}A_n\Psi_0(\rho)\left[e^{ik_n z_n} - R_n e^{ik_n(2h_n - z_n)}\right] \tag{13}$$

where η_n is the characteristic inpedance = $\sqrt{\frac{\mu_0}{\varepsilon_n}}$.

For the (n+1)-th section the electric and magnetic fields are

$$E_{(n+1)\rho}(\rho,z) = A_{n+1}\Psi_0(\rho)\left[e^{ik_{n+1}z_{n+1}} + R_{n+1}e^{ik_{n+1}(2h_{n+1} - z_{n+1})}\right] \tag{14}$$

$$H_{(n+1)\Phi}(\rho,z) = \frac{1}{\eta_{n+1}}A_{n+1}\Psi_0(\rho)\left[e^{ik_{n+1}z_{n+1}} - R_{n+1}e^{ik_{n+1}(2h_{n+1} - z_{n+1})}\right] \tag{15}$$

Boundary conditions require that the transverse components, ρ and Φ, of the electric and magnetic fields of the n-th and (n+1)-th sections to be continuous at the plane of interface, $z_n = h_n$ and $z_{n+1} = 0$.

$$A_n\Psi_0(\rho)\left[1 + R_n\right]e^{ik_n h_n} = A_{n+1}\Psi_0(\rho)\left[1 + R_{n+1}e^{i2k_{n+1}h_{n+1}}\right] \tag{16}$$

$$\frac{1}{\eta_n}A_n\Psi_0(\rho)\left[1 - R_n\right]e^{ik_n h_n} = \frac{1}{\eta_{n+1}}A_{n+1}\Psi_0(\rho)\left[1 - R_{n+1}e^{i2k_{n+1}h_{n+1}}\right] \tag{17}$$

Solving for R_n, the reflection coefficients, the following equation is obtained.

$$R_n = \frac{R_{n,n+1} + R_{n+1} e^{i2k_{n+1}h_{n+1}}}{1 + R_{n,n+1} R_{n+1} e^{i2k_{n+1}h_{n+1}}} \tag{18-a}$$

where

$$R_{n,n+1} = \frac{k_n - k_{n+1}}{k_n + k_{n+1}} = \frac{\eta_{n+1} - \eta_n}{\eta_{n+1} + \eta_n} \tag{18-b}$$

$R_{n,n+1}$ is the reflection coefficient at the boundary, while R_n is the global reflection coefficient. In the case of PMC, R_3, the reflection coefficient at the rightmost plane in Figure 3.2.1.3, is equal to +1. For the case of PEC, R_3 is equal to -1. With the above equations, we can now solve for the reflection coefficient at the measurement plane, where the calibration takes place, for both PMC and PEC cases. We denote the reflection coefficient for the case with PMC as $R_{(m)}$ and for the case with PEC as $R_{(e)}$. To solve the original boundary value problem as presented in Figure 3.2.1, we simply substitute the reflection coefficients, $R_{(m)}$ and $R_{(e)}$, into the following equations:

$$R = \frac{1}{2}(R_{(m)} + R_{(e)}) \tag{19}$$

$$T = \frac{1}{2}(R_{(m)} - R_{(e)}) \tag{20}$$

Realizing that the air section is a no loss 50Ω coaxial section, we do not need to include this section explicitly. It is sufficient to calculate the reflection and transmission coefficients at air/seal interface and to include a phase shift term for the air section. Therefore, the scattering parameters, as measured by the network analyzer, can be denoted by the following equations:

$$S_{11} = S_{22} = \frac{1}{2}(R_{1m} + R_{1e}) e^{j2k_1 h_1} \tag{21}$$

$$S_{12} = S_{21} = \frac{1}{2}(R_{1m} - R_{1e}) e^{j2k_1 h_1} \tag{22}$$

We have developed a FORTRAN code which, given the complex dielectric constants for both the sample and the seal, computes the reflection and transmission coefficients at the measurement plane as a function of frequency. This program uses two input files: one with the dielectric constant and conductivity for the seal and one with the dielectric constant and conductivity for the sample. This code is included in Appendix D.1.

3.2.3 Inversion

The forward model calculates the reflection and transmission coefficients, i.e. the scattering parameters, once the complex dielectric constant of the sample is specified. However, the objective is to retrieve the dielectric information of the sample from the scattering parameter measurements obtained from the network analyzer. This is known as inversion. In the last section, a full-wave model that can predict the response of the coaxial cell (the forward model) was developed. In the following sections, three different inversion schemes for the sample and one inversion scheme for the high-pressure seal are described.

3.2.3.1 Inversion (I) for sample

The first inversion scheme employs the close form solution to the forward model problem. Solving for R_{1m} and R_{1e}, using eqs. (21) and (22), we obtained the following:

$$R_{1m} = \frac{S_{11} + S_{12}}{e^{-j2k_1h_1}} \tag{23}$$

$$R_{1e} = \frac{S_{11} - S_{12}}{e^{-j2k_1h_1}} \tag{24}$$

The set of eqs. (23) and (24) can be repeated using other measured scattering parameters. In general, four sets of such equations can be formed in different combinations of the measured scattering parameters.

Keep in mind that k_1(propagation constant for air), k_2(propagation constant for the high-pressure seal), and h's(lengths of the three sections) are known and k_3(propagation

constant for the sample) is what we are inverting for. Using eq. (18-a) for n=1 and solving for R_2, we get the following:

$$R_{2m} = \frac{R_{1,2} - R_{1m}}{(R_{1m}R_{1,2} - 1)e^{i2k_2h_2}} \tag{25}$$

$$R_{2e} = \frac{R_{1,2} - R_{1e}}{(R_{1e}R_{1,2} - 1)e^{i2k_2h_2}} \tag{26}$$

where R_{1e} and R_{1m} are known from eqs. (23) and (24). Assuming the permittivity of the seal is known, $R_{1,2}$ can be calculated from eq. (18-b). Now that R_{2m} and R_{2e} are known and knowing R_3 is +1 for PMC and -1 for PEC, we can write the following expressions:

$$R_{3m} = +1 = \frac{R_{2,3} - R_{2m}}{(R_{2m}R_{2,3} - 1)e^{i2k_3h_3}} \tag{27}$$

$$R_{3e} = -1 = \frac{R_{2,3} - R_{2e}}{(R_{2e}R_{2,3} - 1)e^{i2k_3h_3}} \tag{28}$$

Letting $\mathbf{b} = e^{i2k_3h_3}$ and $\mathbf{a} = R_{2,3}$, eqs. (27) and (28) take the following form:

$$+1 = \frac{\mathbf{a} - R_{2m}}{(R_{2m}\mathbf{a} - 1)\mathbf{b}} \tag{29}$$

$$-1 = \frac{\mathbf{a} - R_{2e}}{(R_{2e}\mathbf{a} - 1)\mathbf{b}} \tag{30}$$

Isolating a and b into separate equations, the following quadratic relationships are obtained.

$$(R_{2m} + R_{2e})\mathbf{a}^2 - 2(R_{2m}R_{2e} + 1)\mathbf{a} + (R_{2m} + R_{2e}) = 0 \tag{31}$$

$$(R_{2m} - R_{2e})\mathbf{b}^2 + 2(R_{2m}R_{2e} - 1)\mathbf{b} + (R_{2m} - R_{2e}) = 0 \tag{32}$$

Using the conventional quadrical formula, a and b become:

$$a = \frac{(R_{2m}R_{2e}+1) \pm \sqrt{(R_{2m}R_{2e}+1)^2 - (R_{2m}+R_{2e})^2}}{(R_{2m}+R_{2e})} \tag{33}$$

$$b = \frac{-(R_{2m}R_{2e}-1) \pm \sqrt{(R_{2m}R_{2e}-1)^2 - (R_{2m}-R_{2e})^2}}{(R_{2m}-R_{2e})} \tag{34}$$

Finally, k_3 can be retrieved from a or b in the following manner.

$$k_3 = \frac{(1-a)k_2}{1+a} = \frac{\ln(b)}{i2h_3} \tag{35}$$

In this scheme, four identical complex dielectric constants can be derived from four different equations, assuming no measurement error. A FORTRAN code simulating this inversion scheme is included in Appendix E.1.

3.2.3.2 Inversion (II) for sample

The second inversion scheme also utilizes both reflection and transmission coefficients. The analysis is similar to the first inversion scheme up to eqs. (27) and (28). This approach involves solving for k_3 iteratively using either eq. (27) or eq. (28).

$$k_3 = \frac{\ln\left(\frac{R_{2,3}-R_{2m}}{R_{2m}R_{2,3}-1}\right)}{i2h_3} = \frac{\ln\left(\frac{R_{2e}-R_{2,3}}{R_{2e}R_{2,3}-1}\right)}{i2h_3} \tag{36}$$

where the first equality is from eq. (27) and the second is from eq. (28).

Using eq. (18-b), $R_{2,3}$ can be expanded and eq. (36) becomes:

$$k_3 = \frac{\ln\left(\dfrac{\dfrac{k_2-k_3}{k_2+k_3} - R_{2m}}{R_{2m}\left(\dfrac{k_2-k_3}{k_2+k_3}\right)-1}\right)}{i2h_3} = \frac{\ln\left(\dfrac{R_{2e} - \dfrac{k_2-k_3}{k_2+k_3}}{R_{2e}\left(\dfrac{k_2-k_3}{k_2+k_3}\right)-1}\right)}{i2h_3} \tag{37}$$

This equation can not be solved analytically, but we can solve for k_3 iteratively. For this reason, eq. (37) is rewritten in the following form.

$$k_{3(i+1)} = \frac{\ln\left(\dfrac{\dfrac{k_2-k_{3(i)}}{k_2+k_{3(i)}} - R_{2m}}{R_{2m}\left(\dfrac{k_2-k_{3(i)}}{k_2+k_{3(i)}}\right)-1}\right)}{i2h_3} = \frac{\ln\left(\dfrac{R_{2e} - \dfrac{k_2-k_{3(i)}}{k_2+k_{3(i)}}}{R_{2e}\left(\dfrac{k_2-k_{3(i)}}{k_2+k_{3(i)}}\right)-1}\right)}{i2h_3} \tag{38}$$

where the index, i, refers to i-th iteration. Now that k_3 is expressed in an iterative form, we can solve for its value by forming an initial guess for $k_{3(1)}$ and iteratively generating $k_{3(2)}$, $k_{3(3)}$, $k_{3(4)}$, etc., until $(k_{3(i+1)}-k_{3(i)})$ is less than a specified tolerance. A FORTRAN code simulating this inversion scheme is included in Appendix E.2.

3.2.3.3 Inversion (III) for sample

The third inversion scheme uses the individual reflection or transmission coefficient. This method involves using the Newton-Raphson scheme. A broad discussion on the Newton-Raphson approximation may be found in any numerical analysis text book; nevertheless, a brief review of this method is appropriate at this point.

This approach enables us to compute a root of the equation f(x) = 0. We start by guessing at this root, the guess being $x = x_1$. Suppose, however, that the root is actually $x_1 + h$. Then, by the Taylor expansion of f(x), we get

$$f(x_1 + h) = f|_{x=x_1} + hf'|_{x=x_1} + \ldots \tag{39}$$

where the prime refers to the derivative with respect to x.
Now our reasoning takes the following step:

1. The error in our approximation to the actual root is h.
2. This error is small enough to permit us to neglect the terms in the Taylor expansion in which "h" appears to a power higher than the first.
3. Furthermore, and since the actual root is (x_1+h), then $f(x_1) + hf'(x_1) \cong 0$.
4. Thus, the error, $h \approx -\frac{f(x_1)}{f'(x_1)}$.
5. A closer approximation to the actual root will be

$$x_2 = x_1 - \frac{f(x_1)}{f'(x_1)} \tag{40}$$

The iterated use of this method gives us the general formula

$$x_{i+1} = x_i - \frac{f(x_i)}{f'(x_i)} \tag{41}$$

where i represents the i-th iteration.

In our problem, we attempt to use this method to solve for ε_2 with the following equation:

$$\varepsilon_2^{(i)} = \varepsilon_2^{(i-1)} - \frac{F\left(\varepsilon_2^{(i-1)}\right)}{F'\left(\varepsilon_2^{(i-1)}\right)} \tag{42}$$

where $\varepsilon_2^{(i)}$ is the value of ε_2 at the i-th iteration, $\varepsilon_2^{(i-1)}$ is its value at the (i-1)-th iteration, F is a function of ε_2 and F' is the derivative of F with respect to ε_2. We can write this more specifically as:

$$\varepsilon_2^{(i)} = \varepsilon_2^{(i-1)} - \frac{S_{pq}\left(\varepsilon_2^{(i-1)}\right) - S_{pq(ms)}}{S'_{pq}\left(\varepsilon_2^{(i-1)}\right)} \qquad p = 1,2; q = 1,2 \tag{43}$$

where $\mathbf{S}_{pq}\left(\varepsilon_2^{(l-1)}\right)$ are the S-parameters computed from the forward model using $\varepsilon_2^{(l-1)}$. $\mathbf{S}_{pq(ms)}$ is the measured S-parameter. $\mathbf{S'}_{pq}\left(\varepsilon_2^{(l-1)}\right)$ is the derivative of the S-parameter with respect to ε_2, evaluated at $\varepsilon_2^{(l-1)}$.

It is important to note that this approach can be employed for inversions of either the seal or the sample, once the derivative of the scattering parameter is specified. In the remainder of this section we will solve for the derivative of the reflection and transmission coefficient with respect to the dielectric constant of the sample. In the next section we will solve for the derivative of the reflection and transmission coefficient with respect to the dielectric constant of the seal.

Taking the derivatives of the reflection coefficient in eq. (21) and the transmission coefficient in eq. (22) with respect to the dielectric constant of the sample, we get the following:

$$\frac{\partial \mathbf{S}_{11}}{\partial \varepsilon_3} = \frac{1}{2}\left(\frac{\partial \mathbf{R}_{1m}}{\partial \varepsilon_3} + \frac{\partial \mathbf{R}_{1e}}{\partial \varepsilon_3}\right)\mathbf{e}^{i2k_1h_1} \tag{44}$$

$$\frac{\partial \mathbf{S}_{12}}{\partial \varepsilon_3} = \frac{1}{2}\left(\frac{\partial \mathbf{R}_{1m}}{\partial \varepsilon_3} - \frac{\partial \mathbf{R}_{1e}}{\partial \varepsilon_3}\right)\mathbf{e}^{i2k_1h_1} \tag{45}$$

Note that all the terms in eqs. (44) and (45) are known, except for $\frac{\partial \mathbf{R}_{1m}}{\partial \varepsilon_3}$ and $\frac{\partial \mathbf{R}_{1e}}{\partial \varepsilon_3}$. Solving for these unknown, we obtain:

$$\frac{\partial \mathbf{R}_{1m}}{\partial \varepsilon_3} = \frac{\frac{\partial \mathbf{R}_{2m}}{\partial \varepsilon_3} e^{i2k_2h_2}}{1 + R_{1,2}R_{2m}e^{i2k_2h_2}}\left(1 - \frac{\mathbf{R}_{1,2}\left(R_{1,2} + R_{2m}e^{i2k_2h_2}\right)}{1 + R_{1,2}R_{2m}e^{i2k_2h_2}}\right) \tag{46}$$

$$\frac{\partial \mathbf{R}_{1e}}{\partial \varepsilon_3} = \frac{\frac{\partial \mathbf{R}_{2e}}{\partial \varepsilon_3} e^{i2k_2h_2}}{1 + R_{1,2}R_{2e}e^{i2k_2h_2}}\left(1 - \frac{\mathbf{R}_{1,2}\left(R_{1,2} + R_{2e}e^{i2k_2h_2}\right)}{1 + R_{1,2}R_{2e}e^{i2k_2h_2}}\right) \tag{47}$$

From eqs. (46) and (47), we obtain:

$$\frac{\partial R_{2m}}{\partial \varepsilon_3} = \frac{\frac{\partial R_{2,3}}{\partial \varepsilon_3} + \frac{\partial e^{i2k_3h_3}}{\partial \varepsilon_3}}{1 + R_{2,3}e^{i2k_3h_3}} - \frac{\left(R_{2,3} + e^{i2k_3h_3}\right)\left(\frac{\partial R_{2,3}}{\partial \varepsilon_3}e^{i2k_3h_3} + \frac{\partial e^{i2k_3h_3}}{\partial \varepsilon_3}R_{2,3}\right)}{\left(1 + R_{2,3}e^{i2k_3h_3}\right)^2} \tag{48}$$

$$\frac{\partial R_{2e}}{\partial \varepsilon_3} = \frac{\frac{\partial R_{2,3}}{\partial \varepsilon_3} - \frac{\partial e^{i2k_3h_3}}{\partial \varepsilon_3}}{1 - R_{2,3}e^{i2k_3h_3}} + \frac{\left(R_{2,3} - e^{i2k_3h_3}\right)\left(\frac{\partial R_{2,3}}{\partial \varepsilon_3}e^{i2k_3h_3} + \frac{\partial e^{i2k_3h_3}}{\partial \varepsilon_3}R_{2,3}\right)}{\left(1 - R_{2,3}e^{i2k_3h_3}\right)^2} \tag{49}$$

Finally, from eq. (18-b), we obtain:

$$\frac{\partial R_{2,3}}{\partial \varepsilon_3} = -\frac{\sqrt{\varepsilon_2}}{\sqrt{\varepsilon_3}\left(\sqrt{\varepsilon_2} + \sqrt{\varepsilon_3}\right)^2} \tag{50}$$

$$\frac{\partial e^{i2k_3h_3}}{\partial \varepsilon_3} = \frac{ih_3}{k_3}e^{i2k_3h_3} \tag{51}$$

Now that all the terms in eqs (44) and (45) are solved, the derivatives of the scattering parameters can be used in the Newton-Raphson approximation in eq. (43) to solve for the complex dielectric constant of the sample. This inversion scheme is better than either the inversion scheme in section 3.2.3.1 or the one in section 3.2.3.2, because it only requires the knowledge of one scattering parameter. Due to measurement error, sometimes one may only have confidence in either reflection or transmission coefficient. This method allows one to accurately invert for the sample, knowing only one of the four measured parameters. A FORTRAN code simulating this inversion scheme is included in Appendix E.3. In the next section, the derivatives of the scattering parameters with respect to the dielectric constant of the seal are solved, so the Newton-Raphson approximation can be used to invert for the dielectric constant of the seal.

3.2.3.4 Inversion for seal

The dielectric parameters for the high-pressure seals, Kyro-flex, were not known initially, therefore, one of the first steps required to use the cell was to obtain these parameters as a

function of frequency. We extend the Newton-Raphson approach, which was described in previous section, for inversion of the seal. We will solve for the derivatives of the scattering parameters with respect to the dielectric constant of the seal. This solution is based on the assumption that the dielectric parameters of the material in region 3, the sample chamber, is known. This criterion can easily be satisfied by using air as the sample initially. From eqs. (21) and (22), the derivatives are:

$$\frac{\partial S_{11}}{\partial \varepsilon_2} = \frac{1}{2}\left(\frac{\partial R_{1m}}{\partial \varepsilon_2} + \frac{\partial R_{1e}}{\partial \varepsilon_2}\right) e^{j2k_1 h_1} \tag{52}$$

$$\frac{\partial S_{12}}{\partial \varepsilon_2} = \frac{1}{2}\left(\frac{\partial R_{1m}}{\partial \varepsilon_2} - \frac{\partial R_{1e}}{\partial \varepsilon_2}\right) e^{j2k_1 h_1} \tag{53}$$

Using eq. (18-a), we obtain the following:

$$\frac{\partial R_{1m}}{\partial \varepsilon_2} = \frac{\left(\frac{\partial R_{1,2}}{\partial \varepsilon_2} + \frac{\partial e^{i2k_2h_2}}{\partial \varepsilon_2} R_{2m} + \frac{\partial R_{2m}}{\partial \varepsilon_2} e^{i2k_2h_2}\right)}{\left(1 + R_{1,2}R_{2m}e^{i2k_2h_2}\right)} - \frac{\left(R_{1,2} + R_{2m}e^{i2k_2h_2}\right)\left(\frac{\partial R_{1,2}}{\partial \varepsilon_2} R_{2m} e^{i2k_2h_2} + \frac{\partial R_{2m}}{\partial \varepsilon_2} R_{1,2} e^{i2k_2h_2} + \frac{\partial e^{i2k_2h_2}}{\partial \varepsilon_2} R_{2m}R_{1,2}\right)}{\left(1 + R_{1,2}R_{2m}e^{i2k_2h_2}\right)^2} \tag{54}$$

$$\frac{\partial R_{1e}}{\partial \varepsilon_2} = \frac{\left(\frac{\partial R_{1,2}}{\partial \varepsilon_2} + \frac{\partial e^{i2k_2h_2}}{\partial \varepsilon_2} R_{2e} + \frac{\partial R_{2e}}{\partial \varepsilon_2} e^{i2k_2h_2}\right)}{\left(1 + R_{1,2}R_{2e}e^{i2k_2h_2}\right)} - \frac{\left(R_{1,2} + R_{2e}e^{i2k_2h_2}\right)\left(\frac{\partial R_{1,2}}{\partial \varepsilon_2} R_{2e} e^{i2k_2h_2} + \frac{\partial R_{2e}}{\partial \varepsilon_2} R_{1,2} e^{i2k_2h_2} + \frac{\partial e^{i2k_2h_2}}{\partial \varepsilon_2} R_{2e}R_{1,2}\right)}{\left(1 + R_{1,2}R_{2e}e^{i2k_2h_2}\right)^2} \tag{55}$$

The parameters in eqs. (54) and (55) can all be calculated using the following equations.

$$\frac{\partial R_{2m}}{\partial \varepsilon_2} = \frac{\frac{\partial R_{2,3}}{\partial \varepsilon_2}}{1 + R_{2,3}e^{i2k_3h_3}}\left(1 - \frac{e^{i2k_3h_3}\left(R_{2,3} + e^{i2k_3h_3}\right)}{1 + R_{2,3}e^{i2k_3h_3}}\right) \tag{56}$$

$$\frac{\partial R_{2e}}{\partial \varepsilon_2} = \frac{\frac{\partial R_{2,3}}{\partial \varepsilon_2}}{1 - R_{2,3} e^{i2k_3 h_3}} \left(1 + \frac{e^{i2k_3 h_3} \left(R_{2,3} - e^{i2k_3 h_3} \right)}{1 - R_{2,3} e^{i2k_3 h_3}} \right) \tag{57}$$

$$\frac{\partial R_{1,2}}{\partial \varepsilon_2} = -\frac{\sqrt{\varepsilon_1}}{\sqrt{\varepsilon_2} \left(\sqrt{\varepsilon_1} + \sqrt{\varepsilon_2} \right)^2} \tag{58}$$

$$\frac{\partial R_{2,3}}{\partial \varepsilon_2} = \frac{\sqrt{\varepsilon_3}}{\sqrt{\varepsilon_2} \left(\sqrt{\varepsilon_2} + \sqrt{\varepsilon_3} \right)^2} \tag{59}$$

$$\frac{\partial e^{i2k_2 h_2}}{\partial \varepsilon_2} = \frac{ih_2}{k_2} e^{i2k_2 h_2} \tag{60}$$

Using Newton-Raphson approach, we inverted for dielectric constant of the seal in the coaxial configuration. A FORTRAN code simulating this inversion scheme is included in Appendix E.4. The fundamental theoretical model, describing the coaxial system, is established. In the next section, we will explain the procedures involved in preparing the sample and the temperature dependence of sample under pressure.

3.3 Procedure

3.3.1 Preparation of solutions and core samples

In this study, two water solutions and two water-saturated rock samples are measured. The water solutions are pure water and .6 Ω-m water. The rock samples are Berea and Massilon rocks, saturated with 0.1 Ω-m water.

Pure water is obtained from a de-ioninzing chamber. The DC resistivity of this water was 1 mega-ohm. This chamber purifies the water by removing all the ions. The .6 Ω-m and .1 Ω-m water solutions are prepared by mixing tap water with sodium chloride in their

appropriate proportions. The resulting solutions were then measured with a four-terminal resisitivity measurement cell.

The two rock samples are Berea 423 and Massilon 1065, taken from large cores obtained from Ohio. These samples were machined to hollow cylinders with an i.d. of 0.24425", an o.d. of 0.5625", and width of 1.500". The cores were first cut with a diamond core drill in the milling machine to obtain an i.d. of 0.24425". Then a larger diamond core drill is used to cut the o.d. of 0.5625". The ends of the cores were then faced off with a low speed saw and grinded down to precisely 1.500". Once the cores are machined to the specified dimensions, they are placed in a radiant dry heat oven at 60°C for 12 hours to dry out the moisture left in the cores. They are then placed in a vacuum vessel where a vacuum pump, along with Cyrocool freezer, draws a vacuum of down to 7μm of mercury. Once this specified vacuum is attained, the appropriate solution is allowed into the vessel to saturate the rock samples.

3.3.2 Temperature consideration

In the measurements reported here, the temperature of the sample is assumed to be at room temperature between 20°C and 22°C. Application of pressure increases the temperature of the sample in the cell. In this section, a heat transfer equation is used to analyze the rate at which the temperature of the sample will return to equilibrium.

A lump system analysis is assumed. The relevant equation is given in eq (61). (Heat Transfer Textbook by J. Lienhard)

$$\frac{T(t)-T_f}{T_i-T_f}=e^{-\lambda t} \tag{61}$$

where T is the temperature of the cell as a function of time, T_i is the initial temperature, T_f is the final temperature, and λ is a time constant. Note that T_i is the temperature of the cell immediately after the sample is pressurized and T_f is the room temperature. λ is defined in eq. (62).

$$\lambda = \frac{hA_s}{\rho VC} \tag{62}$$

where A_s is the surface area exposed to the heat sink, h is the heat transfer coefficient, ρ is the density, V is the volumn of cell and C is the specific heat of the cell. Since the cell is made from both INCONEL-X750 and MONEL-K500, we chose to use the higher values of C and ρ to obtain the lower limit for our calculations. We used the specific heat constant for INCONEL-X750, 0.103 Btu/lb/°F, and the density for MONEL-K500, 0.306 lb/in^3. (Alcan Corporation's Metalog). The volumn and outer surface area of the cell can be approximated by assuming a hollow-cylinder with an o.d. of 1.90", an i.d. of .5625", and a length of 8.00". We obtained V=20.69 in^3 and A_s=47.75 in^2. The heat transfer coefficient, in general, is determined empirically. But since this empirical information is not available, we will use the free convection heat transfer coefficient, h=1 Btu/hr/sq-ft/°F. This heat transfer coefficient provides an extreme low limit in our calculations. Now substituting appropriate values into eq. (62), we calculated that λ=0.008475015/sec. Eq. (61) can now be rewritten as:

$$T(t) = (T_i - 21.2)e^{-0.008475015*t} + 21.2 \tag{63}$$

In the course of our experiements, the temperature increase of the cell body was never noticeable. So we estimate T_i to be only a few degrees above room temperature. However, since the decay constant of eq. (63), $1/\lambda$, is quite large, the sample will reach thermal equilibrium very first. To demonstrate this, we will use an overly estimated T_i of 50°C and plot the sample temperature as a function of time in Figure 3.3.2.1.

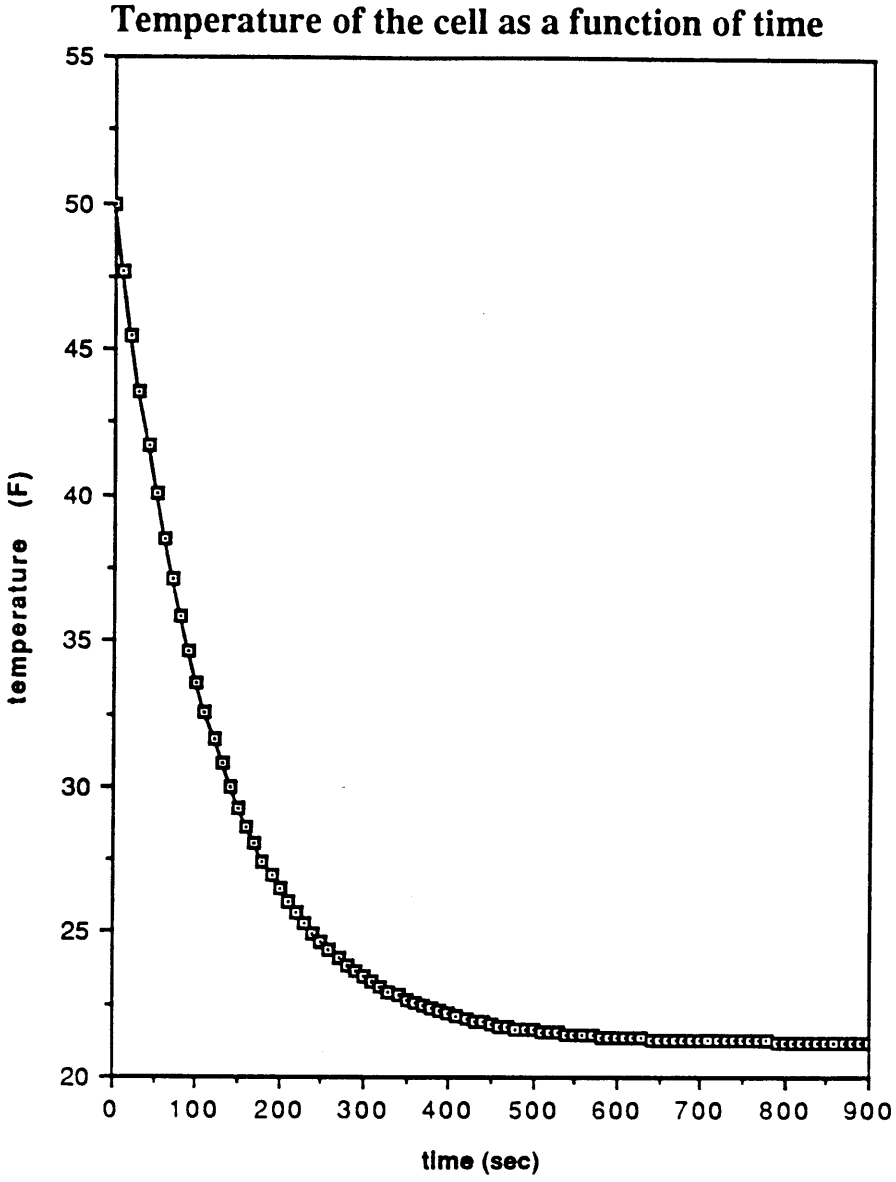

Figure 3.3.2.1: Temperature of the Cell as a Function of Time

Normally, there is a 15 minutes delay between the increase in pressure and the actual measurement. This figure shows the temperature of the cell is back to equilibrium even if the initial temperature were as high as 50°C. If T_i were 30°C, T(900)=21.2043°C. If T_i were 40°C, T(900)=21.2092°C. If T_i were 50°C, T(900)=21.2140°C. It is clear that the temperature at which the measurements were taken is almost independent of T_i. We conclude that the temperature increase of the sample due to pressure can be neglected.

Chapter 4

RESULTS

Two water samples and two water-saturated rock samples have been measured in this study. Before the data is presented, we like to point out that there is no information on high frequency dielectric parameters on either water or water-saturated rocks as a function of pressure in literature. Fortunately, the static dielectric constant of pure water was studied by Srinivasan and Kay in 1974. They used an all-glass, three terminal, Kay-Vidulich-type dielectric cell to measure the static dielectric constant of water at 10°, 25°, and 40°C at pressures of up to 3 kbar. Their results were then fitted to the Tait equation. The Tait equation is defined as:

$$1-\frac{\varepsilon(1)}{\varepsilon(P)}=A\ln\left(\frac{B+P}{B+1}\right) \tag{62}$$

where P is pressure in bars and constants A, B, and $\varepsilon(1)$ are specified for different temperatures. These parameters for 10°, 25°, and 40°C have been given by Srinivasan and Kay and are listed in Table 4.1.

Temperature (°C)	$\varepsilon(1)$	A	B
10	83.95	0.1916	4133
25	78.45	0.2154	4574
40	73.16	0.1824	3672

Table 4.1: Tait Constants for Pure Water

In our measurement on pure water, scattering parameters were measured from 20 MHz to 3 GHz at a number of pressures and at a constant temperature of 21.2°C. The inverted dielectric constants and conductivities at high frequencies are plotted as a function of frequency at various pressures in Figure 4.1 and Figure 4.2.

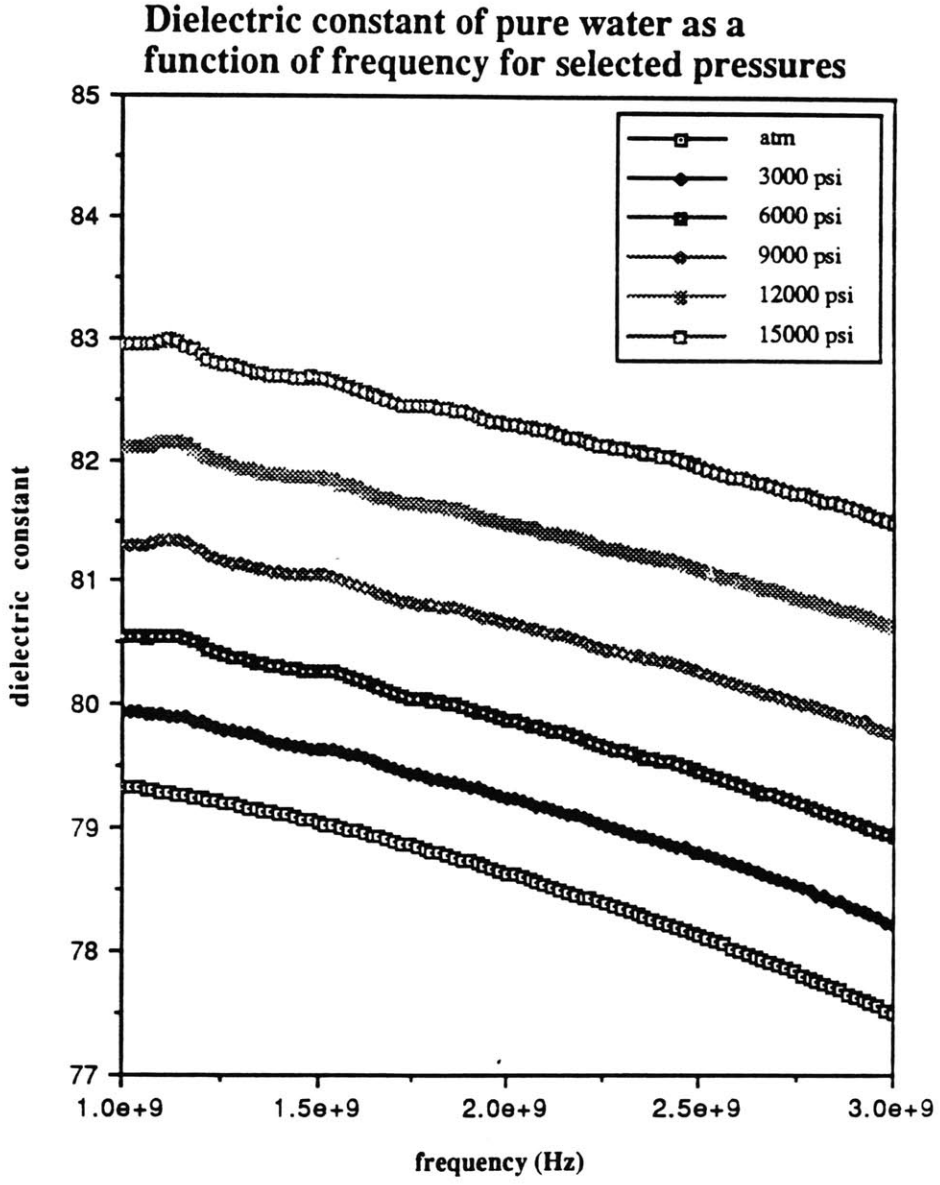

Figure 4.1: Dielectric Constant of Pure Water as a Function of Frequency for Selected Pressures

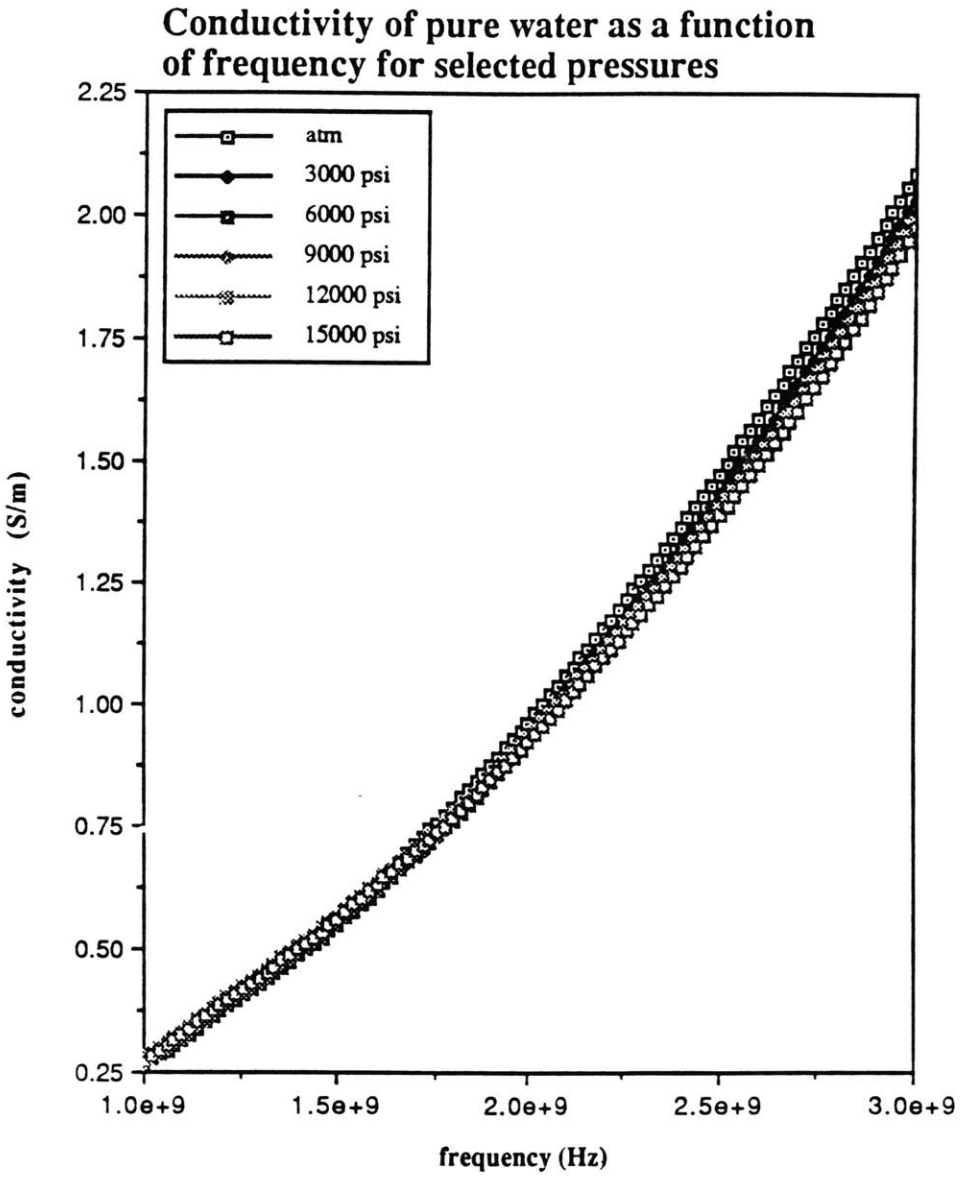

Figure 4.2: Conductivity of Pure Water as a Function of Frequency for Selected Pressures

Although the data in these figures are somewhat corrupted with measurement noise, the increasing trend in the dielectric constant as pressures increases can be observed quite readily. A closer analysis of this trend is warranted. The dielectric constant is plotted as a function of frequency from 1 GHz to 3 GHz at 6 different pressures, ranging from atmospheric pressure to 15,000 psi at intervals of 3,000 psi. The results indicate an increase in the dielectric constant of pure water at all frequencies as pressure is applied. It is interesting to see if the measured high frequency dielectric constants of pure water are

consistent with the previously measured values. But since the high frequency measurements have not been reported before, we will extrapolate these results to DC and compare the results with the data of Srinivasan and Kay. This is done by first curve-fitting the high frequency measurement data at each pressure to a third degree polynomial. A third order polynomial is capable of describing the frequency dependence of these results very well. We then used this polynomial to extrapolate the DC dielectric constant. The curved-fitted dielectric constants as a function of frequency are plotted in Figure 4.3.

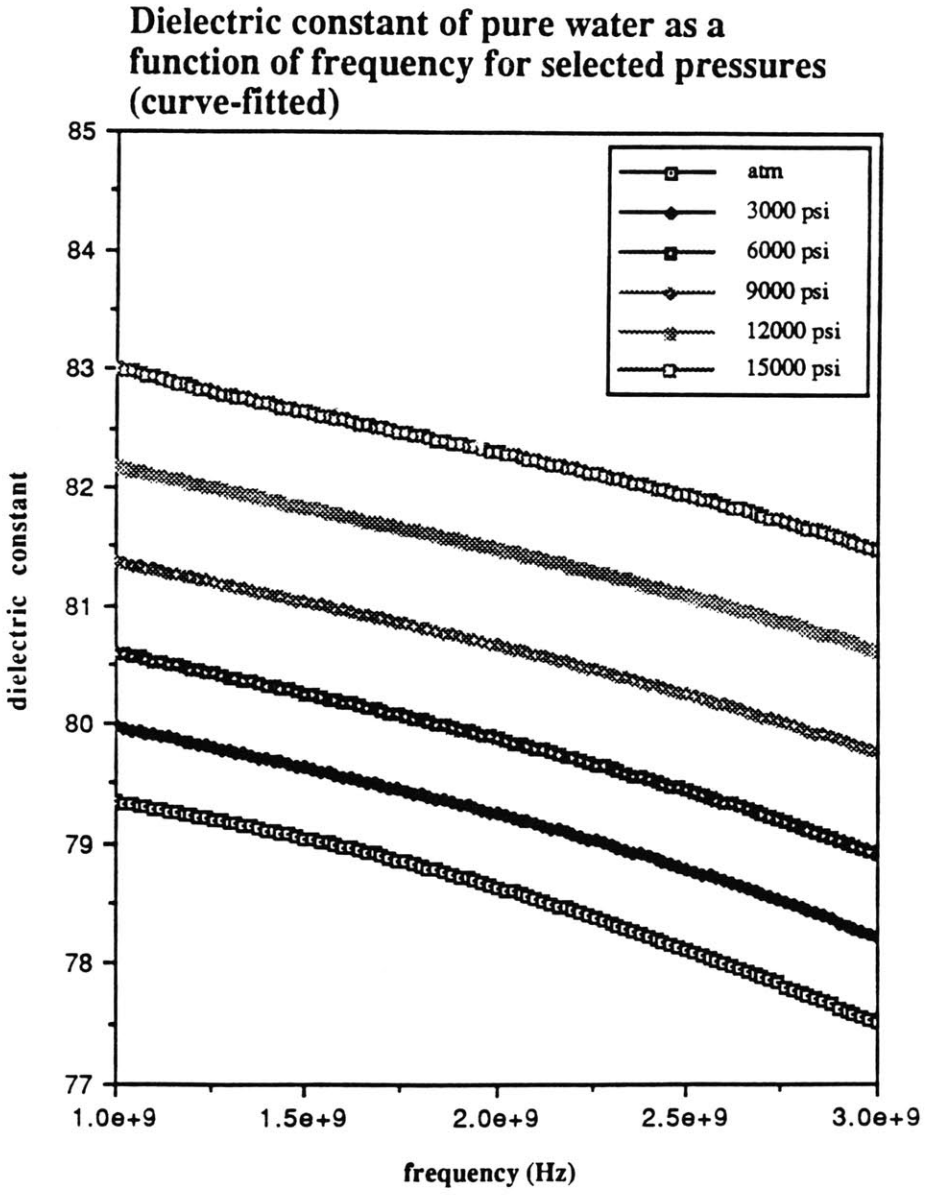

Figure 4.3: Curved-Fitted Dielectric Constant of Pure Water as a Function of Frequency for Selected Pressures

We applied this curve-fitting scheme to the dielectric constant of water as a function of frequency, predicted by Klein-Swift. This exercise showed that the data can always be curve-fitted to a third degree polynomial with a correlation factor of 1. Using this approach, the static dielectric constant as a function of pressure is obtained. The temperature of our measurements is 21.2°C. Constants for the Tait equation are not available for this temperature. But it would be interesting to compare the measured data at 21.2°C with the data from the Tait equation at 10°, 25° , and 40°C. This plot is shown in Figure 4.4.

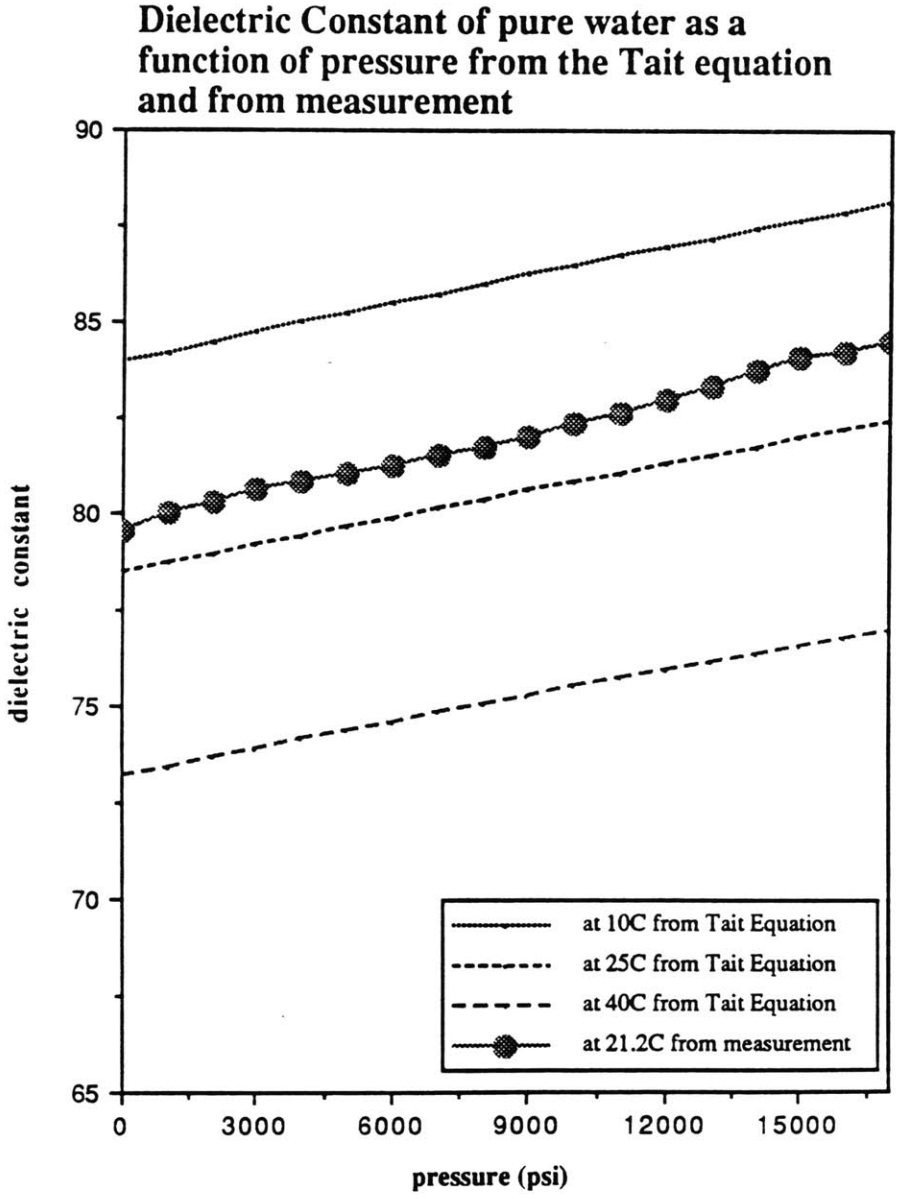

Figure 4.4: Measurement versus Tait Data for Pure Water

The measured data shows the same pressure dependence as the three curves generated from the Tait equation. It also falls between the 10°C and 25°C results as expected.

The conductivity, on the other hand, does not show such apparent pattern as pressure is applied. There seems to be very little, if any, change at frequencies below 2 GHz. Above 2 GHz, it seems that the conductivity is actually decreasing as the pressure is increased.

So far we focus on the effect of pressure on the DC dielectric constant and conductivity of pure water. We now proceed to examine the high frequency data as a function of pressure. Five frequencies, ranging from 1 GHz to 3 GHz at intervals of 500 MHz, were selected for this analysis. At each frequency the dielectric parameters are plotted as a function of pressure. The plots for dielectric constant and conductivity as a function of pressure for the five frequencies are shown in Figure 4.5 and Figure 4.6 respectively. Additional data as a funtion of pressure at 1100 MHz for pure water and subsequent samples are included in Appendix F.1. 1100 MHz is a very important frequency, because most of the available dielectric and resistivity logging tools operate at this frequency.

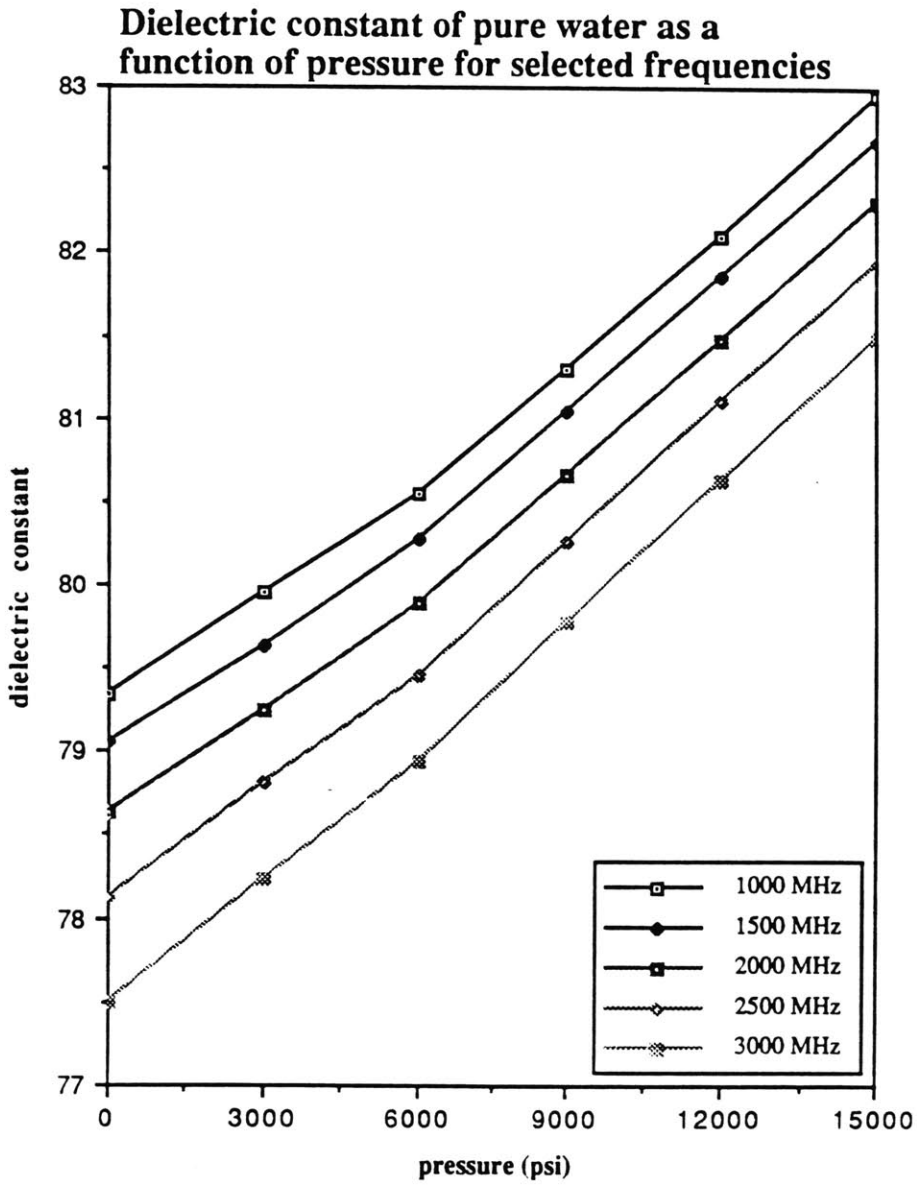

Figure 4.5: Dielectric Constant of Pure Water as a Function of Pressure for Selected Frequencies

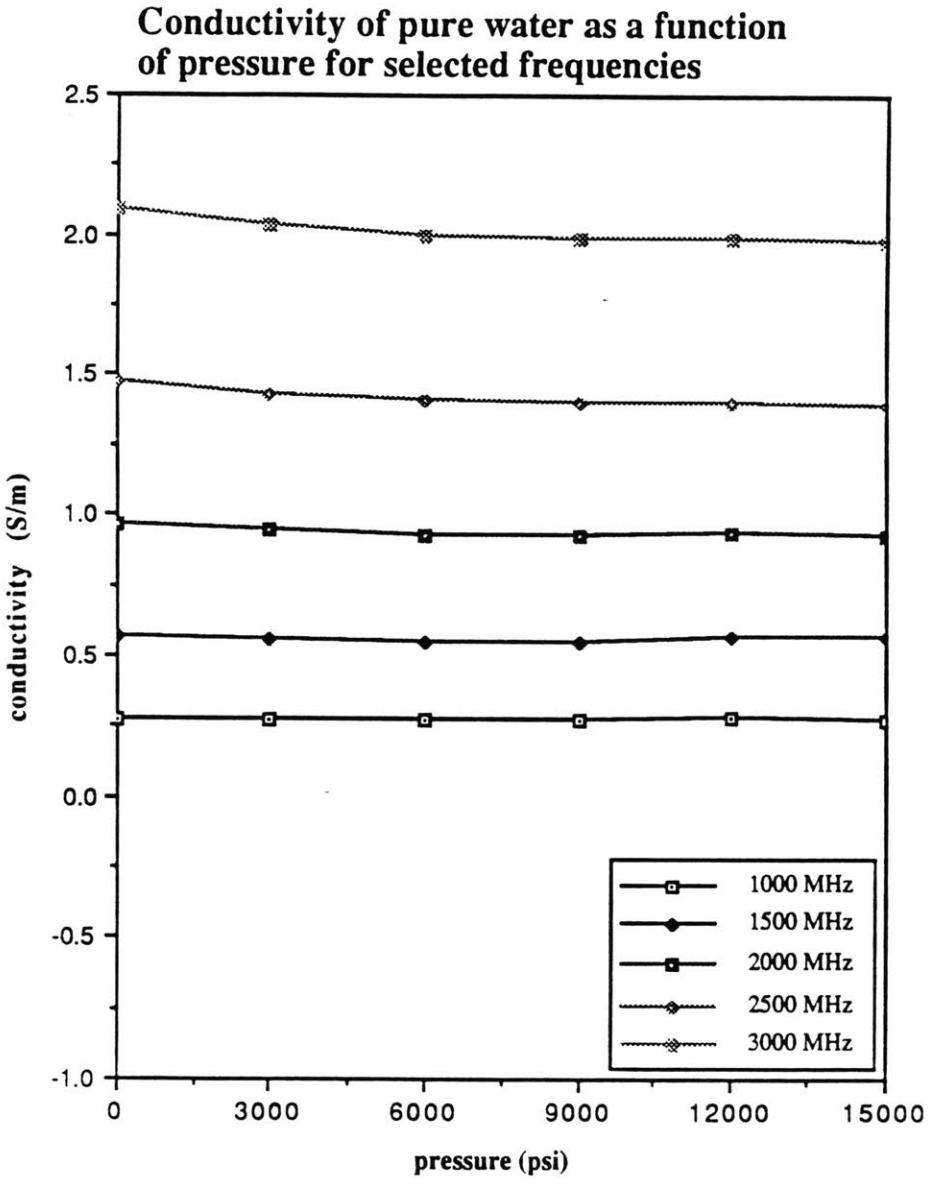

Figure 4.6: Conductivity of Pure Water as a Function of Pressure for Selected Frequencies

The increasing trend in the dielectric constant is apparent at all the selected frequencies. But a closer analysis reveals that the rate of change of dielectric constant as a function of pressure actually increases as the frequency is increased. In order to make this observation more concrete, a linear curve-fit is performed on the data in Figure 4.5. The resulting curve-fitting equations for different frequencies are given in Table 4.2.

Frequency (MHz)	Curve-fitting equations
1000	ε=79.226+2.4090e-4P
1500	ε=78.927+2.4364e-4P
2000	ε=78.530+2.4543e-4P
2500	ε=78.035+2.5520e-4P
3000	ε=77.427+2.6650e-4P

Table 4.2: Curve-Fitting Equations for Dielectric Constant of Pure Water as a Function of Pressure for Selected Frequencies

From the slopes of the fitted curves, it is clear that the rate of increase of dielectric constant increases with frequency.

A similar curve-fitting scheme is performed on the conductivity results. However, a closer analysis of this data set reveals that the change in conductivity as a function of pressure is so small that noise becomes an overshadowing factor. To be more specific, the conductivity as a function of pressure at 3,000 MHz is plotted in Figure 4.7.

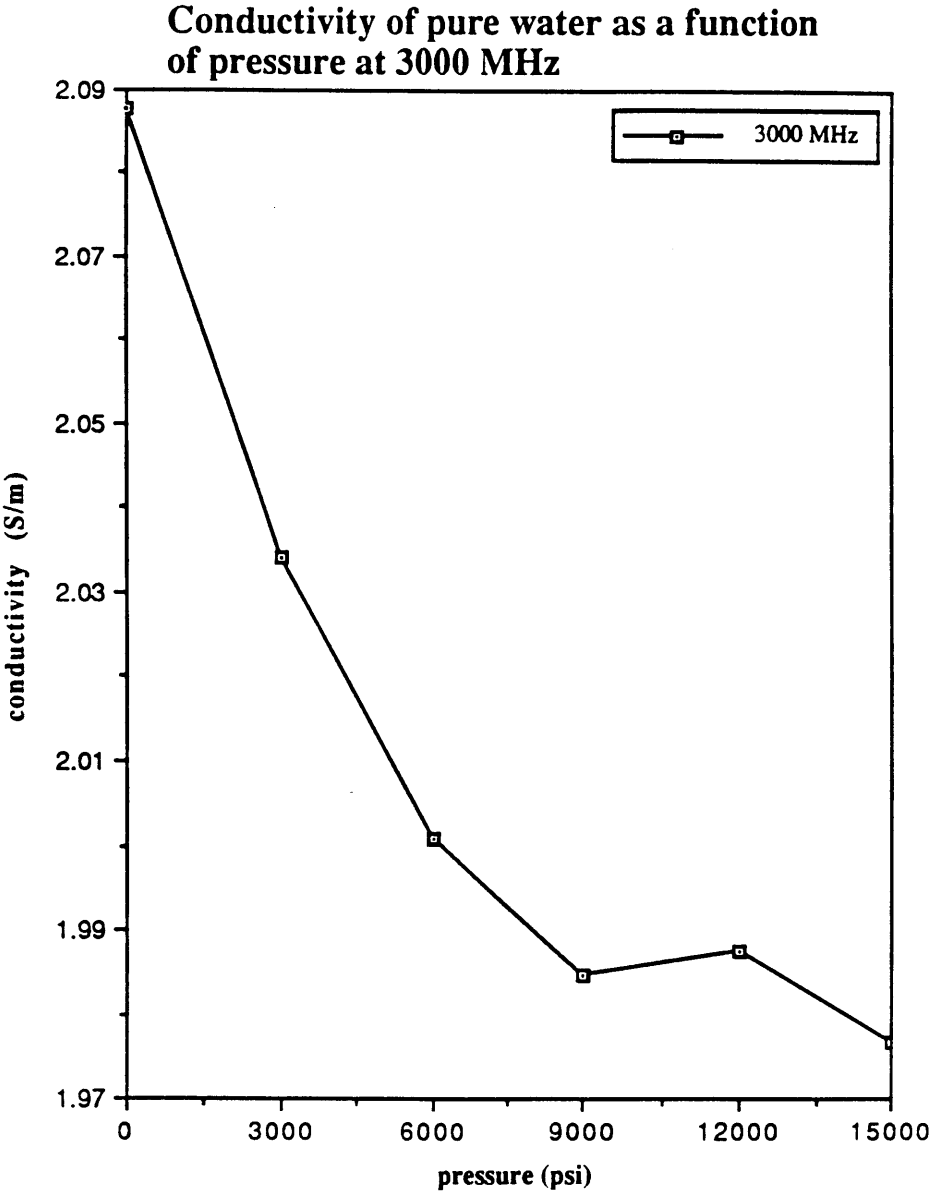

Figure 4.7: Conductivity of Pure Water as a Function of Pressure at 3000 MHz

Although the data shows an overall decreasing trend, the noise makes it very difficult to be certain that this is indeed the behavior of the conductivity of pure water at high frequencies.

The measurement on pure water is interesting in the sense that we were able to compare results with that in literature. These measurements also reflect how the intramolecular structure of liquid water changes with applied pressure. In the following, we present our

results on the dielectric parameters of .6 Ω-m water as a function of pressure. These measurements are more relevant to dielectric logging.

The second sample is a water with a static conductivity of .6 Ω-m. The measurements were taken at frequencies between 20 MHz to 3 GHz. The inverted dielectric constant and conductivity at high frequencies are plotted as a function of frequency at different pressures in Figure 4.8 and Figure 4.9 respectively.

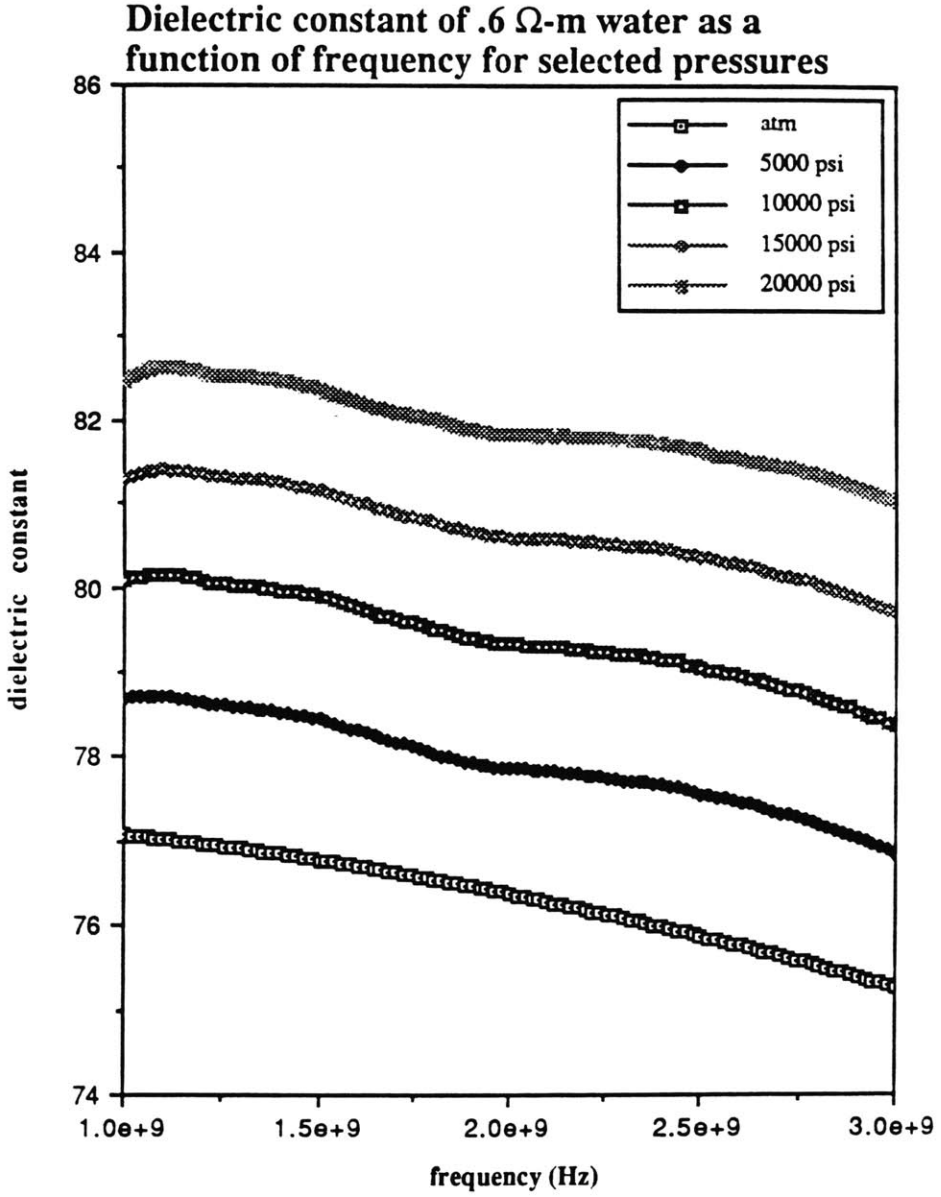

Figure 4.8: Dielectric Constant of .6 Ω-m Water as a Function of Frequency for Selected Pressures

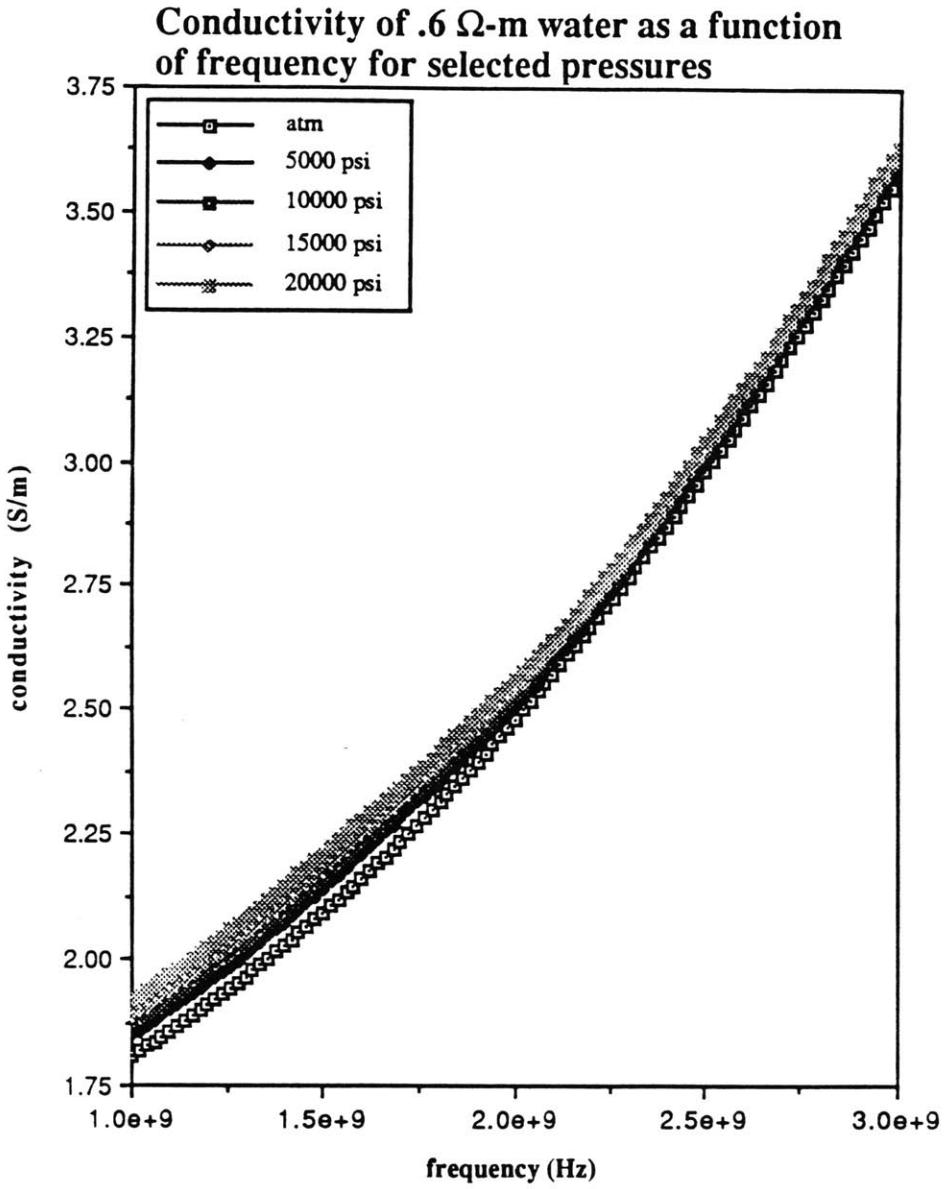

Figure 4.9: Conductivity of .6 Ω-m Water as a Function of Frequency for Selected Pressures

Data at 5 different pressures, between atmospheric pressure and 20,000 psi at intervals of 5,000 psi, are included in these figures. The results on the dielectric constants show behavior similar to that exhibited by pure water. As the pressure is applied, the dielectric constant increases at all frequencies. The curve-fitting to a third order polynomial, utilized for pure water, is also useful in smoothing out the measurement errors. The results of the fit are given in Figure 4.10.

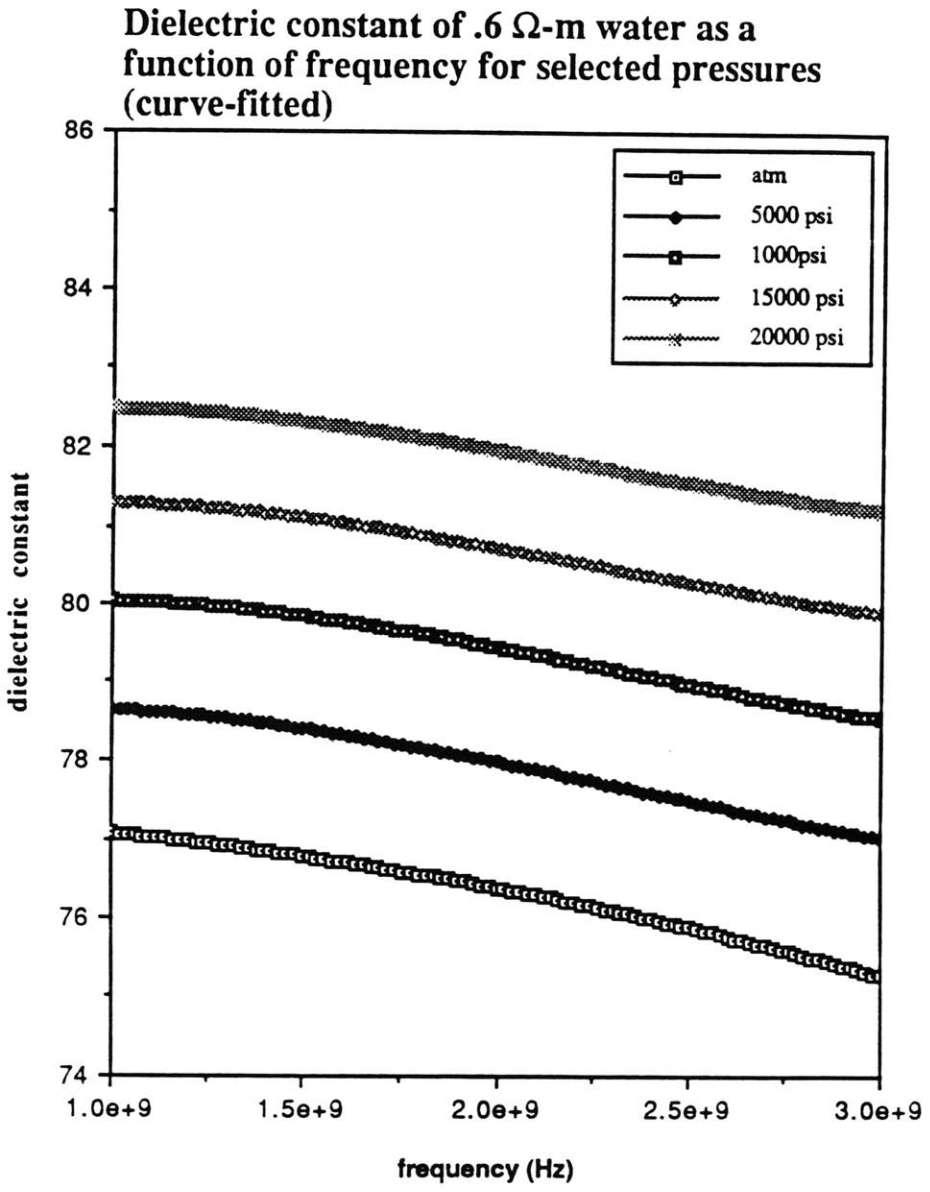

Figure 4.10: Curve-Fitted Dielectric Constant of .6 Ω-m Water as a Function of Frequency for Selected Pressures

It is interesting to see the variation of the DC dielectric constant of .6 Ω-m water compares with that of pure water. In Figure 4.11, the extrapolated DC dielectric constants of pure water and of .6 Ω-m water are plotted.

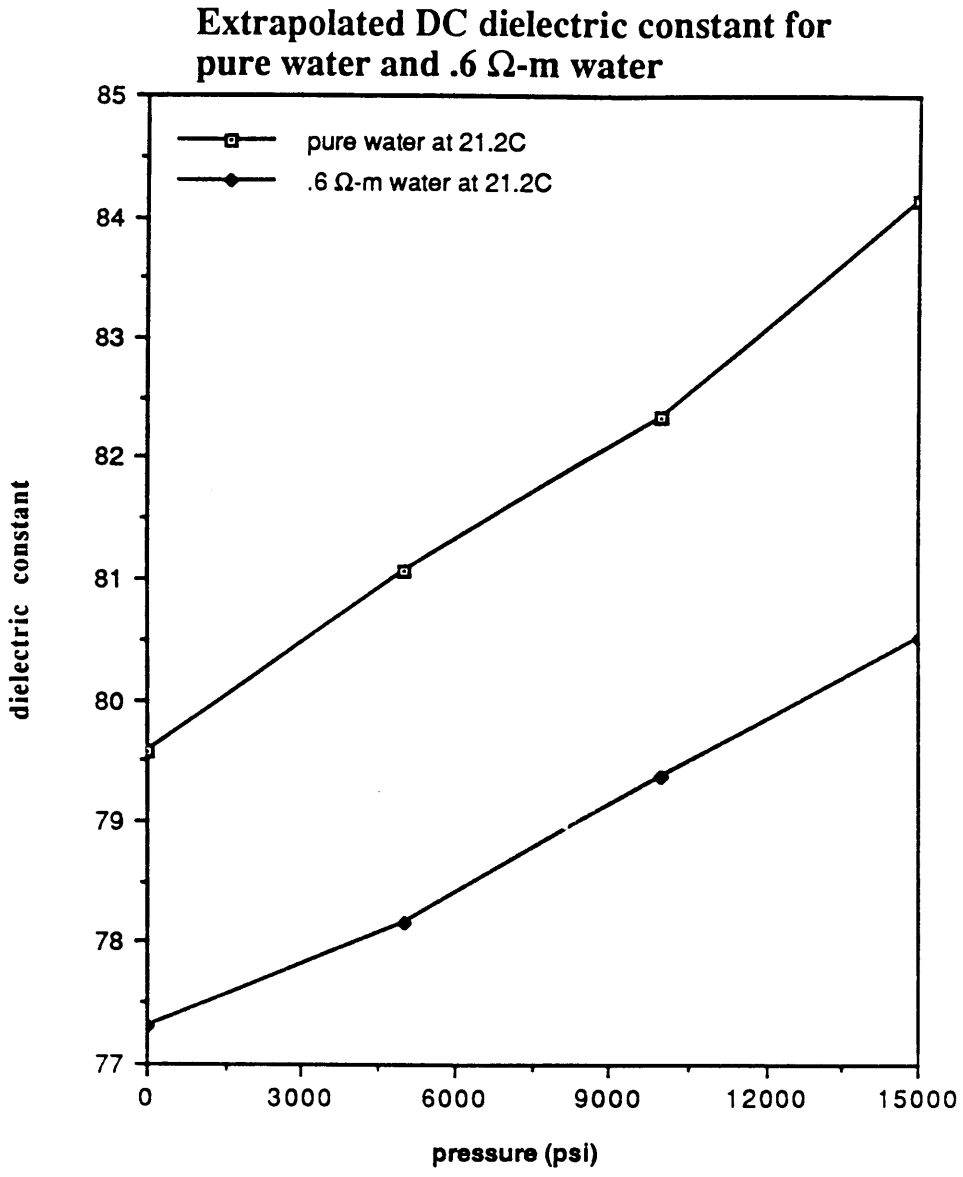

Figure 4.11: Extrapolated DC Dielectric Constant for Pure Water and .6 Ω-m Water

Also it would be interesting to see if the frequency dependence of the pressure effect is consistent with that observed for pure water. Five frequencies were selected, ranging from 1 GHz to 3 GHz at intervals of 500 MHz. At these frequencies, the dielectric constants are plotted as a function of pressure in Figure 4.12.

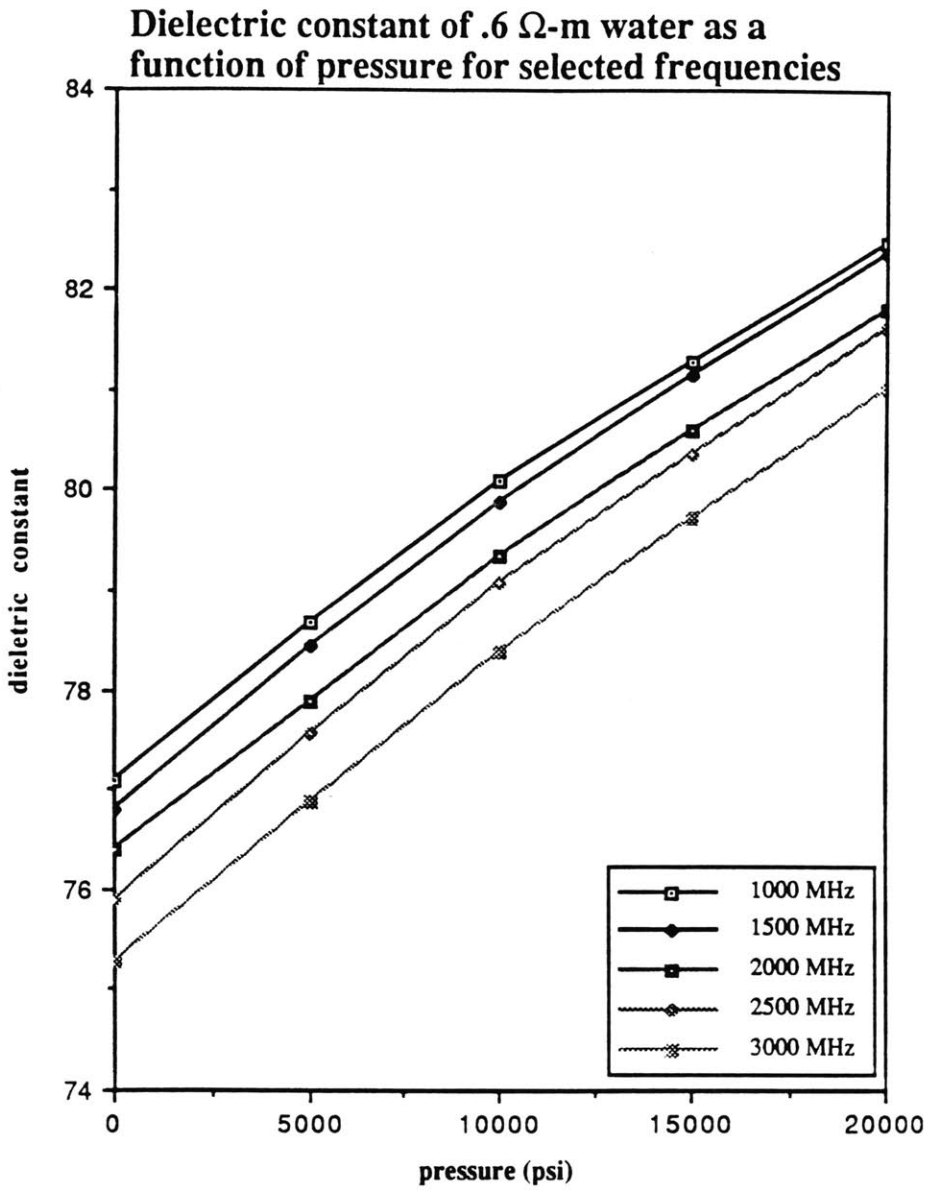

Figure 4.12: Dielectric Constant of .6 Ω-m water as a Function of Pressure for Selected Frequencies

The pressure dependence of dielectric constant is apparent. However, the frequency dependence of this pressure effect is not as linear as that exhibited by the pure water. In order to examine the behavior a bit closer, a linear curve-fitting scheme is utilized to approximate the slopes for the respective curves in Figure 4.12. The curve-fitting equations for different frequencies are given in Table 4.3.

Frequency (MHz)	Curve-fitting equations
1000	ε=77.237+2.6851e-4P
1500	ε=76.964+2.7787e-4P
2000	ε=76.487+2.7211e-4P
2500	ε=76.047+2.8558e-4P
3000	ε=75.389+2.8682e-4P

Table 4.3: Curve-Fitting Equations for Dielectric Constant of .6 Ω-m Water as a Function of Pressure for Selected Frequencies

The overall trend observed in Table 4.3 is that the pressure effect on dielectric constant increases as the frequency increases. This observation is consistent with the pure water data. However, the slope at 1500 MHz is actually greater than that at 2000 MHz. This is probably due to noise in the measurement system.

A similar analysis is carried out for the conductivity to see its frequency dependence of the pressure effect. A plot for the conductivity as a function of pressure is shown in Figure 4.13.

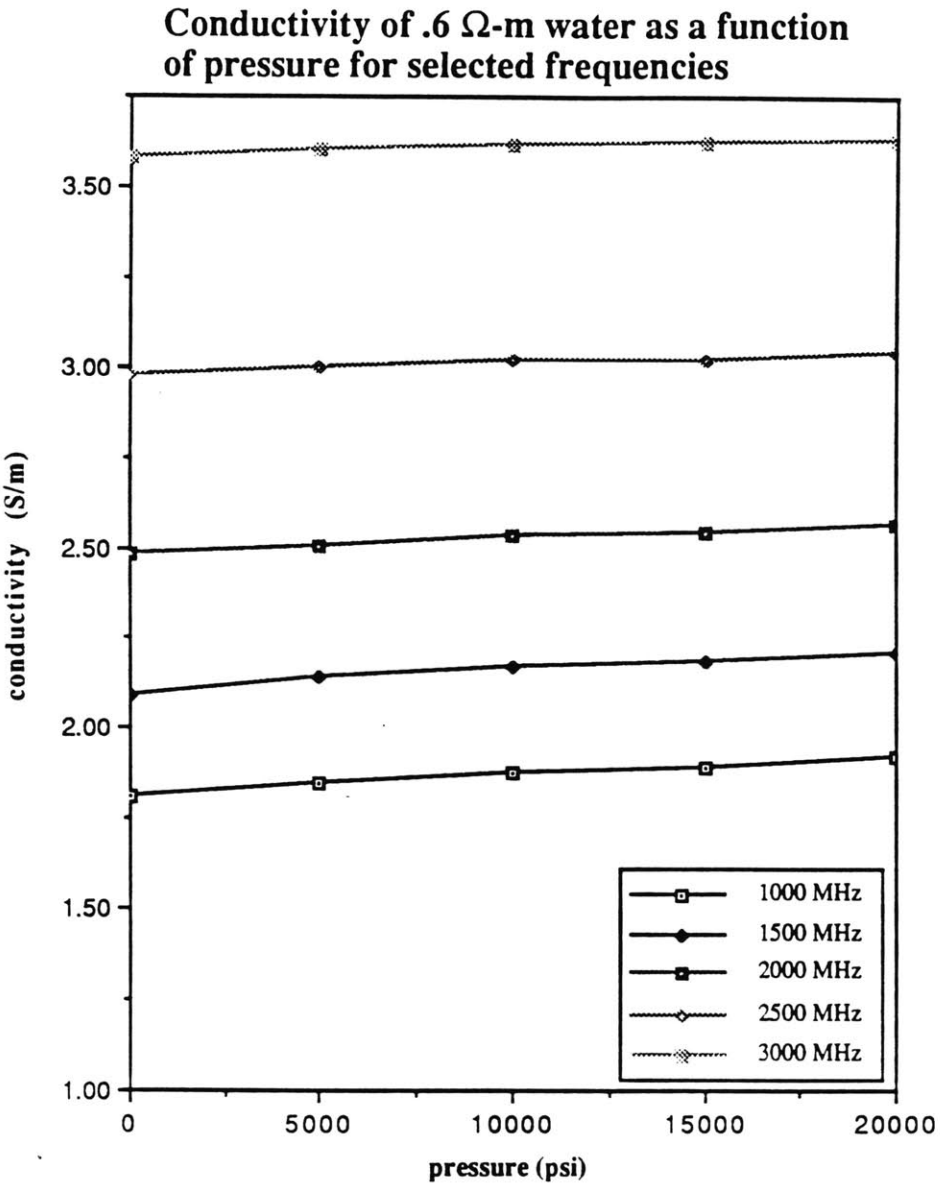

Figure 4.13: Conductivity of .6 Ω-m Water as a Function of Pressure for Selected Frequencies

It is evident from this figure that the conductivity increases as the pressure is increased. However, it is very difficult to see exactly how this increasing trend changes with frequency. One easy way to study this effect is to employ the linear curve-fitting approach used earlier. Linear curves are fitted to each of the five data sets in Figure 4.13 and the resulting curve-fitting equations at different frequencies are given in Table 4.4.

Frequency (MHz)	Curve-fitting equations
1000	σ=1.8171+5.3321e-6P
1500	σ=2.1029+4.6496e-6P
2000	σ=2.4870+3.8073e-6P
2500	σ=2.9829+2.8783e-6P
3000	σ=3.5829+2.7650e-6P

Table 4.4: Curve-Fitting Equations for Conductivity of .6 Ω-m Water as a Function of Pressure for Selected Frequencies

The pressure effect on conductivity is greatest at low frequencies. As the frequency increases, this effect diminishes. From the equations given in Table 4.4, the pressure effect on conductivity at 3 GHz is approximately 50% of that at 1 GHz.

From the water measurements, it is interesting to note the overall behavior of the conductivity under pressure is similar to what Adam and Hall observed in their DC conductivity data in 1931. They realized that the pressure effect has no significant effect on the conductivity of the solutions except in very conductive solutions.

In order to gain some understanding of the effect of pore pressure on the dielectric parameters of water-saturated rocks, we measured Berea and Massilon rocks, saturated with .1 Ω-m water, from 20 MHz to 3 GHz and at a constant temperature of 21.2°C. The dielectric constant and conductivity of Berea are plotted as a function of frequency, from 20 MHz to 3 GHz, at different pressures in Figure 4.14 and Figure 4.15 respectively.

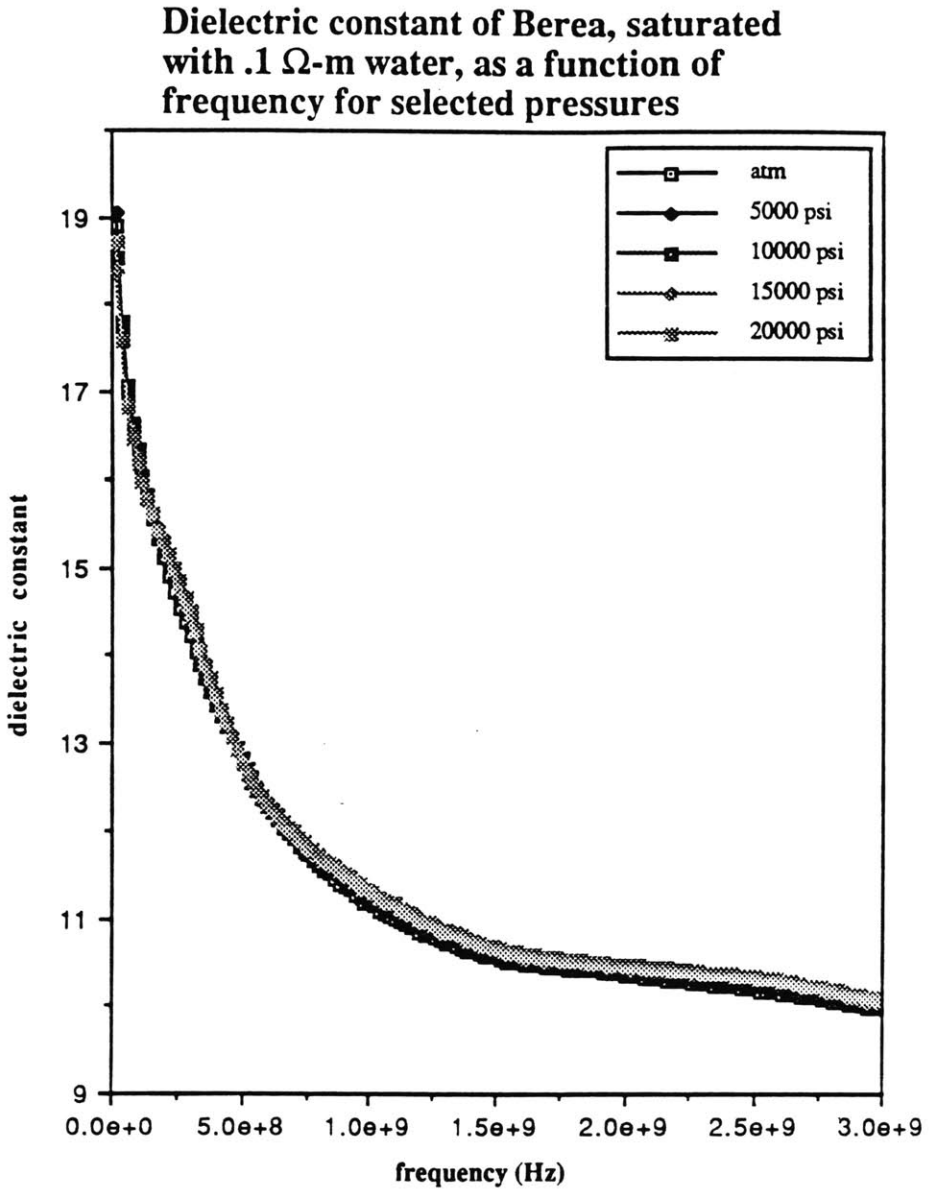

Figure 4.14: Dielectric Constant of Berea, Saturated with .1 Ω-m Water, as a Function of Frequency for Selected Pressures

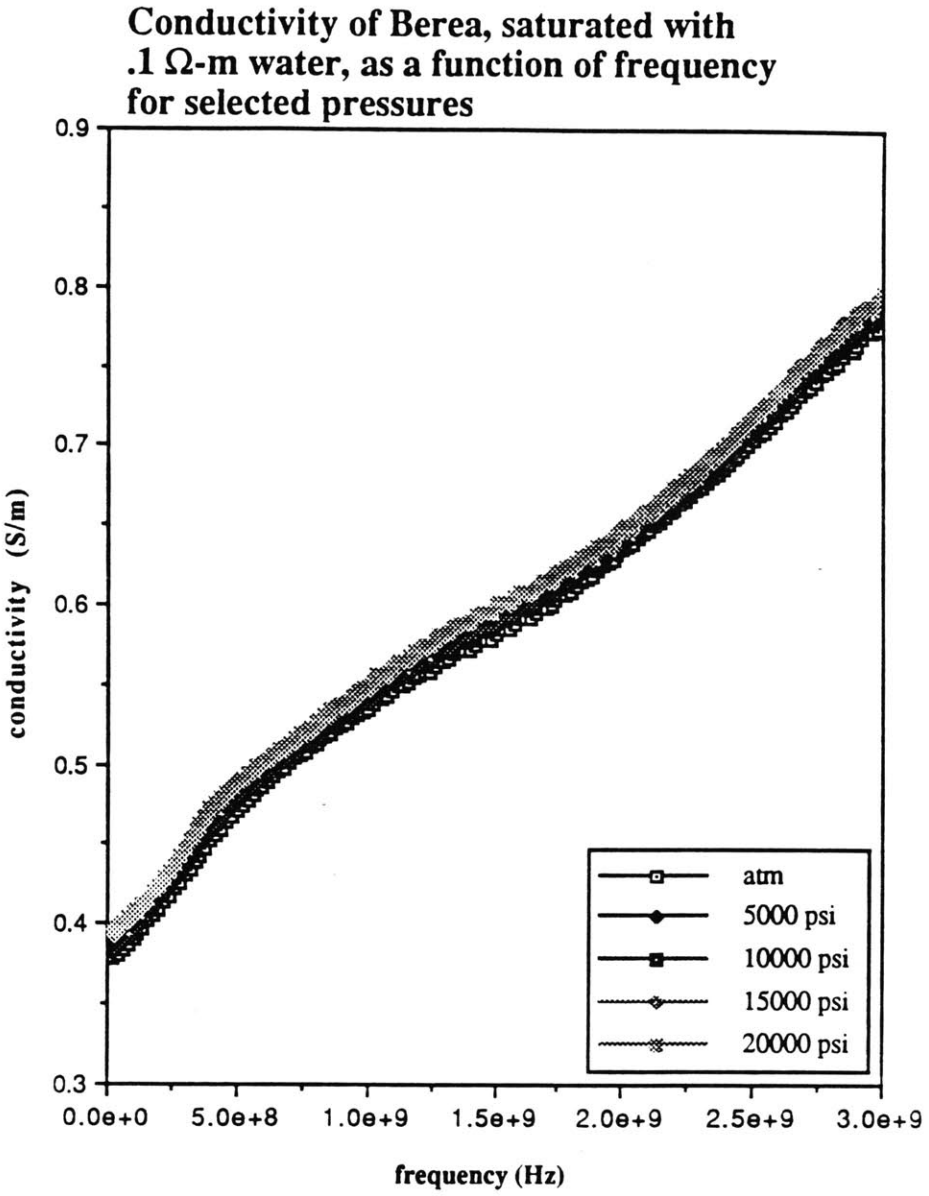

Figure 4.15: Conductivity of Berea, Saturated with .1 Ω-m Water, as a Function of Frequency

In Figure 4.14 the dielectric constant seems to increase slightly. Similarly, the conductivity in Figure 4.15 increases with pressure. In order to see the changes more clearly, the dielectric constant is plotted as a function of pressure for selected frequencies.

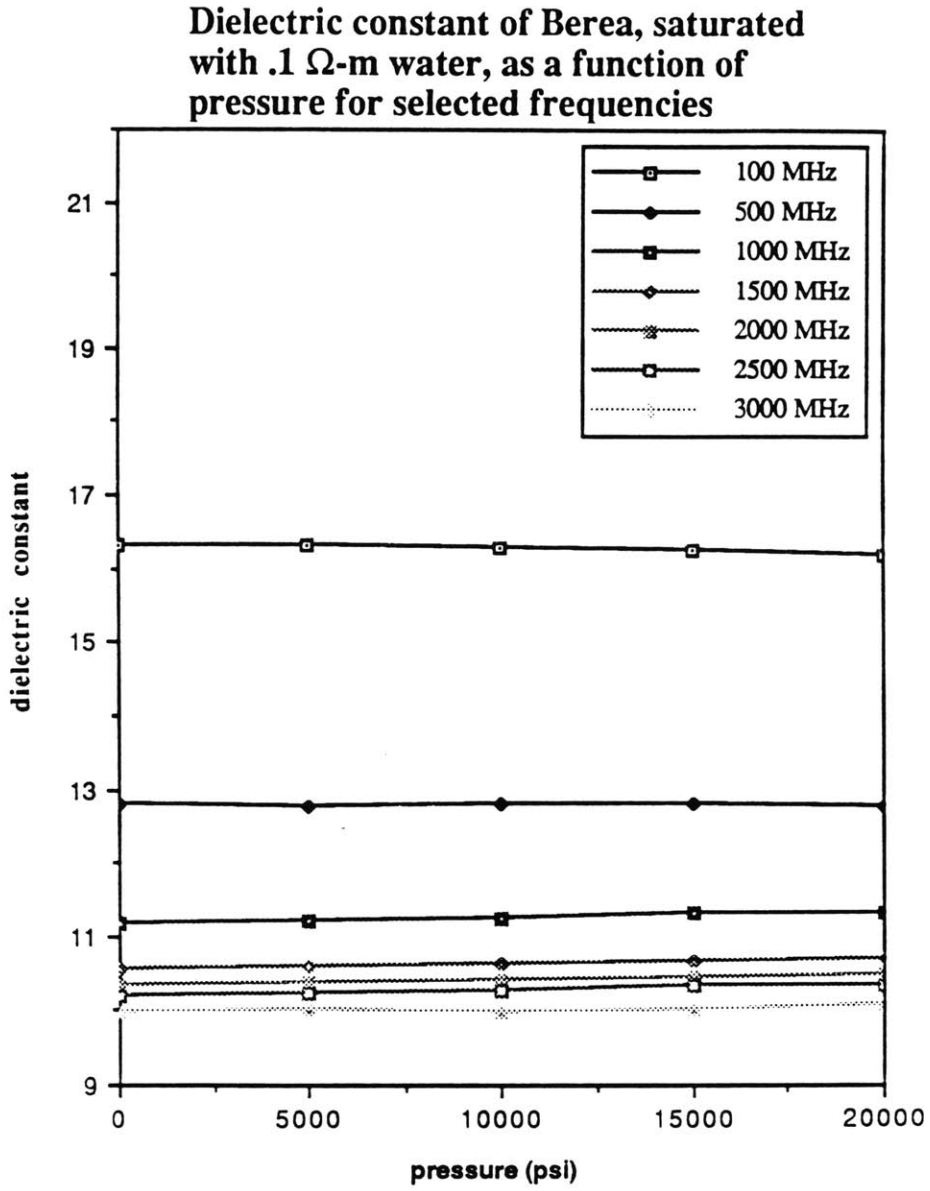

Figure 4.16: Dielectric Constant of Berea, Saturated with .1 Ω-m Water, as a Function of Pressure for Selected Frequencies

The dielectric constant seems to be independent of pressure. A closer observation reveals that the dielectric constant decreases at lower frequencies and increases at higher frequencies. However, these changes are too small and within experimental uncertainties. Therefore, it would be unwise to claim that this is indeed the behavior for this rock sample based on only this set of data. The conductivity is also plotted as a function of pressure for selected frequencies in Figure 4.17.

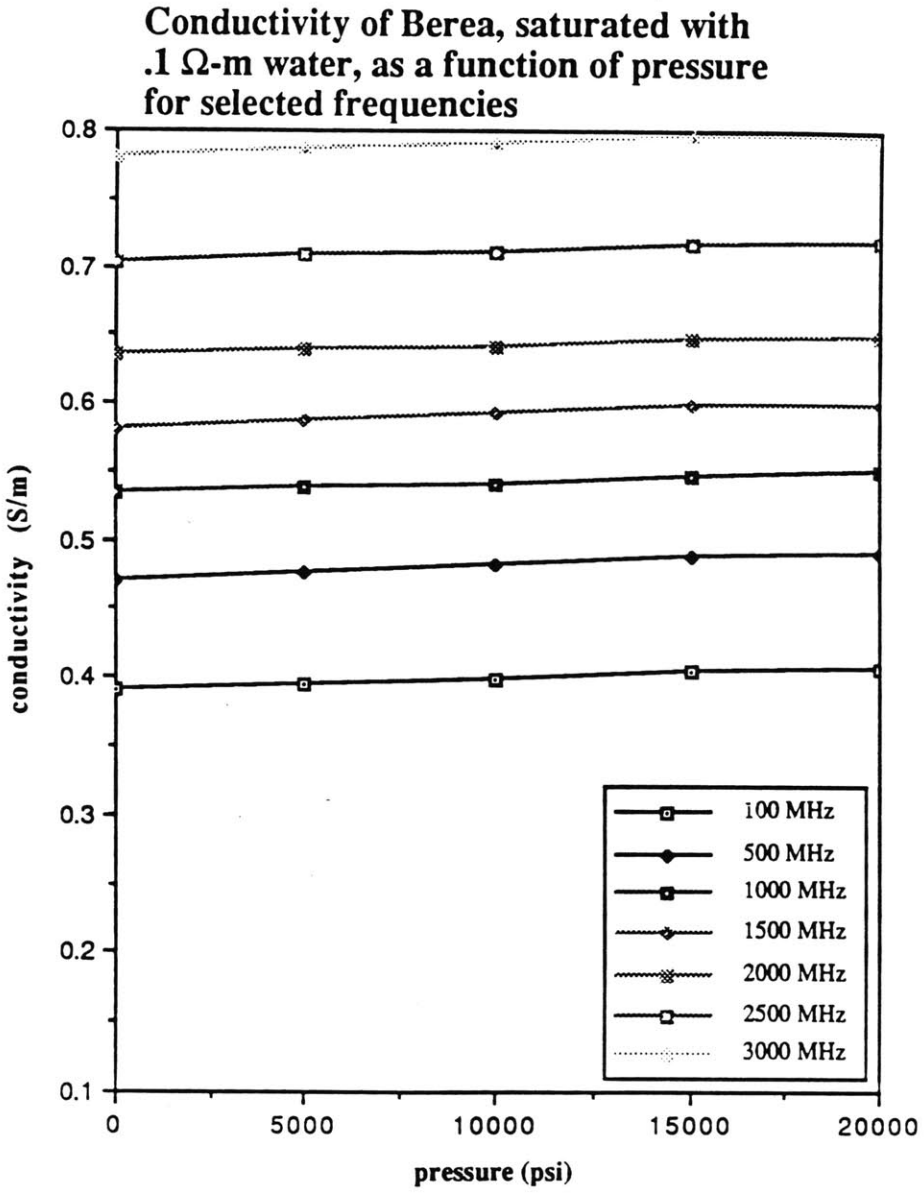

Figure 4.17: Conductivity of Berea, Saturated with .1 Ω-m Water, as a Function of Pressure for Selected Frequencies

The conductivity in Figure 4.17 exhibits a definite increasing trend as a function of pressure. This behavior is similar to that observed for .6 Ω-m water. It would be interesting to see the frequency dependence of the pressure effect on conductivity. Linear curve-fit is again employed and the resulting fitting equations at different frequencies are given in Table 4.5.

Frequency (MHz)	Curve-fitting equations
100	σ=0.39032+8.4077e-7P
500	σ=0.47127+9.7923e-7P
1000	σ=0.53459+7.2759e-7P
1500	σ=0.58228+9.3101e-7P
2000	σ=0.63485+6.8791e-7P
2500	σ=0.70404+7.7557e-7P
3000	σ=0.78161+8.3162e-7P

Table 4.5: Curve-Fitting Equations for Conductivity of Berea, Saturated with .1 Ω-m Water, as a Function of Pressure for Selected Frequencies

The apparent increasing trend of conductivity as a function of pressure is confirmed with the positive slopes in Table 4.5. However, there is no simple pattern of slope variation as the frequency varies. Based on these results, there is significant frequency dependence on the conductivity with pressure.

The last sample is this study is Massilon, saturated with .1 Ω-m water. The dielectric constant and conductivity as a function of frequency for selected pressures are shown in Figure 4.18 and 4.19 respectively.

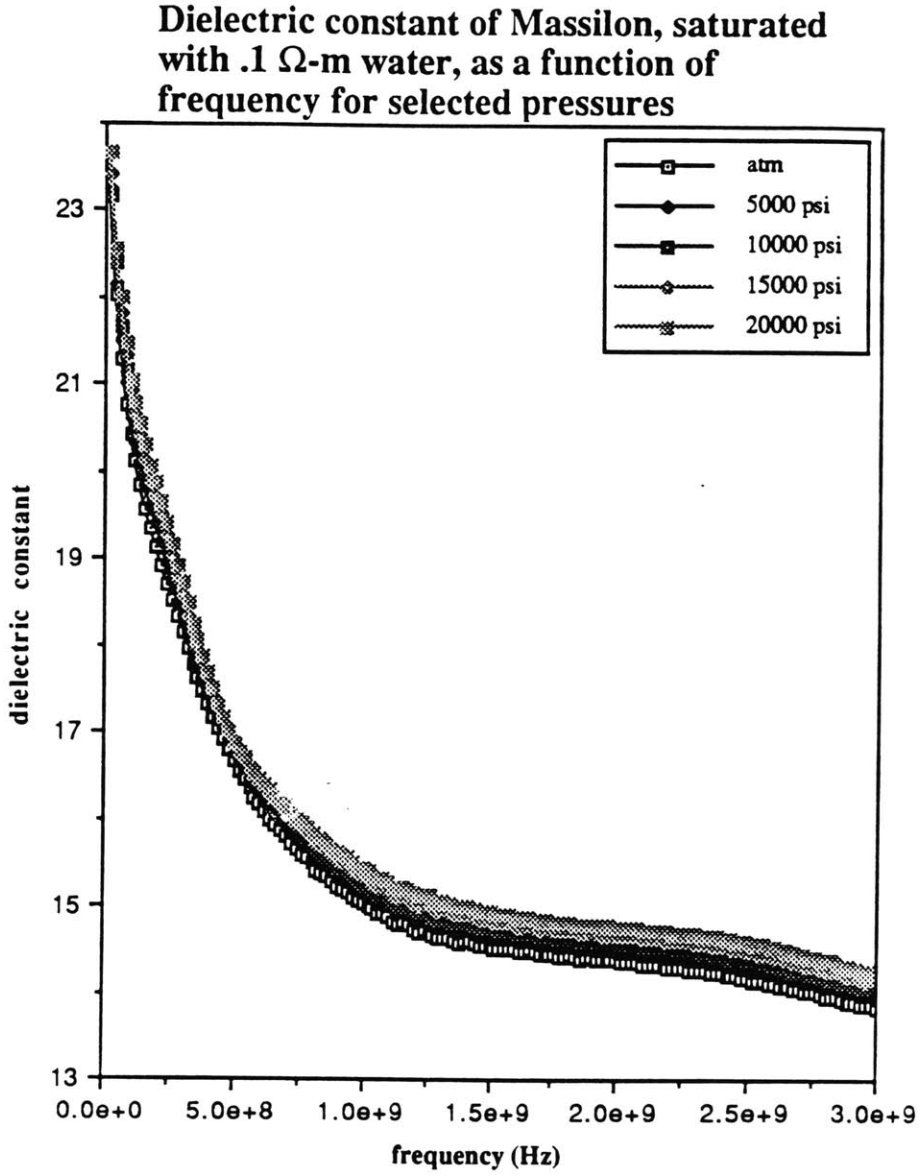

Figure 4.18: Dielectric Constant of Massilon, Saturated with .1 Ω-m Water, as a Function of Frequency for Selected Pressures

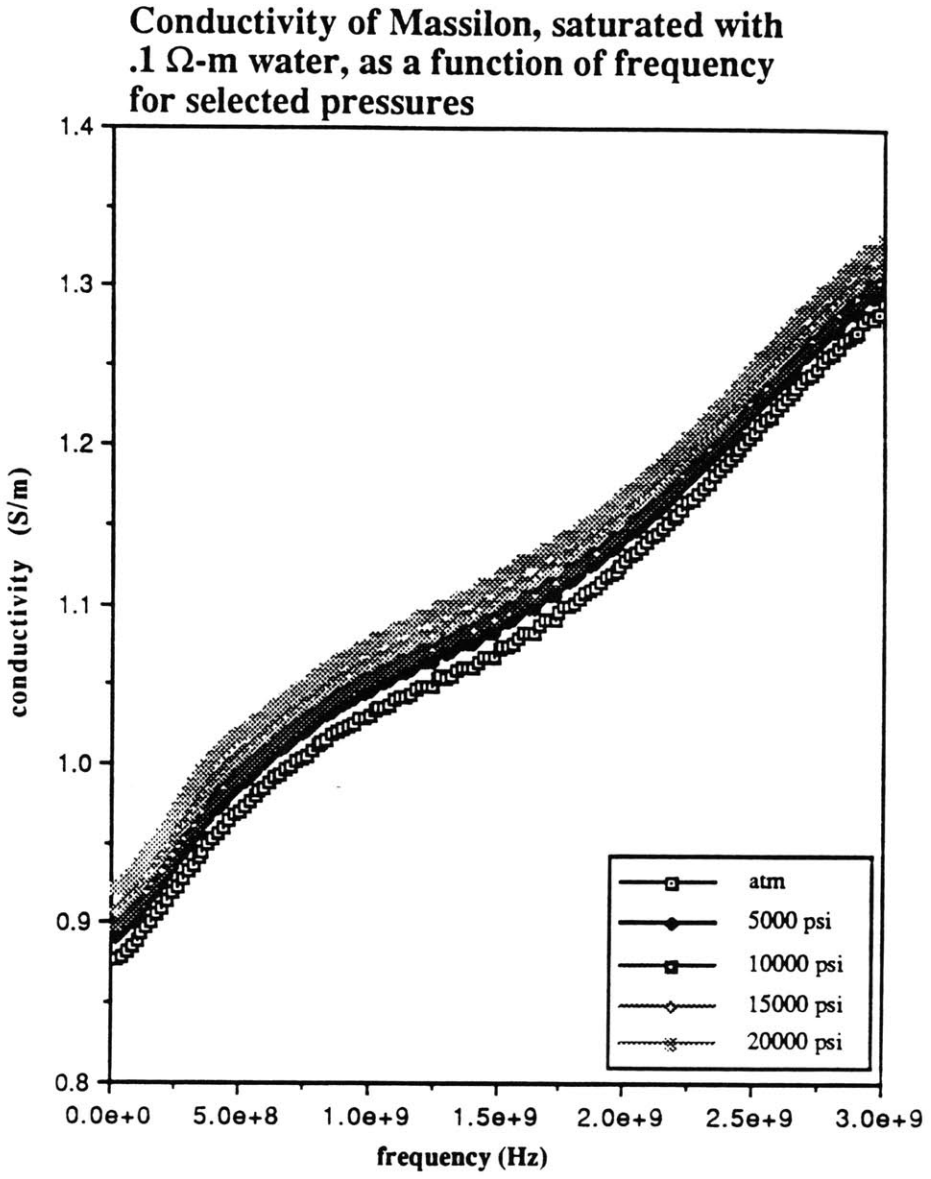

Figure 4.19: Conductivity of Massilon, Saturated with .1 Ω-m Water, as a Function of Frequency for Selected Pressures

Again we will look at the dielectric constant as a function of pressure for selected frequencies. It is plotted in Figure 4.20.

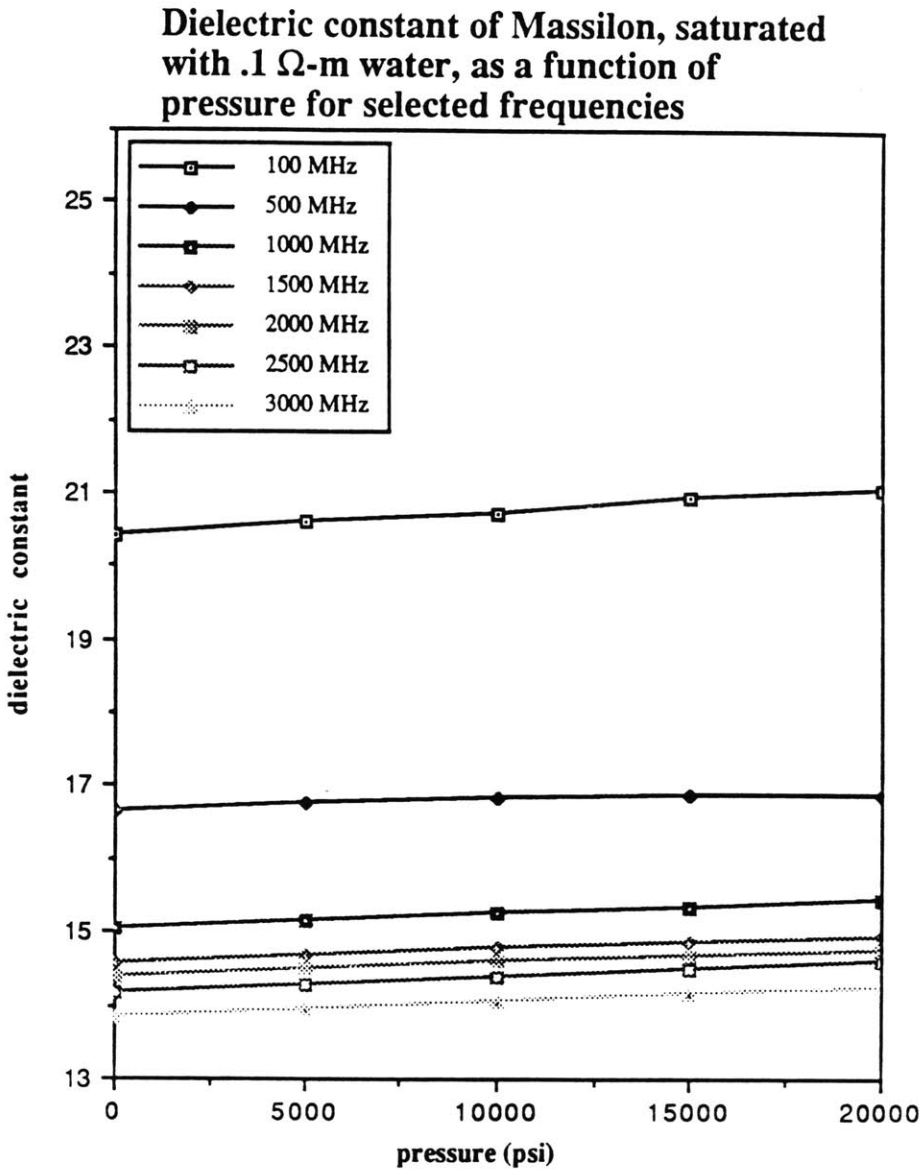

Figure 4.20: Dielectric Constant of Massilon, Saturated with .1 Ω-m Water, as a Function of Pressure for Selected Frequencies

The data shows an increasing trend for dielectric constant as a function of pressure. Linear curve-fitting scheme is applied to the data at 7 different frequencies. The parameters of the resulting curves are given in Table 4.6.

Frequency (MHz)	Curve-fitting equations
100	ε=20.422+3.1757e-5P
500	ε=16.690+1.0715e-5P
1000	ε=15.057+1.9171e-5P
1500	ε=14.570+1.9539e-5P
2000	ε=14.386+1.9485e-5P
2500	ε=14.181+2.0785e-5P
3000	ε=13.858+1.9609e-5P

Table 4.6: Curve-Fitting Equations for Dielectric Constant of Massilon, Saturated with .1 Ω-m Water, as a Function of Pressure for Selected Frequencies

The positive slopes confirms that the dielectric constant does indeed increase as the pressure is increased. However, the slopes as a function of frequency exhibits no clear trend. This means that the frequency dependence of the pressure effect on dielectric constant is within experimental errors. The conductivity as a function of pressures is plotted in Figure 4.21 for selected frequencies.

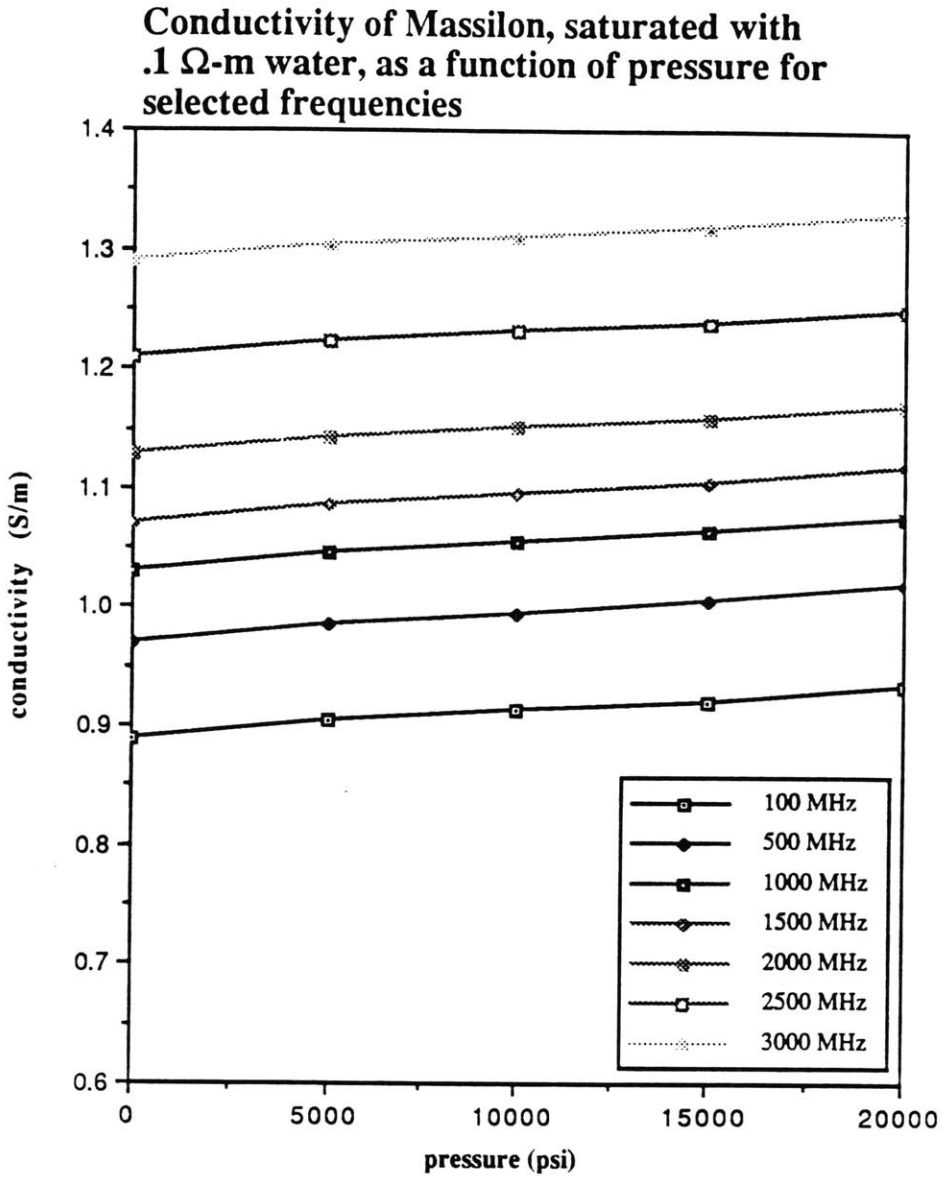

Figure 4.21: Conductivity of Massilon, Saturated with .1 Ω-m Water, as a Function of Pressure for Selected Frequencies

The conductivity also shows an increasing trend as a function of pressure. This behavior is similar to that of both the .6 Ω-m water and Berea. Linear curve-fitting the data for selected frequencies gives the slope of the conductivity as a function of pressure. The slopes are given in Table 4.7.

Frequency (MHz)	Curve-fitting equations
100	σ=0.89129+2.0924e-6P
500	σ=0.97203+2.3091e-6P
1000	σ=1.0327+2.0877e-6P
1500	σ=1.0735+2.1617e-6P
2000	σ=1.1307+1.9523e-6P
2500	σ=1.2110+1.9685e-6P
3000	σ=1.2915+1.9470e-6P

Table 4.7: Curve-Fitting Equations for Conductivity of Massilon, Saturated with .1 Ω-m Water, as a Function of Pressure for Selected Frequencies

The slopes do not indicate any definite pattern. It seems that for both Berea and Massilon, the pressure effect on conductivity is not a function of frequency. It should be noted that the porosity for Berea 423 is 19% and that for Massilon is 24.6%. From the data in Table 4.5 and Table 4.7, it is obvious that the pressure effect on conductivity is more significant for Massilon than for Berea. There are two possible expanations. Since Massilon is more porous than Berea, there is a greater number of ions entering Massilon when pressurized. Another explanation is that Massilon is "softer" than Berea, therefore more susceptible to pressure.

Chapter 5

SUMMARY

A two-port coaxial cell is designed and manufactured to make scattering parameter measurement of fluids and fluid-saturated rocks at high pressures of up to 20,000 psi. It is essentially a coaxial line, filled with sections of different dielectric materials. When assembled, the cell has neither discontinuities nor abrupt jump in both inner and outer conductors. Inversion models were developed to retrieve the dielectric information from the measured scattering parameters.

Two water solutions and two rock samples were examined in this study. This study concerned with the effect of pressure on the high frequency dielectric constant and conductivity of the samples. The extrapolated DC dielectric constant of the pure water at 21.2°C displayed a pattern similar to that at 10°C, 25°C, and 40°C reported in literature by Srinivasan and Kay. The overall behavior of the conductivity of pure water and .6 Ω-m water under pressure is similar to what Adam and Hall observed in their conductivity data.

Our results on the high frequency, high pressure complex dielectric constant of rocks are the first in literature. In these measurements, the pore pressure was varied.

In order to gain a complete understanding of the pressure effect on the dielectric parameters of rocks, it would be interesting to make similar measurements, varying the confining pressure. This requires a new design for the dielectric cell.

Chapter 6

APPENDICES

A.1 Measurement Setup

In order to make an accurate measurement, the pressurizing unit must be set up correctly. The oil section needs to be filled up with a 200 cs. viscosity oil from Dow Corning only once. The fluid section needs to be filled up with the fluid under study. That means filling up with a different fluid in the fluid section each time the fluid of interest changes. The procedures to filling up both the oil and fluid sections are given in the following steps. (Please refer to Figure 3.1.3.1 for specific notations)

Filling the oil section: (To be done only once)

1. Shut V1 to isolate the oil section from the oil reservoir.
2. Crank the PP handle up to the highest position.
3. Open V2.
4. Open V3.
5. Push piston to the bottom of the accumulator.
6. Open V4 and operate VP1.
7. Shut V3 to isolate the pressure gauge from the rest of the system, when the vacuum meter reads a vacuum of 10μm in the oil section.
8. Shut V4 and stop VP1, when the vacuum meter reads a vaccuum of 2μm.
9. Open V1 to allow the inflow of oil from the oil reservoir.

10. After the oil section has been filled with oil, open V3 to allow additional oil into the PG1.
11. Shut V1 to again isolate the oil section from the oil reservoir.

Filling the fluid section: (To be done everytime the measuring fluid changes)

1. Dry the sample compartment of the high-pressure cell.
2. Put the seals in place and install the high-pressure cell in the system.
3. Shut V5 to isolate the fluid section from the fluid reservoir.
4. Open V7.
5. Open V8.
6. Open V6 and operate VP2.
7. Shut V8 to isolate the pressure gauge from the rest of the system, when the vacuum meter reads a vacuum of 10μm in the fluid section.
8. Shut V6 and stop VP2, when the vacuum meter reads a vacuum of 2μm.
9. Open V6 to allow the inflow of fluid from the fluid reservoir.
10. After the fluid section has been filled with fluid, open V8 to allow additional fluid into PG2.
11. Shut V5 to again isolate the fluid section from the fluid reservoir.

In the case of measuring fluid, the above setup procedure is sufficient. In the case of measuring fluid-saturated rock, additional steps are necessary and are listed below.

12. Remove the top seal from the high-pressure cell.
13. Open V5.
14. Using a fluid pump, pump fluid into the fluid section until fluid overflows the high-pressure cell.
15. Submerge the fluid-saturated sample in the fluid and push it into the sample chamber.
16. Stop the stop pump.
17. With V5 still open, put the top seal back into place.
18. Shut V5.

The pressure pump has a volumn of 11 cc. This small volumn of oil is insufficient to pressurize the entire system to 20,000 psi. The following procedure was devised to enable us to pump more oil into the system, thereby generating pressures of up to 20,000 psi.

1. With the entire system in order, crank the PP all the way down.
2. Shut V2 to maintain the pressure in the accumulator.
3. Crank the PP all the way up to create a partial vacuum in the pressure pump.
4. Open V1 to allow inflow of oil into the pressure pump.
5. Shut V1 after the pressure pump is filled.
6. Crank PP partially downward to minimize the differential pressure across V2.
7. Open V2 to allow more oil into the accumulator by cranking the PP.
8. Repeat 1 if necessary.

B.1 Clamping Force versus Thread Friction Coefficient

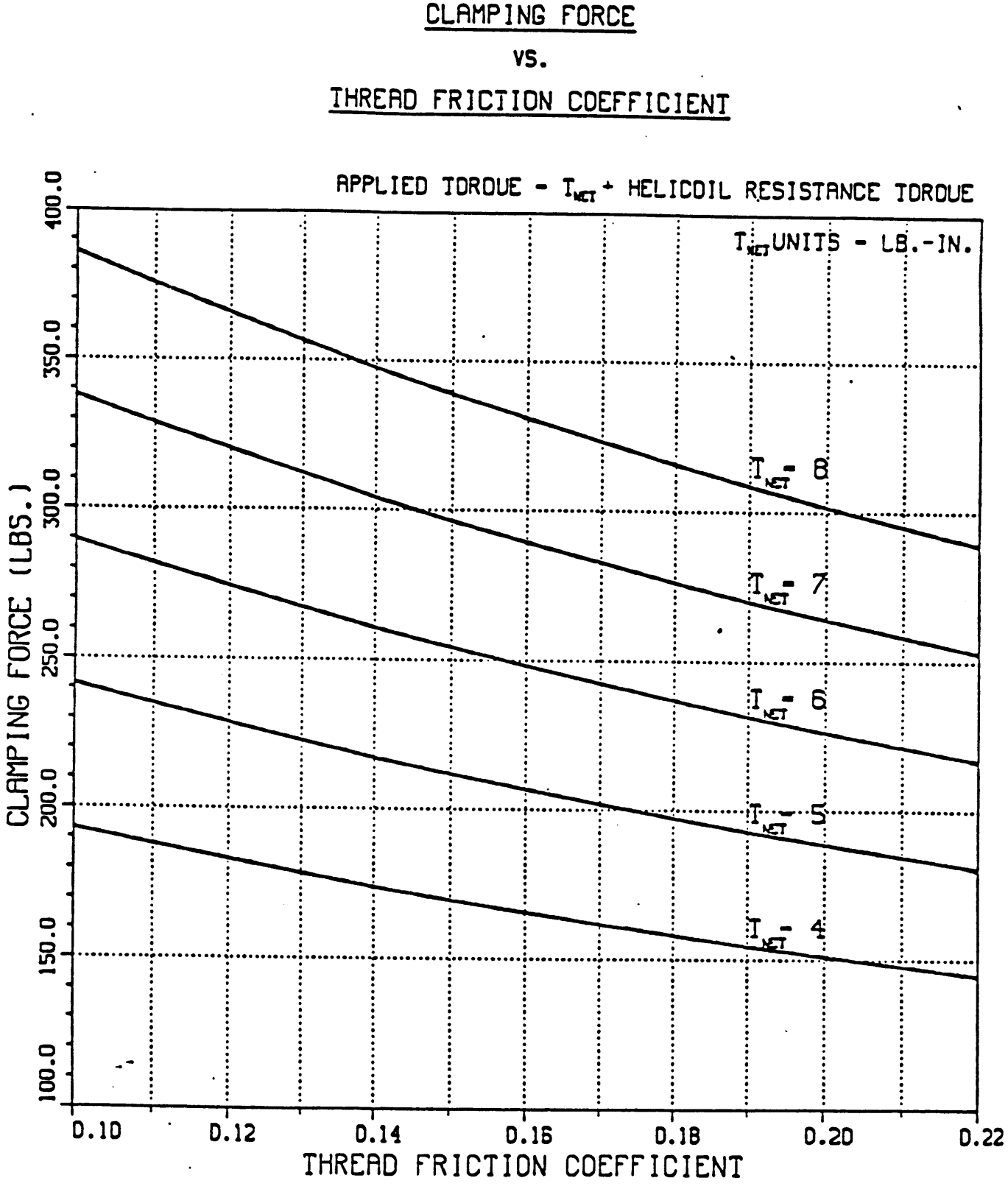

CLAMPING FORCE
VS.
THREAD FRICTION COEFFICIENT

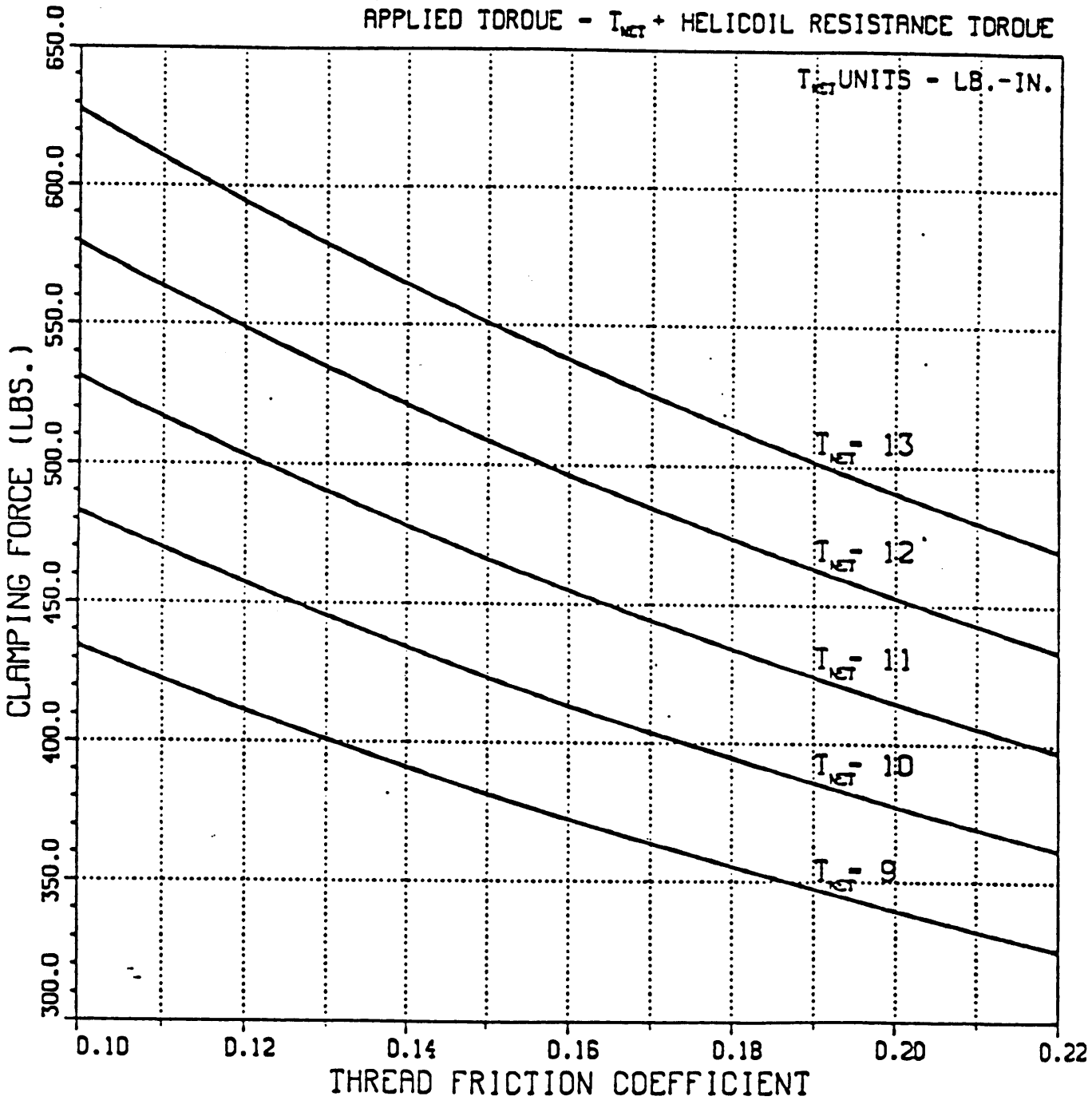

C.1 Acquisition Code

The following code is written in Microsoft BASIC and stored on the Macintosh computer. It automates the data acquisition process on the HP8753A/85046A. The code enables the user to perform a variety of functions, such as calibrating the network analyzer with standard terminations, measuring scattering parameters, saving raw data to an external memory device, retrieving data from an external memory device, printing data on a line printer, and plotting data in various graphic forms.

```
REM       Title: Data_Acquisition_version_2.
REM       This code (Data_Acquisition_version_2) is developed to make S-parameter
REM       measurement with either the coaxial-circular or the coaxial cell on the
REM       HP8753A network analyzer and 85046A S-parameter test set.
REM       Done in June 1989 by David Yuen.
    OPTION BASE 1
    CLEAR, 200000!
    DIM   freq(1000),PHAS11(1000),LMAGS11(1000),PHAS12(1000)
    DIM   LMAGS12(1000),PHAS21(1000),LMAGS21(1000),PHAS22(1000)
    DIM   LMAGS22(1000),PPHAS11(1000),PLMAGS11(1000)
    DIM   PPHAS12(1000),PLMAGS12(1000),PPHAS21(1000)
    DIM   PLMAGS21(1000),PPHAS22(1000),PLMAGS22(1000)
    DIM   EX(4,151),EY(4,151),SX(4,151),SY(4,151),S(12,151)
    PI=3.14159265358979#
    F1 = 20
    F2 = 3000
    BAND = 10
    DELTAF = 20
    prog$="Data_Acquisition_version_2"
    savflag=1
    PRINT"Type in the necessary information or press return for the default values:"
    PRINT"DEFAULTS:";TAB(15);"Starting-freq = ";F1;"MHz"
    PRINT TAB(15);"Ending-freq = ";F2;"MHz"
    PRINT TAB(15);"IF-bandwidth = ";BAND;"Hz"
    PRINT TAB(15);"Delta-freq = ";DELTAF;"MHz"
    PRINT"Enter the starting frequency in MHz: "
    INPUT ANS1$
    IF LEN(ANS1$) =0 THEN PRINT F1 ELSE F1=VAL(ANS1$):
    PRINT"Enter the stopping frequency in MHz: "
    INPUT ANS2$
    IF LEN(ANS2$) =0 THEN PRINT F2 ELSE F2=VAL(ANS2$)
    PRINT"Enter the If-bandwidth in Hz: "
    PRINT"Note that the range is 10,30,100,300,1000,and 3000Hz."
```

```
      INPUT ANS3$
      IF LEN(ANS3$) =0 THEN PRINT BAND ELSE BAND=VAL(ANS3$)
      PRINT"Enter the frequency increment in MHz: "
      INPUT ANS4$
      IF LEN(ANS4$)=0 THEN PRINT DELTAF ELSE
      DELTAF=VAL(ANS4$)
      npt=INT((F2-F1)/DELTAF)+1
      PRINT"The number of data point is "npt

      MENU 6,0,1,"Commands"
      MENU 6,1,1,"Calibration"
      MENU 6,2,1,"Measurement"
      MENU 6,3,1,"Save data"
      MENU 6,4,1,"Read data from disk"
      MENU 6,5,1,"Print data"
      MENU 6,6,1,"Plot data"
      MENU ON

100   CALL TEXTFACE(8)
      PRINT ""
      PRINT "Select a Command"
      CALL TEXTFACE(0)
      WHILE MENU(0)<>6
      WEND
      ON MENU(1) GOSUB
      calibration,measurement,savdata,readdata,prindata,plotdata
      GOTO 100

calibration:

      LIBRARY "MacDriver488"
      CALFLG=1
      RST
      WR"RESET"
      WR"EOL IN NONE"
      WR"HELLO"
      A$=""
      RD A$
      PRINT A$
      WR"REMOTE 16;"
      WR"OUTPUT 16;PRES;"
      WR"OUTPUT 16;HOLD;"
      F1$=STR$(F1)
      F2$=STR$(F2)
      BAND$=STR$(BAND)
      DELTAF$=STR$(DELTAF)
      UNIT1$="MHz"
      UNIT2$="Hz"
      WR"OUTPUT 16;EDITLIST;"
      WR"OUTPUT 16;SADD;"
      WR"OUTPUT 16;STAR";F1$;UNIT1$;CHR$(59)
      WR"OUTPUT 16;STOP";F2$;UNIT1$;CHR$(59)
      WR"OUTPUT 16;STPSIZE",DELTAF$;UNIT1$;CHR$(59)
      WR"OUTPUT 16;SDON;"
```

```
        WR"OUTPUT 16;EDITDONE;"
        WR"OUTPUT 16;LISFREQ;"
        WR"OUTPUT 16;SING;"
        WR"OUTPUT 16;IFBW";BAND$;UNIT2$;CHR$(59)
        WR"OUTPUT 16;CALIFUL2;"
        WR"OUTPUT 16;REFL;"
        INPUT"Please connect an open to port 1.",DUMMY$
        PRINT"Calibration in progress."
        WR"OUTPUT 16;CLASS11A;"
        WR"OUTPUT 16;AUTO;"
        INPUT"Please connect a short to port 1.",DUMMY$
        PRINT"Calibration in progress."
        WR"OUTPUT 16;CLASS11B;"
        WR"OUTPUT 16;AUTO;"
        INPUT"Please connect a load to port 1.",DUMMY$
        PRINT"Calibration in progress."
        WR"OUTPUT 16;CLASS11C;"
        WR"OUTPUT 16;AUTO;"
        INPUT"Please connect an open to port 2.",DUMMY$
        PRINT"Calibration in progress."
        WR"OUTPUT 16;CLASS22A;"
        WR"OUTPUT 16;AUTO;"
        INPUT"Please connect a short to port 2.",DUMMY$
        PRINT"Calibration in progress."
        WR"OUTPUT 16;CLASS22B;"
        WR"OUTPUT 16;AUTO;"
        INPUT"Please connect a load to port 2.",DUMMY$
        PRINT"Calibration in progress."
        WR"OUTPUT 16;CLASS22C;"
        WR"OUTPUT 16;AUTO;"
        WR"OUTPUT 16;REFD;"
        WR"OUTPUT 16;TRAN;"
        INPUT"Please connect the two ports together",DUMMY$
        PRINT"Calibration in progress."
        WR"OUTPUT 16;FWDT;"
        WR"OUTPUT 16;REVT;"
        WR"OUTPUT 16;FWDM;"
        WR"OUTPUT 16;REVM;"
        WR"OUTPUT 16;TRAD;"
        WR"OUTPUT 16;ISOL;"
        WR"OUTPUT 16;OMII;"
        WR"OUTPUT 16;ISOD;"
        WR"OUTPUT 16;SAV2;"
        FOR i=1 TO 50000!
        NEXT i
        PRINT"Calibration finished."
        RETURN

measurement:

                                                                IF savflag

        PRINT b$
        IF b$="R" OR b$="r" THEN RETURN
        b$="d"
```

```
      TDEGC = 21.2
      RW = .25
      MAT$="water"
      PRINT "Type in the necessary information or press return for the default values:"
      PRINT "DEFAULTS:";TAB(15);"Temperature-C = ";TDEGC;"
      PRINT TAB(15);"Resistivity-W = ";RW;"
      PRINT TAB(15);"Material = ";MAT$;"
      INPUT"Enter the temperature in degree Celsius: ",ANS5$
      IF LEN(ANS5$) =0 THEN PRINT TDEGC ELSE   TDEGC=VAL(ANS5$)
      INPUT"Enter the water resistivity: ",ANS6$
      IF LEN(ANS6$) =0 THEN PRINT RW ELSE RW=VAL(ANS6$)
      INPUT "Enter the type of material: ",ANS7$
      IF LEN(ANS7$) =0 THEN PRINT MAT$ ELSE MAT$ = ANS7$
      savflag=0
      TODAY$=DATE$
      MTIME$=TIME$
      WR"RESET"
      WR"OUTPUT 16;FORM4;"
      INPUT"Please connect the cell to the two ports.",DUMMY$
REM         Calculating the phase for S11
      PRINT"Measurement for S11(phase) in progress."
      WR"OUTPUT 16;S11;"
      WR"OUTPUT 16;CHAN2;S11;PHAS;"
      WR"OUTPUT 16;SING;"
      WR"OUTPUT 16;AUTO;"
      WR"OUTPUT 16;OUTPFORM;"
      FOR i= 1 TO npt
      WR"ENTER 16 #50"
      RD DAT$
      PHAS11(i)=VAL(MID$(DAT$,1,25))
      NEXT i
REM         Calculating the magnitude for S11
      PRINT"Measurement for S11(magnitude) in progress."
      WR"OUTPUT 16;CHAN2;S11;LOGM;"
      WR"OUTPUT 16;AUTO;"
      WR"OUTPUT 16;OUTPFORM;"
      FOR i= 1 TO npt
      WR"ENTER 16 #50"
      RD DAT$
      LMAGS11(i)=VAL(MID$(DAT$,1,25))
      NEXT i
REM         Calculating the phase for S12
      PRINT"Measurement for S12(phase) in progress."
      WR"OUTPUT 16;S12;"
      WR"OUTPUT 16;CHAN2;S12;PHAS;"
      WR"OUTPUT 16;AUTO;"
      WR"OUTPUT 16;OUTPFORM;"
      FOR i= 1 TO npt
      WR"ENTER 16 #50"
      RD DAT$
      PHAS12(i)=VAL(MID$(DAT$,1,25))
      NEXT i
REM         Calculating the magnitude for S12
      PRINT"Measurement for S12(magnitude) in progress."
```

```
      WR"OUTPUT 16;CHAN2;S12;LOGM;"
      WR"OUTPUT 16;AUTO;"
      WR"OUTPUT 16;OUTPFORM;"
      FOR i= 1 TO npt
      WR"ENTER 16 #50"
      RD DAT$
      LMAGS12(i)=VAL(MID$(DAT$,1,25))
      NEXT i
REM         Calculating the phase for S21
      PRINT"Measurement for S21(phase) in progress."
      WR "OUTPUT 16;S21;"
      WR "OUTPUT 16;CHAN2;PHAS;"
      WR "OUTPUT 16;AUTO;"
      WR "OUTPUT 16;OUTPFORM;"
      FOR i= 1 TO npt
      WR"ENTER 16 #50"
      RD DAT$
      PHAS21(i)=VAL(MID$(DAT$,1,25))
      NEXT i
REM         Calculating the magnitude for S21
      PRINT"Measurement for S21(magnitude) in progress."
      WR"OUTPUT 16;CHAN2;S21;LOGM;"
      WR"OUTPUT 16;AUTO;"
      WR"OUTPUT 16;OUTPFORM;"
      FOR i= 1 TO npt
      WR"ENTER 16 #50"
      RD DAT$
      LMAGS21(i)=VAL(MID$(DAT$,1,25))
      NEXT i
REM         Calculating the phase for S22
      PRINT"Measurement for S22(phase) in progress."
      WR"OUTPUT 16;S22;"
      WR"OUTPUT 16;CHAN2;S22;PHAS;"
      WR"OUTPUT 16;AUTO;"
      WR"OUTPUT 16;OUTPFORM;"
      FOR i= 1 TO npt
      WR"ENTER 16 #50"
      RD DAT$
      PHAS22(i)=VAL(MID$(DAT$,1,25))
      NEXT i
REM         Calculating the magnitude for S22
      PRINT"Measurement for S22(magnitude) in progress."
      WR"OUTPUT 16;CHAN2;S22;LOGM;"
      WR"OUTPUT 16;AUTO;"
      WR"OUTPUT 16;OUTPFORM;"
      FOR i= 1 TO npt
      WR"ENTER 16 #50"
      RD DAT$
      LMAGS22(i)=VAL(MID$(DAT$,1,25))
      NEXT i
      fr=F1
      FOR i=1 TO npt
      freq(i)=fr
      fr=fr+DELTAF
```

```
        NEXT i
        PRINT "Measurement finished."
        RETURN

savdata:

        nameout$=FILES$(0,"Enter filename to save raw data")
        comment1$="NONE"
        comment2$="NONE"
        fr=F1
        FOR i=1 TO npt
        freq(i)=fr
        fr=fr+DELTAF
        NEXT i
        PRINT "Please enter the first line of comment :"
        INPUT com1$
        IF LEN(com1$)=0 THEN PRINT comment1$ ELSE comment1$=com1$
        PRINT "Now enter the second line of comment :"
        INPUT com2$
        IF LEN(com2$)=0 THEN PRINT comment2$ ELSE comment2$=com2$
        OPEN nameout$ FOR OUTPUT AS #2
        PRINT "Raw data saving in progress."
        PRINT #2,""
        PRINT #2,TAB(28);"Date:      ";TODAY$;"    Time:       ";MTIME$
        PRINT #2,""
        PRINT #2,TAB(5);"FILENAME                ";nameout$
        PRINT #2,TAB(5);"ACQUISITION CODE    ";prog$
        PRINT #2,""
        PRINT #2,TAB(5);"Number of points per measurement is ";npt
        PRINT #2,TAB(5);"The material used is ";MAT$
        PRINT #2,TAB(5);"The temperature in Celsius is ";TDEGC
        PRINT #2,TAB(5);"The water resistivity is ";RW
        PRINT #2,""
        PRINT #2,TAB(5);"COMMENT:"
        PRINT #2,TAB(5);comment1$
        PRINT #2,TAB(5);comment2$
        PRINT #2,""
        PRINT #2,""
        PRINT #2,TAB(5);"For S11"
        PRINT #2,TAB(5);"Frequency(i) , Phase(i) , Magnitude(i)"
        PRINT #2,""
        FOR i=1 TO npt
        PRINT #2,TAB(5);freq(i);" , ";PHAS11(i);" , ";LMAGS11(i)
        NEXT i
        PRINT #2,""
        PRINT #2,TAB(5);"For S12    "
        PRINT #2,TAB(5);"Frequency(i) , Phase(i) , Magnitude(i)"
        PRINT #2,""
        FOR i=1 TO npt
        PRINT #2,TAB(5);freq(i);" , ";PHAS12(i);" , ";LMAGS12(i)
        NEXT i
        PRINT #2,""
        PRINT #2,TAB(5);"For  S21    "
        PRINT #2,TAB(5);"Frequency(i) , Phase(i) , Magnitude(i)"
```

```
        PRINT #2,""
        FOR i=1 TO npt
        PRINT #2,TAB(5);freq(i);" , ";PHAS21(i);" , ";LMAGS21(i)
        NEXT i
        PRINT #2,""
        PRINT #2,TAB(5);"For S22     "
        PRINT #2,TAB(5);"Frequency(i) , Phase(i) , Magnitude(i)"
        PRINT #2,""
        FOR i=1 TO npt
        PRINT #2,TAB(5);freq(i);" , ";PHAS22(i);" , ";LMAGS22(i)
        NEXT i
        PRINT #2,""
        savflag=1
        CLOSE #2
        PRINT "Data saving finished."
        RETURN

readdata:

        namein$=FILES$(1,"TEXT")
        OPEN namein$ FOR INPUT AS #2
        nameout$=namein$
        INPUT #2,L$
        PRINT L$
        INPUT #2,L$
        PRINT L$
        TODAY$=MID$(L$,14,10)
        MTIME$=MID$(L$,45,8)
        INPUT #2,L$
        PRINT L$
        INPUT #2,L$
        PRINT L$
        INPUT #2,L$
        PRINT L$
        prog$=MID$(L$,23,23)
        INPUT #2,L$
        PRINT L$
        INPUT #2,L$
        PRINT L$
        npt=VAL(MID$(L$,37))
        INPUT #2,L$
        PRINT L$
        MAT$=MID$(L$,21)
        INPUT #2,L$
        PRINT L$
        TGDEC=VAL(MID$(L$,30))
        INPUT #2,L$
        PRINT L$
        RW=VAL(MID$(L$,25))
        INPUT #2,L$
        PRINT L$
        INPUT #2,L$
        PRINT L$
        INPUT #2,L$
```

```
      PRINT L$
      comment1$=L$
      INPUT #2,L$
      PRINT L$
      comment2$=L$
      INPUT"Type R(return) for more:",R$
      INPUT #2,L$
      PRINT L$
      INPUT #2,L$
      PRINT L$
      IF R$="R" OR R$="r" THEN GOTO 10
10    INPUT #2,L$
      PRINT L$
      INPUT #2,h$,L$,k$
      PRINT h$,L$,k$
      INPUT #2,L$
      PRINT L$
      FOR i=1 TO npt
      INPUT #2,h$,L$,k$
      freq(i)=VAL(MID$(h$,1))
      PHAS11(i)=VAL(MID$(L$,1))
      LMAGS11(i)=VAL(MID$(k$,1))
      PRINT freq(i),PHAS11(i),LMAGS11(i)
      NEXT i
      INPUT #2,L$
      PRINT L$
      INPUT"Type R(return) for more:",R$
      IF R$="R" OR R$="r" THEN GOTO 11
11    INPUT #2,L$
      PRINT L$
      INPUT #2,h$,L$,k$
      PRINT h$,L$,k$
      INPUT #2,L$
      PRINT L$
      FOR i=1 TO npt
      INPUT #2,h$,L$,k$
      PHAS12(i)=VAL(MID$(L$,1))
      LMAGS12(i)=VAL(MID$(k$,1))
      PRINT freq(i),PHAS12(i),LMAGS12(i)
      NEXT i
      INPUT #2,L$
      PRINT L$
      INPUT"Type R(return) for more:",R$
      IF R$="R" OR R$="r" THEN GOTO 12
12    INPUT #2,L$
      PRINT L$
      INPUT #2,h$,L$,k$
      PRINT h$,L$,k$
      INPUT #2,L$
      PRINT L$
      FOR i=1 TO npt
      INPUT #2,h$,L$,k$
      PHAS21(i)=VAL(MID$(L$,1))
      LMAGS21(i)=VAL(MID$(k$,1))
```

```
        PRINT freq(i),PHAS21(i),LMAGS21(i)
        NEXT i
        INPUT #2,L$
        PRINT L$
        INPUT"Type R(return) for more:",R$
        IF R$="R" OR R$="r" THEN GOTO 13
13      INPUT #2,L$
        PRINT L$
        INPUT #2,h$,L$,k$
        PRINT h$,L$,k$
        INPUT #2,L$
        PRINT L$
        FOR i=1 TO npt
        INPUT #2,h$,L$,k$
        PHAS22(i)=VAL(MID$(L$,1))
        LMAGS22(i)=VAL(MID$(k$,1))
        PRINT freq(i),PHAS22(i),LMAGS22(i)
        NEXT i
        savflag=1
        CLOSE #2
        PRINT "Data reading finished."
        RETURN

prindata:

        PRINT "Data printing in progress"
        OPEN "O", #2,"lpt1:"
        PRINT #2,"FILENAME ";TAB(30);nameout$
        PRINT #2,"ACQUISITION CODE ";TAB(30);prog$
        PRINT #2,""
        PRINT #2,"Number of points per measurement is ";npt
        PRINT #2,"The material used is ";MAT$
        PRINT #2,"The temperature in Celsius is ";TDEGC
        PRINT #2,"The water resistivity is ";RW
        PRINT #2,""
        PRINT #2,"Date and time of the measurement"
        PRINT #2,TAB(7);"Date: ";TAB(14);TODAY$
        PRINT #2,TAB(7);"Time: ";TAB(14);MTIME$
        PRINT #2,""
        PRINT #2,"COMMENT"
        PRINT #2,comment1$
        PRINT #2,comment2$
        PRINT #2,""
        PRINT #2,"FOR S11"
        PRINT #2,"Frequency(i)        Phase(i)          Magnitude(i)"
        PRINT #2,""
        FOR i=1 TO npt
        PRINT #2,freq(i),PHAS11(i),LMAGS11(i)
        NEXT i
        PRINT #2,""
        PRINT #2,"FOR S12"
        PRINT #2,"Frequency(i)        Phase(i)          Magnitude(i)"
        PRINT #2,""
        FOR i=1 TO npt
```

```
        PRINT #2,freq(i),PHAS12(i),LMAGS12(i)
        NEXT i
        PRINT #2,""
        PRINT #2,"FOR S21"
        PRINT #2,"Frequency(i)        Phase(i)          Magnitude(i)"
        PRINT #2,""
        FOR i=1 TO npt
        PRINT #2,freq(i),PHAS21(i),LMAGS21(i)
        NEXT i
        PRINT #2,""
        PRINT #2,"FOR S22"
        PRINT #2,"Frequency(i)        Phase(i)          Magnitude(i)"
        PRINT #2,""
        FOR i=1 TO npt
        PRINT #2,freq(i),PHAS22(i),LMAGS22(i)
        NEXT i
        PRINT #2,""
        CLOSE #2
        PRINT "Data printing finished."
        RETURN

plotdata:

        OPEN "clip:" FOR OUTPUT AS #3
        FOR i=1 TO npt
        WRITE #3,freq(i),PHAS11(i),LMAGS11(i),PHAS12(i),LMAGS12(i),
        PHAS21(i),LMAGS21(i),PHAS22(i),LMAGS22(i)
        NEXT i
        CLOSE #3
        PRINT "Finished sending data to clipboard;"
        PRINT "You can now use CRICKET GRAPH to plot the data."
        RETURN
```

D.1 Forward Model

The following code is written in FORTRAN and runs on the VAX. It simulates the forward model for the coaxial cell in Figure 3.2.1. The first input file contains the dielectric constant and conductivity of the high-pressure seal. The second input file contains the dielectric constant and conductivity of the sample. The output file contains the scattering parameters. All the data are given at a range of frequencies.

```
C**********************************************************************
C     This FORTRAN code computes the scattering parameters, as measured with the
C     HP8753A network analyzer and 85046A S-parameter test set, based on the given
C     complex dielectric constant of the sample in the high-pressure coaxial cell.
C**********************************************************************

      real*8 pi,freq,k0,aep(3),asig(3),alen(3),alenn(3)
      complex*16 ci,aeps(3),temp1,temp2
      complex*16 ar(2,3),are(3),arm(3)
      complex*16 ref,tra,num1,num2
      character*40 out

C     Input file "coaxin1" contains the dielectric constant and conductivity of the high-
C     pressure seal at a range of frequencies.
C     Input file "coaxin2" contains the dielectric constant and conductivity of the sample
C     at a range of frequencies.
C     Output file "coaxout" contains the S-parameters for the coaxial cell at a range of
C     frequencies.

      open(unit=1,file='coaxin1',status='old')
      open(unit=2,file='coaxin2',status='old')
      open(unit=3,file='coaxout',status='new')

C     n is the number of sections in the coaxial cell. In this particular case, I am assuming
C     a three section coaxial line.

      n=3
      ci=(0.d0,1.d0)
      pi=3.141592653589793d0

C     aep(i) and asig(i) represent the dielectric constant and conductivity of the i-th section
C     in the coaxial cell.

      aep(1)=1.d0
```

```
      asig(1)=0.d0

C     alen(i) represents the length of the i-th section in meter.

      alen(1)=1.210939d-1
      alen(2)=2.83464d-2
      alen(3)=1.90373d-2

      do 10 j=1,150
      read(1,*) freq,aep(2),asig(2)
      read(2,*) freq,aep(3),asig(3)
      k0=2.d0*pi*freq*1.d-8/3.d0
      do 20 i=1,n
      aeps(i)=aep(i)+ci*1.7975078d+10*asig(i)/freq
      alenn(i)=alen(i)*k0
20    continue
      aeps(2)=aeps(2)+(j-1)*0.01*aeps(2)
      do 30 i=1,n-1
      ar(i,i+1)=(cdsqrt(aeps(i))-cdsqrt(aeps(i+1)))/
     1(cdsqrt(aeps(i))+cdsqrt(aeps(i+1)))
30    continue
      are(n)=-1.d0
      arm(n)=1.d0
      do 40 i=0,n-2
      k=n-i
      temp1=ar(k-1,k)+are(k)*cdexp(ci*2.d0*cdsqrt(aeps(k))*alenn(k))
      temp2=1.d0+ar(k-1,k)*are(k)*cdexp(ci*2.d0*cdsqrt(aeps(k))*alenn(k))
      are(k-1)=temp1/temp2
      temp1=ar(k-1,k)+arm(k)*cdexp(ci*2.d0*cdsqrt(aeps(k))*alenn(k))
      temp2=1.d0+ar(k-1,k)*arm(k)*cdexp(ci*2.d0*cdsqrt(aeps(k))*alenn(k))
      arm(k-1)=temp1/temp2
40    continue
      ref=dconjg((arm(1)+are(1))*cdexp(ci*2.d0*cdsqrt(aeps(1))
     1*alenn(1))/2.d0)
      tra=dconjg((arm(1)-are(1))*cdexp(ci*2.d0*cdsqrt(aeps(1))
     1*alenn(1))/2.d0)
      call comphase(ref,tra)

      write(3,60) freq,char(9),dreal(ref),char(9),dimag(ref),char(9),dreal(tra),char(9),
     1dimag(tra)

10    continue
60    format(sp,1x,1pe13.6,4(a1,1pe13.6))
      end

C**********************************************************************
C     This subroutine changes S-parameters from (real,imaginary) to (phase,amplitude).

      subroutine comphase(ref,tra)
      complex*16 ref,tra,ci
      real*8 freq,real,imag

      ci=(0.d0,1.d0)
      real=datan2d(dimag(ref),dreal(ref))
```

```
      imag=20.d0*dlog10(cdabs(ref))
      ref=real+ci*imag
      real=datan2d(dimag(tra),dreal(tra))
      imag=20.d0*dlog10(cdabs(tra))
      tra=real+ci*imag
      return
      end

C*********************************************************************
```

E.1 Inversion (I) for sample

The following code is written in FORTRAN and runs on the VAX. It implements the inversion scheme described in section 2.3.1 using the Newton-Raphson approach. Various subroutines are integrated to provide greater flexibility. Parameters, such as frequency range, length of the sample, and measured scattering parameters, are taken as input. The output is the dielectric constant and conductivity of the sample under test.

```
C**********************************************************************
C     This FORTRAN code computes the complex dielectric constant of the sample using
C     both measured reflection and transmission coefficients by solving a set of
C     simultaneous equations, given the complex dielectric constant of the high-pressure
C     seal.
C**********************************************************************

      real*8 pi,freq,k0,aep(2),asig(2),alen(3),alenn(3)
      complex*16 ci,aeps(2),unknown1,unknown2,unknown3,unknown4
      complex*16 ar(2,3),are(3),arm(3),temp1,temp2
      complex*16 s11,s12,s21,s22,ref,tra
      complex*16 eps1,eps2,eps3,eps4

C     Input file "coaxinv1in1" contains the measured scattering parameters at a range of
C     frequencies.
C     Input file "coaxinv1in2" contains the dielectric constant and conductivity of the
C     high-pressure seal at a range of frequencies.
C     Output file "coaxinv1out" contains the dielectric constant and conductivity of the
C     sample at a range of frequencies.

      open (unit=1,file='coaxinv1in1',status='old')
      open (unit=2,file='coaxinv1in2',status='old')
      open (unit=3,file='coaxinv1out',status='new')

C     n is the number of sections in the coaxial cell. In this particular case, I am assuming
C     a three section coaxial line.

      n=3
      ci=(0.d0,1.d0)
      pi=3.141592653589793d0

C     aep(i) and asig(i) represent the dielectric constant and conductivity of the i-th section
C     in the coaxial cell.
```

```
      aep(1)=1.d0
      asig(1)=0.d0

C     alen(i) represents the length of the i-th section in meter.

      alen(1)=1.210939d-1
      alen(2)=2.83464d-2
      alen(3)=1.90373d-2

      do 10 j=1,150
      read(1,*) freq,s11,s12
      read(1,*) freq,s21,s22
      read(2,*) freq,aep(2),asig(2)
      s11=dconjg(s11)
      s12=dconjg(s12)
      s21=dconjg(s21)
      s22=dconjg(s22)
      k0=2.d0*pi*freq*1.d-8/3.d0
      do 20 i=1,n
      alenn(i)=alen(i)*k0
20    continue
      do 30 i=1,n-1
      aeps(i)=aep(i)+ci*1.7975078d+10*asig(i)/freq
30    continue
      ar(1,2)=(cdsqrt(aeps(1))-cdsqrt(aeps(2)))/
     1(cdsqrt(aeps(1))+cdsqrt(aeps(2)))

C     Moving the plane of measurement to the interface between air and the seal.

      ref=s11/cdexp(ci*2.d0*cdsqrt(aeps(1))*alenn(1))
      tra=s12/cdexp(ci*2.d0*cdsqrt(aeps(1))*alenn(1))
      arm(1)=tra+ref
      are(1)=ref-tra
      temp1=ar(1,2)-arm(1)
      temp2=(arm(1)*ar(1,2)-1.d0)*cdexp(ci*2.d0*cdsqrt(aeps(2))*alenn(2))
      arm(2)=temp1/temp2
      temp1=ar(1,2)-are(1)
      temp2=(are(1)*ar(1,2)-1.d0)*cdexp(ci*2.d0*cdsqrt(aeps(2))*alenn(2))
      are(2)=temp1/temp2

C     Solving the quadratic equation.

      temp1=arm(2)+are(2)
      temp2=-2.d0*(are(2)*arm(2)+1.d0)
      unknown1=(-1.d0*temp2+cdsqrt(temp2*temp2-4.d0*temp1*temp1))
     1/(2.d0*temp1)
      unknown2=(-1.d0*temp2-cdsqrt(temp2*temp2-4.d0*temp1*temp1))
     1/(2.d0*temp1)
      temp1=arm(2)-are(2)
      temp2=2.d0*(are(2)*arm(2)-1.d0)
      unknown3=(-1.d0*temp2+cdsqrt(temp2*temp2-4.d0*temp1*temp1))
     1/(2.d0*temp1)
      unknown4=(-1.d0*temp2-cdsqrt(temp2*temp2-4.d0*temp1*temp1))
     1/(2.d0*temp1)
```

```
C     Solving for eps from the roots obtained from the quadratic equation.

      eps1=(cdsqrt(aeps(2))-unknown1*cdsqrt(aeps(2)))/
     1(unknown1+1.d0)**2
      eps2=(cdsqrt(aeps(2))-unknown2*cdsqrt(aeps(2)))/
     1(unknown2+1.d0)**2
      eps3=(cdlog(unknown3)/(2.d0*ci*alenn(3)))**2
      eps4=(cdlog(unknown4)/(2.d0*ci*alenn(3)))**2

      write (3,60) freq,dreal(eps1),dimag(eps1)*freq/1.7975078d10
      write (3,60) freq,dreal(eps2),dimag(eps2)*freq/1.7975078d10
      write (3,60) freq,dreal(eps3),dimag(eps3)*freq/1.7975078d10
      write (3,60) freq,dreal(eps4),dimag(eps4)*freq/1.7975078d10

10    continue
60    format(sp,1x,1pe13.6,2(a1,1pe13.6))
      end

C*********************************************************************
```

E.2 Inversion (II) for sample

The following code is written in FORTRAN and stored on the VAX. It implements the inversion scheme described in section 2.3.1 using the Newton-Raphson approach. Various subroutines are integrated to provide greater flexibility. Parameters, such as frequency range, length of the sample, and measured scattering parameters, are taken as input. The output is the dielectric constant and conductivity of the sample under test.

```
C**********************************************************************
C     This FORTRAN code computes the complex dielectric constant of the sample using
C     both measured reflection and transmission coefficients with an iterative approach,
C     given the complex dielectric constant of the high-pressure seal.
C**********************************************************************

      real*8 pi,tol,freq,k0,aep(3),asig(3),alen(3),alenn(3)
      complex*16 ci,aeps(3),unknown1,unknown2,unknown3,unknown4
      complex*16 ar(2,3),are(3),arm(3),temp1,temp2
      complex*16 s11,s12,s21,s22,ref,tra,aeps31,aeps32
      complex*16 eps1,eps2,eps3,eps4
      real*8 alenn3
      complex*16 aeps2,arm2,are2
      common /par/aeps2,alenn3,ci,tol
      common /par1/arm2
      common /par2/are2

C     Input file "coaxinv2in1" contains the measured scattering parameters at a range of
C     frequencies.
C     Input file "coaxinv2in2" contains the dielectric constant and conductivity of the
C     high-pressure seal at a range of frequencies.
C     Output file "coaxinv2out" contains the dielectric constant and conductivity of the
C     sample at a range of frequencies.

      open (unit=1,file='coaxinv2in1',status='old')
      open (unit=2,file='coaxinv2in2',status='old')
      open (unit=3,file='coaxinv2out',status='new')

C     n is the number of sections in the coaxial cell. In this particular case, I am assuming
C     a three section coaxial line.

      n=3

C     aep(i) and asig(i) represent the dielectric constant and conductivity of the i-th section
```

```
C     in the coaxial cell.

      aep(1)=1.d0
      asig(1)=0.d0

C     alen(i) represents the length of the i-th section in meter.

      alen(1)=1.210939d-1
      alen(2)=2.83464d-2
      alen(3)=1.90373d-2

C     tol represents the tolerance for the iteration process.

      tol=1.d-10

C     Initial guess for the complex dielectric constant for the sample.

      aep(3)=30.d0
      asig(3)=3.d-3

      ci=(0.d0,1.d0)
      pi=3.141592653589793d0
      do 10 j=1,150
      read(1,*) freq,s11,s12
      read(1,*) freq,s21,s22
      read(2,*) freq,aep(2),asig(2)
      s11=dconjg(s11)
      s12=dconjg(s12)
      s21=dconjg(s21)
      s22=dconjg(s22)
      k0=2.d0*pi*freq*1.d-8/3.d0
      do 20 i=1,n
      alenn(i)=alen(i)*k0
20    continue
      do 30 i=1,n
      aeps(i)=aep(i)+ci*1.7975078d+10*asig(i)/freq
30    continue
      ar(1,2)=(cdsqrt(aeps(1))-cdsqrt(aeps(2)))/
     1(cdsqrt(aeps(1))+cdsqrt(aeps(2)))

C     Moving the plane of measurement to the interface between the seal and sample.

      ref=s11/cdexp(ci*2.d0*cdsqrt(aeps(1))*alenn(1))
      tra=s12/cdexp(ci*2.d0*cdsqrt(aeps(1))*alenn(1))
      arm(1)=tra+ref
      are(1)=ref-tra
      temp1=ar(1,2)-arm(1)
      temp2=(arm(1)*ar(1,2)-1.d0)*cdexp(ci*2.d0*cdsqrt(aeps(2))*alenn(2))
      arm(2)=temp1/temp2
      temp1=ar(1,2)-are(1)
      temp2=(are(1)*ar(1,2)-1.d0)*cdexp(ci*2.d0*cdsqrt(aeps(2))*alenn(2))
      are(2)=temp1/temp2
      aeps31=aeps(3)
      aeps32=aeps(3)
```

```
      alenn3=alenn(3)
      aeps2=aeps(2)
      arm2=arm(2)
      are2=are(2)
      call f1(aeps31)
      call f2(aeps32)

      write (3,60) freq,char(9),dreal(aeps31),char(9),dimag(aeps31)*freq/1.7975078d10
      write (3,60) freq,char(9),dreal(aeps32),char(9),dimag(aeps32)*freq/1.7975078d10

10    continue
60    format(sp,1x,1pe13.6,2(a1,1pe13.6))
      end

C*********************************************************************
C     This subroutine f1() computes the complex dielectric constant assuming a PMC.

      subroutine f1(aeps31)
      real*8 alenn3,tol
      complex*16 aeps3,aeps31,aeps2,arm2,ar23,ci
      common /par/aeps2,alenn3,ci,tol
      common /par1/arm2

10    ar23=(cdsqrt(aeps2)-cdsqrt(aeps31))/(cdsqrt(aeps2)+cdsqrt(aeps31))
      aeps3=(cdlog((arm2-ar23)/(1.d0-arm2*ar23))/(2.d0*ci*alenn3))**2
      if(cdabs(aeps3-aeps31).lt.cdabs(tol*aeps31)) then
      aeps31=aeps3
      return
      else
      aeps31=aeps3
      goto 10
      endif
      return
      end

C*********************************************************************
C     This subroutine f2() computes the complex dielectric constant assuming a PEC.

      subroutine f2(aeps32)
      real*8 alenn3,tol
      complex*16 aeps3,aeps32,aeps2,are2,ar23,ci
      common /par/aeps2,alenn3,ci,tol
      common /par2/are2

10    ar23=(cdsqrt(aeps2)-cdsqrt(aeps32))/(cdsqrt(aeps2)+cdsqrt(aeps32))
      aeps3=(cdlog((are2-ar23)/(are2*ar23-1.d0))/(2.d0*ci*alenn3))**2
      if(cdabs(aeps3-aeps32).lt.cdabs(tol*aeps32)) then
      aeps32=aeps3
      return
      else
      aeps32=aeps3
      goto 10
      endif
      return
```

```
      end
C**********************************************************************
```

E.3 Inversion (III) for sample

The following code is written in FORTRAN and stored on the VAX. It implements the inversion scheme described in section 2.3.1 using the Newton-Raphson approach. Various subroutines are integrated to provide greater flexibility. Parameters, such as frequency range, length of the sample, and measured scattering parameters, are taken as input. The output is the dielectric constant and conductivity of the sample under test.

```
C**********************************************************************
C     This FORTRAN code computes the complex dielectric constant of the sample using
C     either reflection or transmission coefficient with a Newton-Raphson approximation
C     approach, given the complex dielectric constant of the high-pressure seal.
C**********************************************************************

      real*8 pi,freq,k0,aep(3),asig(3),alen(3),alenn(3)
      real*8 re11,sig11,re12,sig12,re21,sig21,re22,sig22
      complex*16 ci,aeps(3),tem11,tem12,tem21,tem22
      complex*16 ar(2,3),are(3),arm(3)
      complex*16 s11,s12,s21,s22
      common /par1/ci
      common /par2/aeps,alenn,ar
      common /par3/are,arm
      common /par4/n

C     Input file "coaxinv3in1" contains the measured scattering parameters at a range of
C     frequencies.
C     Input file "coaxinv3in2" contains the dielectric constant and conductivity of the
C     high-pressure seal at a range of frequencies.
C     Output file "coaxinv3out" contains the dielectric constant and conductivity of the
C     sample at a range of frequencies.

      open (unit=1,file='coaxinv3in1',status='old')
      open (unit=2,file='coaxinv3in2',status='old')
      open (unit=3,file='coaxinv3out',status='new')

C     n is the number of sections in the coaxial cell. In this particular case, I am assuming
C     a three section coaxial line.

      n=3

C     aep(i) and asig(i) represent the dielectric constant and conductivity of the i-th section
C     in the coaxial cell.
```

```
      aep(1)=1.d0
      asig(1)=0.d0

C     alen(i) represents the length of the i-th section in meter.

      alen(1)=1.210939d-1
      alen(2)=2.83464d-2
      alen(3)=1.90373d-2


C     Initial guess for the complex dielectric constant for the sample.

      aep(3)=30.d0
      asig(3)=3.d-3

      ci=(0.d0,1.d0)
      pi=3.141592653589793d0
      do 10 j=1,150
      read(1,*) freq,s11,s12
      read(1,*) freq,s21,s22
      read(2,*) freq,aep(2)asig(2)
      s11=dconjg(s11)
      s12=dconjg(s12)
      s21=dconjg(s21)
      s22=dconjg(s22)
      k0=2.d0*pi*freq*1.d-8/3.d0
      do 20 i=1,3
      alenn(i)=alen(i)*k0
20    continue
      do 30 i=1,3
      aeps(i)=aep(i)+ci*1.7975078d+10*asig(i)/freq
30    continue
      ar(1,2)=(cdsqrt(aeps(1))-cdsqrt(aeps(2)))/
     1(cdsqrt(aeps(1))+cdsqrt(aeps(2)))
      are(3)=-1.d0
      arm(3)=1.d0
      tem11=aeps(3)
      tem12=aeps(3)
      tem21=aeps(3)
      tem22=aeps(3)

      call fs11(tem11,s11)
      re11=dreal(tem11)
      sig11=dimag(tem11)*freq/1.7975078d10
      write(3,60) freq,char(9),re11,char(9),sig11

      call fs12(tem12,s12)
      re12=dreal(tem12)
      sig12=dimag(tem12)*freq/1.7975078d10
      write(3,60) freq,char(9),re12,char(9),sig12

      call fs12(tem21,s21)
      re21=dreal(tem21)
```

```
      sig21=dimag(tem21)*freq/1.7975078d10
      write(3,60) freq,char(9),re21,char(9),sig21

      call fs11(tem22,s22)
      re22=dreal(tem22)
      sig22=dimag(tem22)*freq/1.7975078d10
      write(3,60) freq,aep(3),asig(3)

      aep(3)=re22
      asig(3)=sig22
10    continue
60    format(sp,1x,1pe13.6,2(a1,1pe13.6))
      end

C*********************************************************************
C     The subroutine fs11() compute complex dielectric based on s11.

      subroutine fs11(weps,s11)
      real*8 tol
      complex*16 weps,s11,reps,deps,ref,deref,detra,epsn

      tol=1.d-13
      reps=weps
      deps=weps
10    call refl(reps,ref)
      call der(deps,deref,detra)
      epsn=weps-(ref-s11)/deref
      if (cdabs(epsn-weps).lt.cdabs(tol*epsn)) then
      weps=epsn
      return
      else
      weps=epsn
      reps=weps
      deps=weps
      go to 10
      endif
      return
      end

C*********************************************************************
C     The subroutine refl() computes s11 based on (ep,sig).

      subroutine refl(reps,ref)
      real*8 alenn(3)
      complex*16 ci,reps,aeps(3),temp1,temp2,ref
      complex*16 ar(2,3),are(3),arm(3)
      common /par1/ci
      common /par2/aeps,alenn,ar
      common /par3/are,arm

      aeps(3)=reps
      ar(2,3)=(cdsqrt(aeps(2))-cdsqrt(aeps(3)))/
     1(cdsqrt(aeps(2))+cdsqrt(aeps(3)))
      do 10 i=0,1
```

```
      k=3-i
      temp1=ar(k-1,k)+are(k)*cdexp(ci*2.d0*cdsqrt(aeps(k))*alenn(k))
      temp2=1.d0+ar(k-1,k)*are(k)*cdexp(ci*2.d0*cdsqrt(aeps(k))*alenn(k))
      are(k-1)=temp1/temp2
      temp1=ar(k-1,k)+arm(k)*cdexp(ci*2.d0*cdsqrt(aeps(k))*alenn(k))
      temp2=1.d0+ar(k-1,k)*arm(k)*cdexp(ci*2.d0*cdsqrt(aeps(k))*alenn(k))
      arm(k-1)=temp1/temp2
10    continue
      ref=(arm(1)+are(1))*cdexp(ci*2.d0*cdsqrt(aeps(1))*alenn(1))/2.d0
      return
      end

C**********************************************************************
C     The subroutine fs12() computes complex dielectric constant based on s12.

      subroutine fs12(weps,s12)
      real*8 tol
      complex*16 s12,weps,reps,deps,tra,deref,detra,epsn

      tol=1.d-13
      reps=weps
      deps=weps
10    call tran(reps,tra)
      call der(deps,deref,detra)
      epsn=weps-(tra-s12)/detra
      if (cdabs(epsn-weps).lt.cdabs(tol*epsn)) then
      weps=epsn
      return
      else
      weps=epsn
      reps=weps
      deps=weps
      go to 10
      endif
      return
      end

C**********************************************************************
C     The subroutine tran() computes s12 based on (ep,sig).

      subroutine tran(reps,tra)
      real*8 alenn(3)
      complex*16 ci,reps,aeps(3),temp1,temp2,tra
      complex*16 ar(2,3),are(3),arm(3)
      common /par1/ci
      common /par2/aeps,alenn,ar
      common /par3/are,arm

      aeps(3)=reps
      ar(2,3)=(cdsqrt(aeps(2))-cdsqrt(aeps(3)))/
     1(cdsqrt(aeps(2))+cdsqrt(aeps(3)))
      do 10 i=0,1
      k=3-i
      temp1=ar(k-1,k)+are(k)*cdexp(ci*2.d0*cdsqrt(aeps(k))*alenn(k))
```

```
      temp2=1.d0+ar(k-1,k)*are(k)*cdexp(ci*2.d0*cdsqrt(aeps(k))*alenn(k))
      are(k-1)=temp1/temp2
      temp1=ar(k-1,k)+arm(k)*cdexp(ci*2.d0*cdsqrt(aeps(k))*alenn(k))
      temp2=1.d0+ar(k-1,k)*arm(k)*cdexp(ci*2.d0*cdsqrt(aeps(k))*alenn(k))
      arm(k-1)=temp1/temp2
10    continue
      tra=(arm(1)-are(1))*cdexp(ci*2.d0*cdsqrt(aeps(1))*alenn(1))/2.d0
      return
      end

C**********************************************************************
C     The subroutine der() computes the derivative of refl() and tran() at eps3.

      subroutine der(eps3,deref,detra)
      real*8 alenn(3)
      complex*16 eps3,deref,detra
      complex*16 ci,aeps(3),ar(2,3),k1,k2,k3
      complex*16 con1,decon1,con2,decon2,con3,decon3,con4,decon4
      complex*16 con5,derm,dere
      common /par1/ci
      common /par2/aeps,alenn,ar

      aeps(3)=eps3
      k1=cdsqrt(aeps(1))
      k2=cdsqrt(aeps(2))
      k3=cdsqrt(aeps(3))

C     The value of (k2-k3)/(k2+k3).
      con1=(k2-k3)/(k2+k3)

C     The derivative of con1 with respect to eps3.
      decon1=-1.d0*k2/(k3*(k2+k3)**2)

C     The value of cdexp(ci*2.d0*k3*h3)
      con2=cdexp(ci*2.d0*k3*alenn(3))

C     The derivative of con2 with respect to eps3.
      decon2=ci*alenn(3)*con2/k3

C     The value of R2M or (con1+con2)/(1.d0+con1*con2).
      con3=(con1+con2)/(1.d0+con1*con2)

C     The derivative of R2M with respect to eps3.
      decon3=-1.d0*(con1+con2)*(con1*decon2+con2*decon1)/
     1(1.d0+con1*con2)**2+(decon1+decon2)/(1.d0+con1*con2)

C     The value of R2E or (con1-con2)/(1.d0-con1*con2).
      con4=(con1-con2)/(1.d0-con1*con2)

C     The derivative of R2E with respect to eps3.
      decon4=(con1-con2)*(con1*decon2+con2*decon1)/
     1(1.d0-con1*con2)**2+(decon1-decon2)/(1.d0-con1*con2)

C     The value of cdexp(ci*2.d0*k2*alenn(2)).
```

```
      con5=cdexp(ci*2.d0*k2*alenn(2))

C     The derivative of R1M with respect to eps3.
      derm=-1.d0*(ar(1,2)+con3*con5)*ar(1,2)*con5*decon3/
     1(1.d0+ar(1,2)*con3*con5)**2+decon3*con5/(1.d0+ar(1,2)*
     1con3*con5)

C     The derivative of R1E with respect to eps3.
      dere=-1.d0*(ar(1,2)+con4*con5)*ar(1,2)*con5*decon4/
     1(1.d0+ar(1,2)*con4*con5)**2+decon4*con5/(1.d0+ar(1,2)*
     1con4*con5)

      deref=(derm+dere)*cdexp(ci*2.d0*k1*alenn(1))/2.d0
      detra=(derm-dere)*cdexp(ci*2.d0*k1*alenn(1))/2.d0
      return
      end

C*********************************************************************
```

E.4 Inversion for seal

The following code is written in FORTRAN and stored on the VAX. It implements the inversion scheme described in section 2.3.1 using the Newton-Raphson approach. Various subroutines are integrated to provide greater flexibility. Parameters, such as frequency range, length of the sample, and measured scattering parameters, are taken as input. The output is the dielectric constant and conductivity of the sample under test.

```
C**********************************************************************
C     This FORTRAN code computes the complex dielectric constant of the high-
C     pressure seal using either reflection or transmission coefficient with a Newton-
C     Raphson approximation approach, given the complex dielectric constant of the
C     sample.
C**********************************************************************

      real*8 pi,freq,k0,aep(3),asig(3),alen(3),alenn(3)
      real*8 sr(6),si(6),temp3,junk,junk1
      complex*16 ci,aeps(3),tem1,tem2,tem3,tem4,tem5,tem6
      complex*16 are(3),arm(3)
      complex*16 s11ave,s12ave,s11,s12,s21,s22
      common /par1/ci
      common /par2/aeps,alenn
      common /par3/are,arm
      common /par4/n

C     Input file "coaxinv4in1" contains the measured scattering parameters at a range of
C     frequencies.
C     Input file "coaxinv4in2" contains the dielectric constant and conductivity of the
C     sample at a range of frequencies.
C     Output file "coaxinv4out" contains the dielectric constant and conductivity of the
C     high-pressure seal at a range of frequencies.

      open(unit=1,file='coaxinv4in1',status='old')
      open(unit=2,file='coaxinv4in2',status='old')
      open(unit=3,file='coaxinv4out',status='new')

C     n is the number of sections in the coaxial cell. In this particular case, I am assuming
C     a three section coaxial line.

      n=3
```

```
C     aep(i) and asig(i) represent the dielectric constant and conductivity of the i-th section
C     in the coaxial cell.

      aep(1)=1.d0
      asig(1)=0.d0

C     alen(i) represents the length of the i-th section in meter.

      alen(1)=1.210939d-1
      alen(2)=2.83464d-2
      alen(3)=1.90373d-2

C     Initial guess for the complex dielectric constant for the seal.

      aep(2)=16.d0
      asig(2)=3.d-4

      ci=(0.d0,1.d0)
      pi=3.141592653589793d0
      do 10 j=1,150
      read(1,*) freq,s11,s12
      read(1,*) freq,s21,s22
      read(2,*) freq,aep(3),asig(3)
      s11=dconjg(s11)
      s12=dconjg(s12)
      s21=dconjg(s21)
      s22=dconjg(s22)
      k0=2.d0*pi*freq*1.d-8/3.d0
      do 20 i=1,3
      alenn(i)=alen(i)*k0
20    continue
      do 30 i=1,3
      aeps(i)=aep(i)+ci*1.7975078d+10*asig(i)/freq
30    continue
      are(3)=-1.d0
      arm(3)=1.d0
      tem1=aeps(2)
      tem2=aeps(2)
      tem3=aeps(2)
      tem4=aeps(2)

      call fs11(tem1,s11)
      sr(1)=dreal(tem1)
      si(1)=dimag(tem1)*freq/1.7975078d10
      write(3,60) freq,sr(1),si(1)

      call fs12(tem2,s12)
      sr(2)=dreal(tem2)
      si(2)=dimag(tem2)*freq/1.7975078d10
      write(3,60) freq,sr(2),si(2)

      call fs12(tem3,s21)
      sr(3)=dreal(tem3)
      si(3)=dimag(tem3)*freq/1.7975078d10
```

```
      write(3,60) freq,sr(3),si(3)

      call fs11(tem4,s22)
      sr(4)=dreal(tem4)
      si(4)=dimag(tem4)*freq/1.7975078d10
      write(3,60) freq,sr(4),si(4)

      aep(2)=sr(4)
      asig(2)=si(4)
10    continue
60    format(sp,1x,1pe13.6,2(a1,1pe13.6))
      end

C*********************************************************************
C     The subroutine fs11() compute complex dielectric based on s11.

      subroutine fs11(weps,s11)
      real*8 tol
      complex*16 weps,s11,reps,deps,ref,deref,detra,epsn

      tol=1.d-10
      reps=weps
      deps=weps
10    call refl(reps,ref)
      call der(deps,deref,detra)
      epsn=weps-(ref-s11)/deref
      if (cdabs(epsn-weps).lt.cdabs(tol*epsn)) then
      weps=epsn
      return
      else
      weps=epsn
      reps=weps
      deps=weps
      go to 10
      endif
      return
      end

C*********************************************************************
C     The subroutine refl() computes s11 based on (ep,sig).

      subroutine refl(reps,ref)
      real*8 alenn(3)
      complex*16 ci,reps,aeps(3),temp1,temp2,ref
      complex*16 ar(2,3),are(3),arm(3)
      common /par1/ci
      common /par2/aeps,alenn
      common /par3/are,arm

      aeps(2)=reps
      ar(1,2)=(cdsqrt(aeps(1))-cdsqrt(aeps(2)))/
     1(cdsqrt(aeps(1))+cdsqrt(aeps(2)))
      ar(2,3)=(cdsqrt(aeps(2))-cdsqrt(aeps(3)))/
     1(cdsqrt(aeps(2))+cdsqrt(aeps(3)))
```

```
      do 10 i=0,1
      k=3-i
      temp1=ar(k-1,k)+are(k)*cdexp(ci*2.d0*cdsqrt(aeps(k))*alenn(k))
      temp2=1.d0+ar(k-1,k)*are(k)*cdexp(ci*2.d0*cdsqrt(aeps(k))*alenn(k))
      are(k-1)=temp1/temp2
      temp1=ar(k-1,k)+arm(k)*cdexp(ci*2.d0*cdsqrt(aeps(k))*alenn(k))
      temp2=1.d0+ar(k-1,k)*arm(k)*cdexp(ci*2.d0*cdsqrt(aeps(k))*alenn(k))
      arm(k-1)=temp1/temp2
10    continue
      ref=(arm(1)+are(1))*cdexp(ci*2.d0*cdsqrt(aeps(1))*alenn(1))/2.d0
      return
      end

C**********************************************************************
C     The subroutine fs12() computes complex dielectric constant based on s12.

      subroutine fs12(weps,s12)
      real*8 tol
      complex*16 s12,weps,reps,deps,tra,deref,detra,epsn

      tol=1.d-10
      reps=weps
      deps=weps
10    call tran(reps,tra)
      call der(deps,deref,detra)
      epsn=weps-(tra-s12)/detra
      if (cdabs(epsn-weps).lt.cdabs(tol*epsn)) then
      weps=epsn
      return
      else
      weps=epsn
      reps=weps
      deps=weps
      go to 10
      endif
      return
      end

C**********************************************************************
C     The subroutine tran() computes s12 based on (ep,sig).

      subroutine tran(reps,tra)
      real*8 alenn(3)
      complex*16 ci,reps,aeps(3),temp1,temp2,tra
      complex*16 ar(2,3),are(3),arm(3)
      common /par1/ci
      common /par2/aeps,alenn
      common /par3/are,arm

      aeps(2)=reps
      ar(1,2)=(cdsqrt(aeps(1))-cdsqrt(aeps(2)))/
     1(cdsqrt(aeps(1))+cdsqrt(aeps(2)))
      ar(2,3)=(cdsqrt(aeps(2))-cdsqrt(aeps(3)))/
     1(cdsqrt(aeps(2))+cdsqrt(aeps(3)))
```

```
      do 10 i=0,1
      k=3-i
      temp1=ar(k-1,k)+are(k)*cdexp(ci*2.d0*cdsqrt(aeps(k))*alenn(k))
      temp2=1.d0+ar(k-1,k)*are(k)*cdexp(ci*2.d0*cdsqrt(aeps(k))*alenn(k))
      are(k-1)=temp1/temp2
      temp1=ar(k-1,k)+arm(k)*cdexp(ci*2.d0*cdsqrt(aeps(k))*alenn(k))
      temp2=1.d0+ar(k-1,k)*arm(k)*cdexp(ci*2.d0*cdsqrt(aeps(k))*alenn(k))
      arm(k-1)=temp1/temp2
10    continue
      tra=(arm(1)-are(1))*cdexp(ci*2.d0*cdsqrt(aeps(1))*alenn(1))/2.d0
      return
      end

C*********************************************************************
C     The subroutine der() computes the derivative of refl() and tran() at eps2.

      subroutine der(eps2,deref,detra)
      real*8 alenn(3)
      complex*16 eps2,deref,detra
      complex*16 ci,aeps(3),k1,k2,k3
      complex*16 R12,DR12,R23,DR23,E1,E2,DE2,E3,RM2,DRM2
      complex*16 RE2,DRE2,DRM1,DRE1
      common /par1/ci
      common /par2/aeps,alenn

      aeps(2)=eps2
      k1=cdsqrt(aeps(1))
      k2=cdsqrt(aeps(2))
      k3=cdsqrt(aeps(3))

C     The value of R12.
      R12=(k1-k2)/(k1+k2)

C     The derivative of R12 with respect to eps2.
      DR12=-1.d0*k1/(k2*(k1+k2)**2)

C     The value of R23.
      R23=(k2-k3)/(k2+k3)

C     The derivative of R23 with respect to eps2.
      DR23=k3/(k2*(k2+k3)**2)

C     The value of E1.
      E1=cdexp(ci*2.d0*k1*alenn(1))

C     The value of E2.
      E2=cdexp(ci*2.d0*k2*alenn(2))

C     The derivative of E2 with respect to eps2.
      DE2=ci*alenn(2)*E2/k2

C     The value of E3.
      E3=cdexp(ci*2.d0*k3*alenn(3))
```

```
C     The value of R2M.
      RM2=(R23+E3)/(1.d0+R23*E3)

C     The derivative of R2M with respect to eps2.
      DRM2=-1.d0*(R23+E3)*E3*DR23/(1.d0+R23*E3)**2+
     1DR23/(1.d0+R23*E3)

C     The value of R2E.
      RE2=(R23-E3)/(1.d0-R23*E3)

C     The derivative of R2E with respect to eps2.
      DRE2=(R23-E3)*DR23*E3/(1.d0-R23*E3)**2+
     1DR23/(1.d0-R23*E3)

C     The derivative of R1M with respect to eps2.
      DRM1=-1.d0*(R12+RM2*E2)*(DR12*RM2*E2+DRM2*R12*E2+
     1DE2*R12*RM2)/(1.d0+R12*RM2*E2)**2+(DR12+DE2*RM2+
     1DRM2*E2)/(1.d0+R12*RM2*E2)

C     The derivative of R1E with respect to eps2.
      DRE1=-1.d0*(R12+RE2*E2)*(DR12*RE2*E2+DRE2*R12*E2+
     1DE2*R12*RE2)/(1.d0+R12*RE2*E2)**2+(DR12+DE2*RE2+
     1DRE2*E2)/(1.d0+R12*RE2*E2)

      deref=(DRM1+DRE1)*E1/2.d0
      detra=(DRM1-DRE1)*E1/2.d0
      return
      end

C*********************************************************************
```

F.1 Data as a Function of Frequency at 1100 MHz

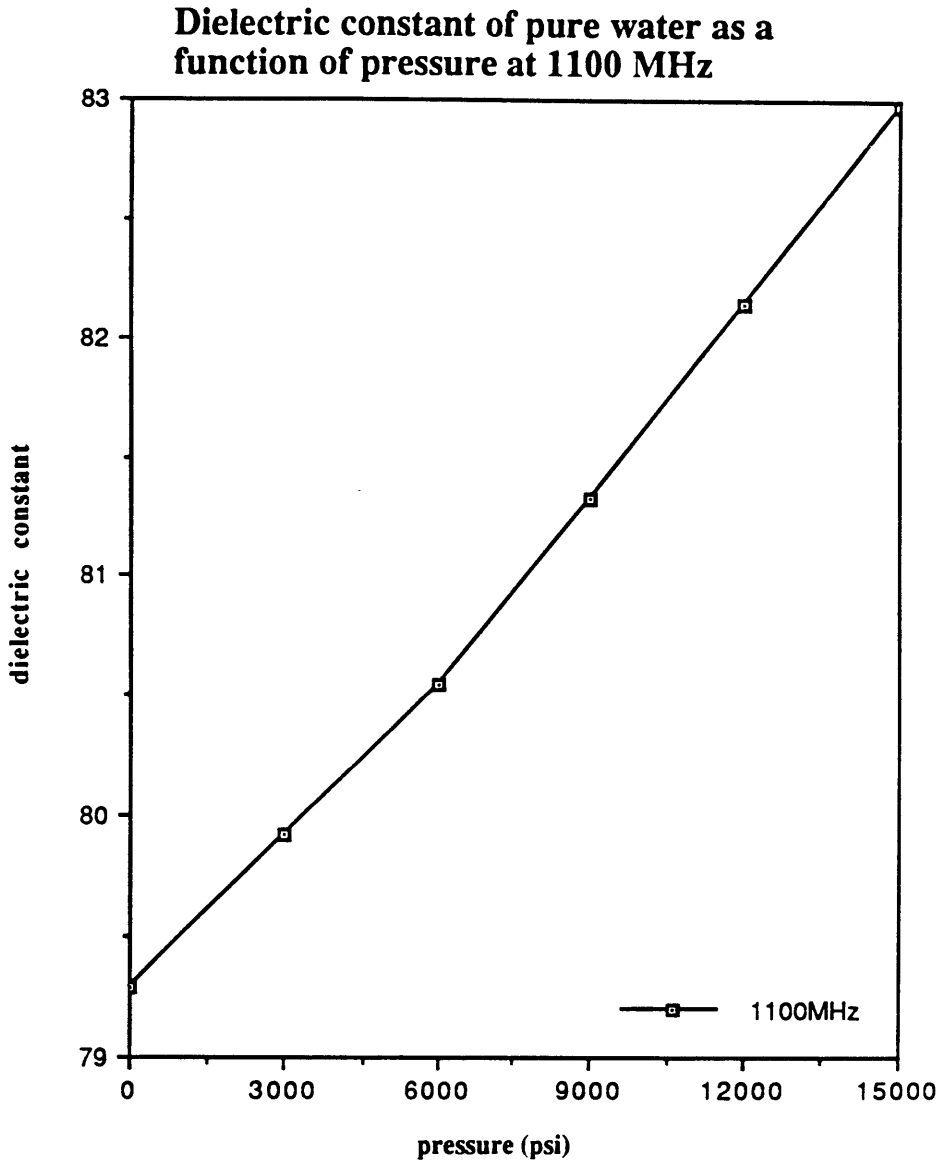

Figure F.1.1: Dielectric Constant of Pure Water as a Function of Pressure at 1100 MHz

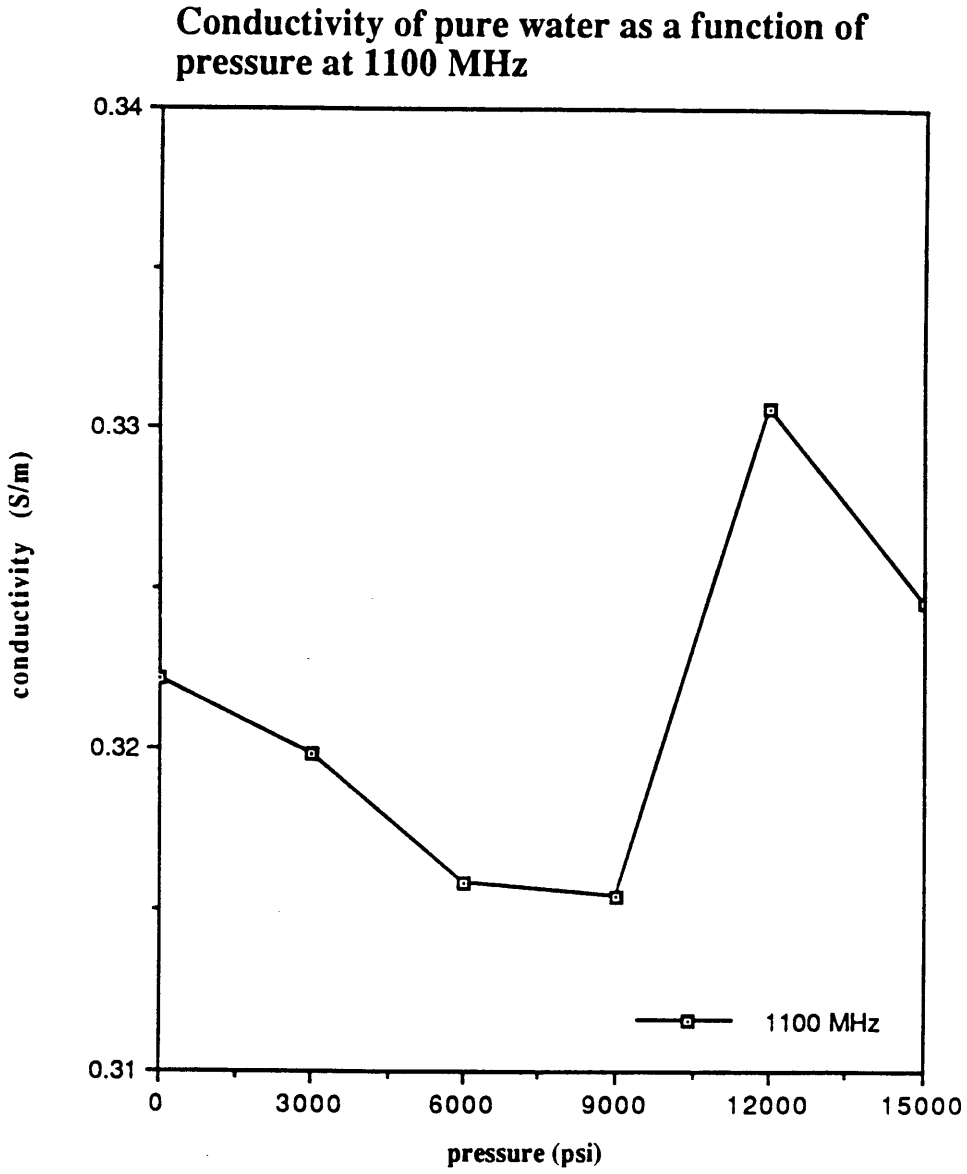

Figure F.1.2: Conductivity of Pure Water as a Function of Pressure at 1100 MHz

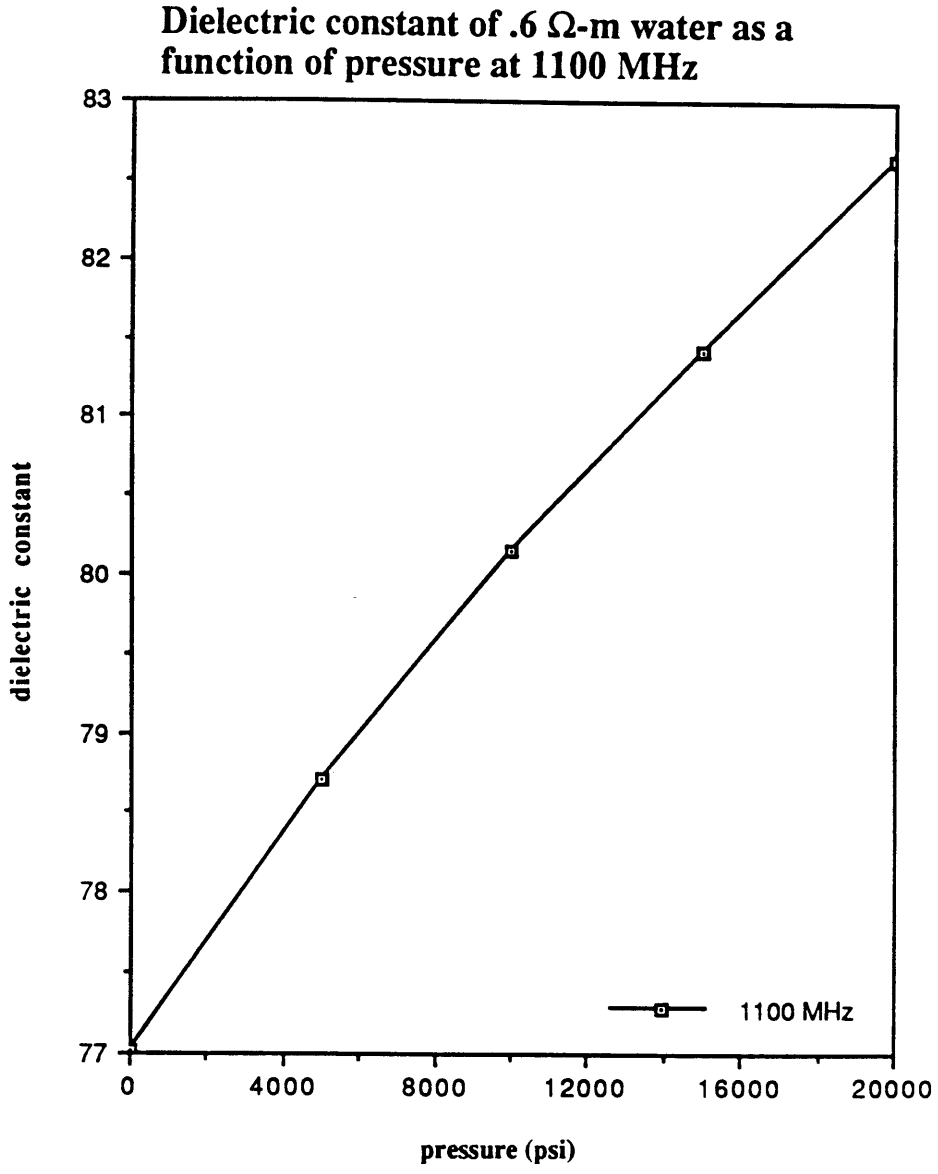

Figure F.1.3: Dielectric Constant of .6 Ω-m Water as a Function of Pressure at 1100 MHz

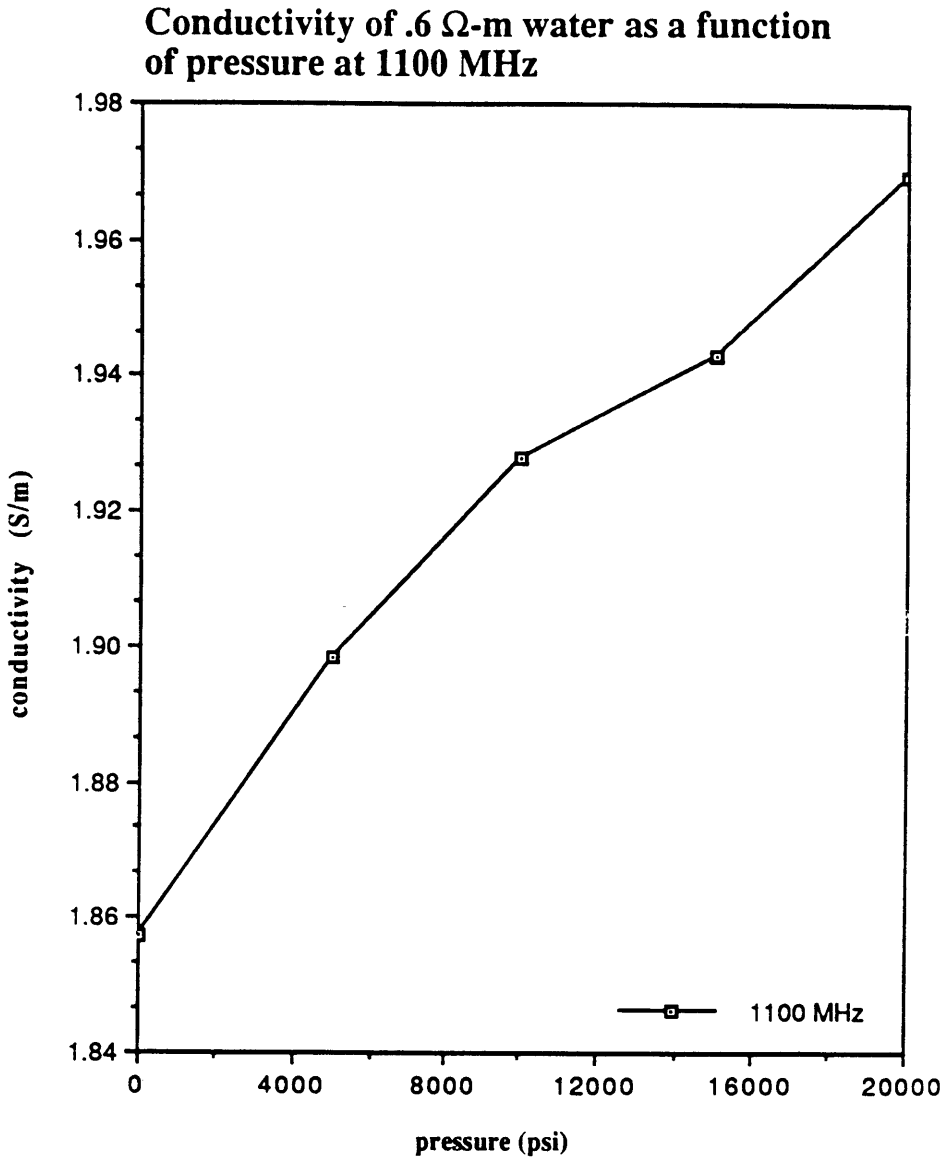

Figure F.1.4: Conductivity of .6 Ω-m Water as a Function of Pressure at 1100 MHz

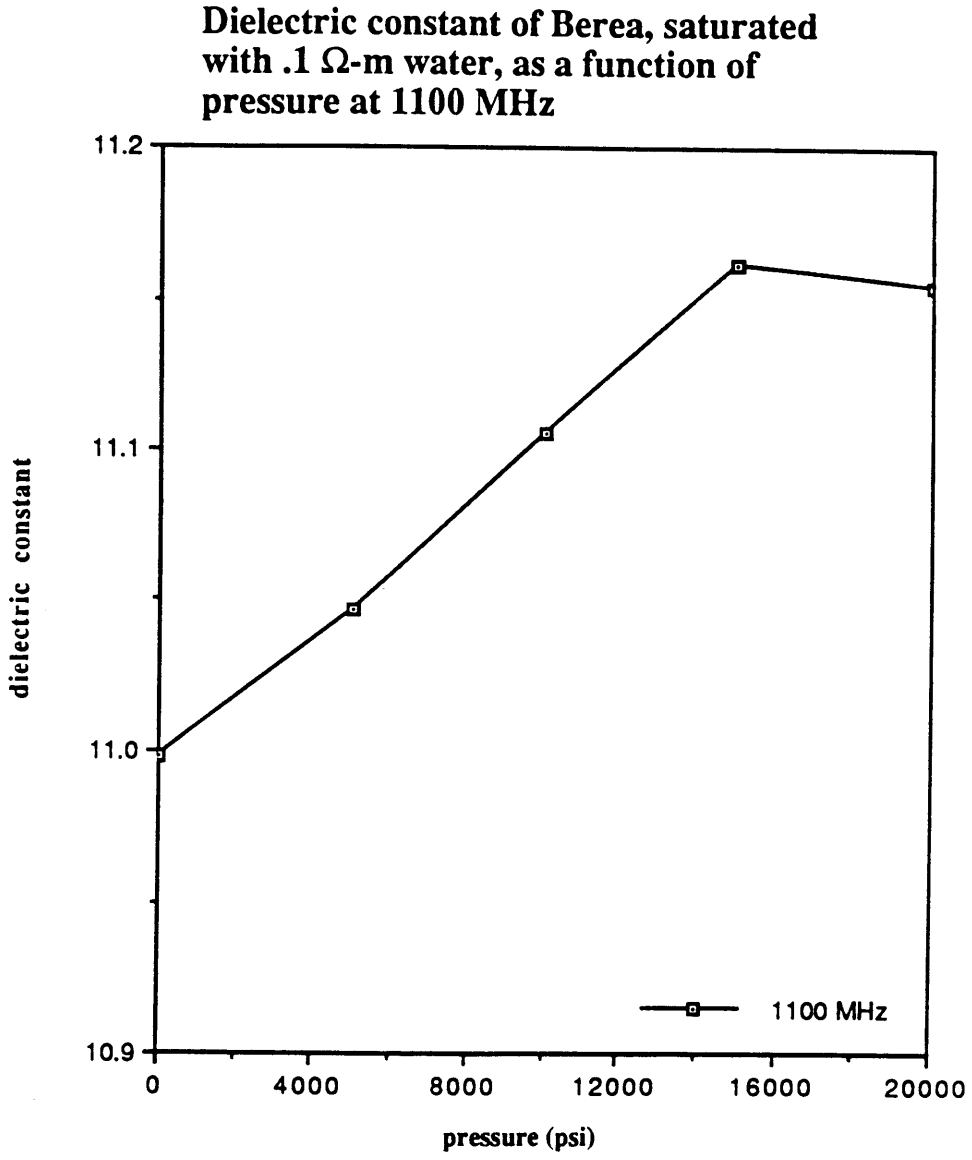

Figure F.1.5: Dielectric Constant of Berea, Saturated with .1 Ω-m Water, as a Function of Pressure at 1100 MHz

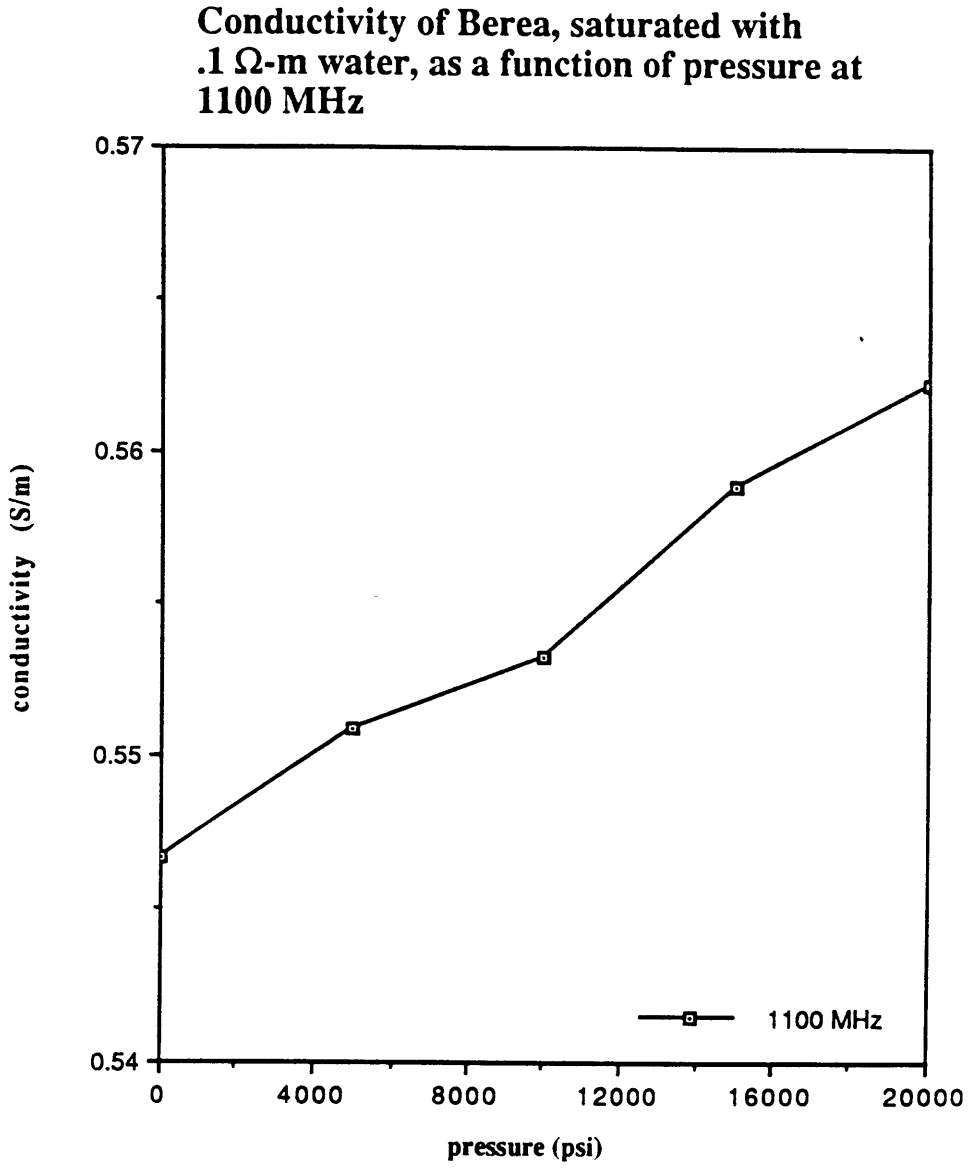

Figure F.1.6: Conductivity of Berea, Saturated with .1 Ω-m Water, as a Function of Pressure at 1100 MHz

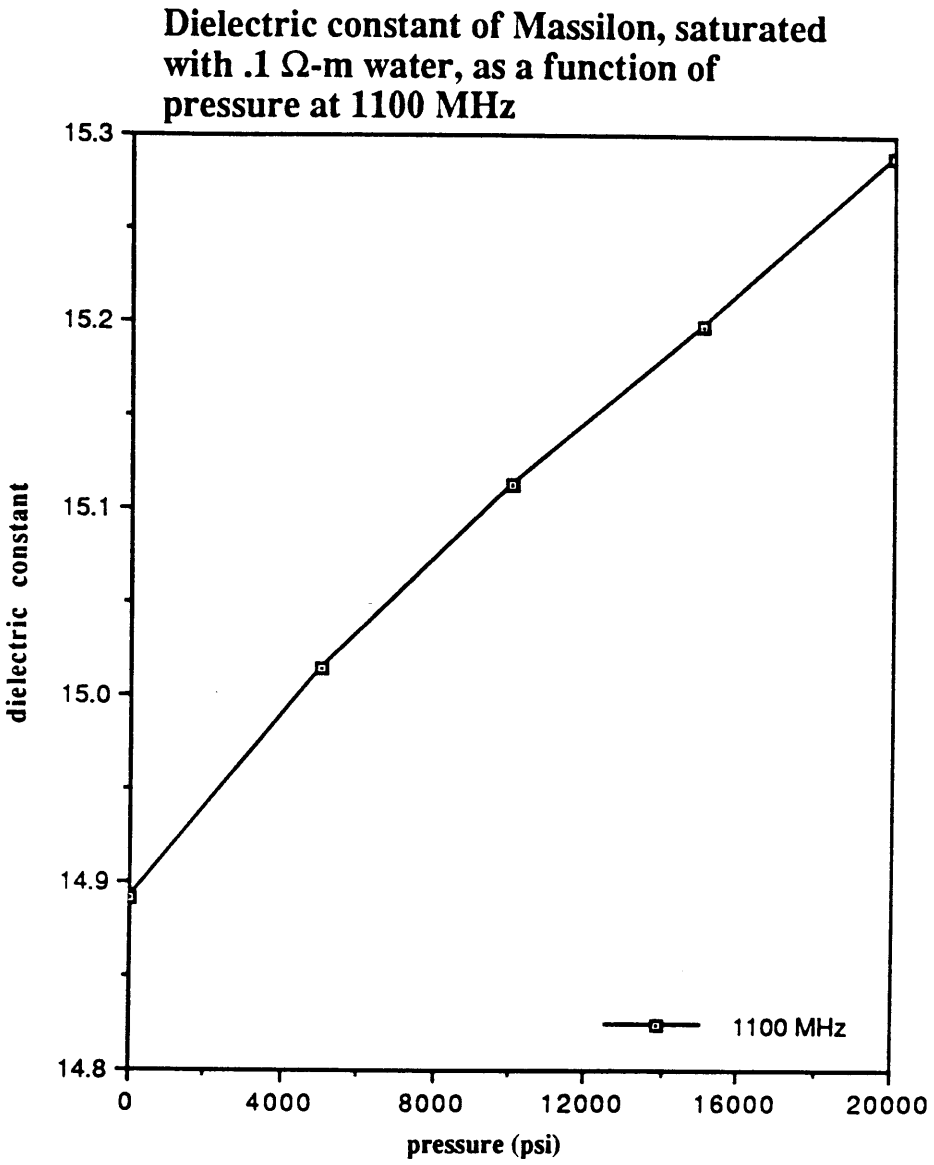

Figure F.1.7: Dielectric Constant of Massilon, Saturated with .1 Ω-m Water, as a Function of Pressure at 1100 MHz

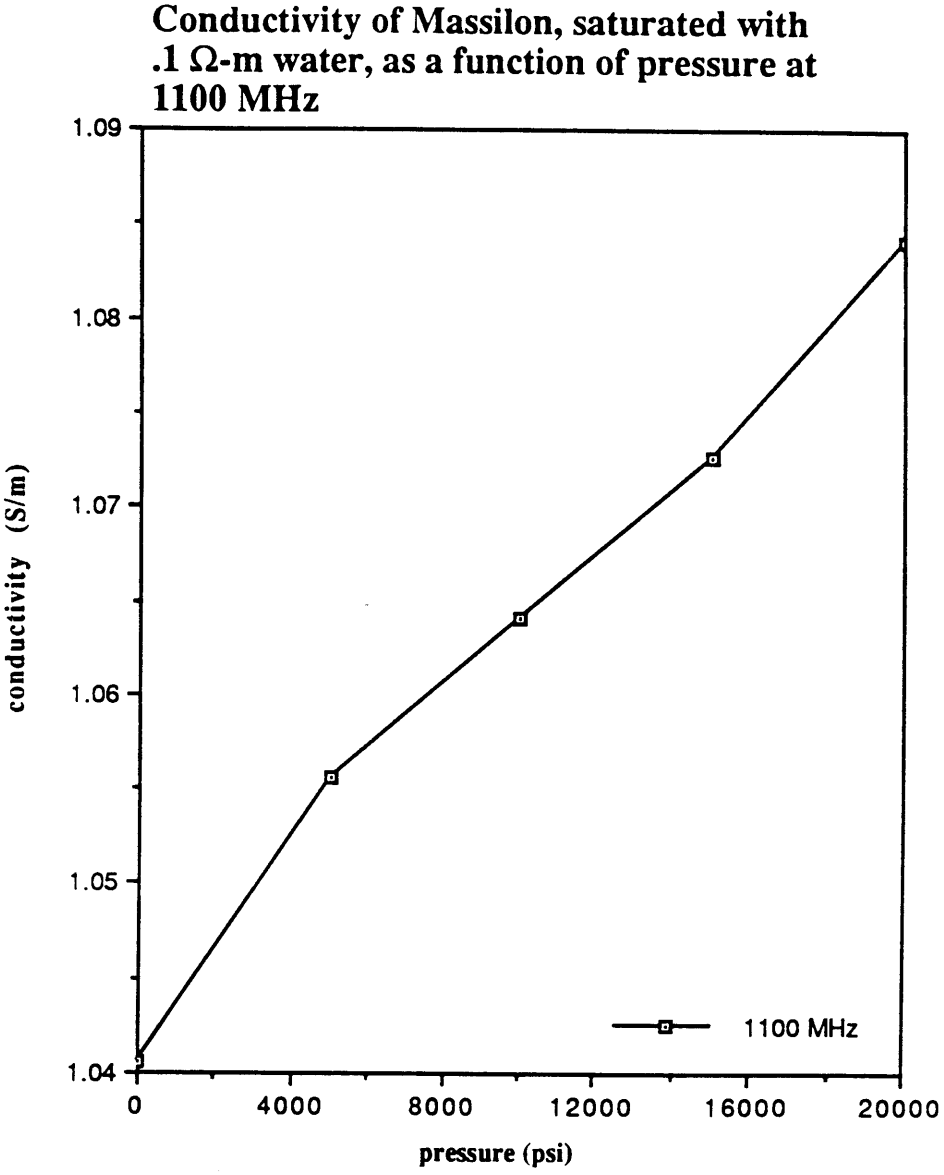

Figure F.1.8: Conductivity of Massilon, Saturated with .1 Ω-m Water, as a Function of Pressure at 1100 MHz

Reference

[1] Adam L.H. and Hall R.E., *The Effect of Pressure on the Electrical Conductivity of Solutions of Sodium Chloride and of Other Electrolytes*, Journal of Physical Chemistry, Volumn 35, pp. 2145-2163, 1931.

[2] Archie G.E., *The Electrical Resistivity Log as an Aid in Determining Some Reservoir Characteristics*, Tran. AIME, 1942, Volumn 146, pp. 54-67.

[3] Arps J.J., *The Effect of Temperature on the Density and Electrical Resistivity of Sodium Chloride Solutions*, Tran. AIME, 1953, Volumn 198, pp. 327-330.

[4] Banavar J.R., Sen P.N., Tomanic J., and Wong P., *Inversion Method for Obtaining Dielectric Data from Scattering Parameters*, Internal Publication, Schlumberger-Doll Research, 1984.

[5] Barus C., *The Effect of Pressure on the Electrical Conductivity of Liquids*, American Journal of Science, Volumn 140, pp. 219-222, 1890.

[6] Baumeister T., *Mark's Mechanical Engineers' Handbook* , McGraw-Hill Book Company, Inc., 1958.

[7] Brace W.F., Orange A.S., and Madden T.R., *The Effect of Pressure on the Electrical Resistivity of Water Saturated Crystalline Rocks*, Journal of Geophysical Research, 1965, Volumn 70, pp. 5669-5678.

[8] Brace W.F. and Orange A.S., *Further Studies of the Effect of Pressure on Electrical Resistivity of Rocks*, Journal of Geophysical Research, 1968, Volumn 73, pp. 5407-5420.

[9] Bradley R.S., *High Pressure Physics and Chemistry* , Volume 1 and 2, Academic Press Ltd.

[10] Bridgman P.W., *The Physics of High Pressure* , Strangeways Press Ltd., 1958.

[11] Buckley F. and Maryott A.A., *Tables of Dielectric Dispersion Data for Pure Liquids and Dilute Solutions*, National Bureau of Standards, November 1, 1958.

[12] Danforth W.E.Jr., *The Dielectric Constant of Liquids under High Pressure*, Physical Review, Volumn 38, 1224-1235, 1931.

[13] Fatt I., *Effect of Overburden and Reservoir Pressure on Electric Logging Formation Factor*, AAPG Bull., Volumn 41, No. 11, pp.2456-2466, 1957.

[14] Franks Felix, *Water, A Comprehensive Treatise*, Plenum Press, 1972.

[15] Giardini A.A. and Lloyd E.C., *High-Pressure Measurement* , Waverly Press Inc., 1963.

[16] Gilchrist A., Earley J.E., and Cole R.H., *Effect of Pressure on Dielectric Properties and Volumn of 1-Propanol and Glycerol*, Journal of Chemical Physics, Volumn 26, No. 1, 1957.

[17] Gilkerson W.R., *The Importance of the Effect of the Solvent Dielectric Constant on Ion-Pair*, Journal of Physical Chemistry, Volumn 74, No. 4, 1970.

[18] Glanville C.R., *Laboratory Study Indicates Significant Effect of Pressure on Resistivity of Reservoir Rock*, Journal of Petroleum Technology, Volumn 11, No. 4, pp. 20-26.

[19] Haynes W.M., *Measurements of Densities and Dielectric Constants of Liquid Isobutane from 120 to 300 K at Pressures to 35 MPa* , J. Chemistry Engineering Data, 28, 367-369, 1983.

[20] Haynes W.M., *Measurements of Densities and Dielectric Constants of Liquid Normal Butane from 140 to 300 K at Pressures to 35 MPa* , J. Chemistry Thermodynamics, 15, 801-805, 1983.

[21] Haynes W.M., *Measurements of Densities and Dielectric Constants of Liquid Propane from 90 to 300 K at Pressures to 35 MPa* , J. Chemistry Thermodynamics, 15, 419-424, 1983.

[22] Haynes W.M. and Frederick N.V., *Apparatus for Density and Dielectric Constant Measurements to 35 MPa on Fluids of Cryogenic Interest* , Journal of Research of the National Bureau of Standards, Volume 88, No.4, July-August 1983.

[23] Heacock J.G., *The Structure and Physical Properties of the Earth's Crust* , Geophysical Monograph 14, American Geophysical Union, 1971.

[24] Hilchie D.W., *The Effect of Pressure and Temperature on the Resistivity of Rocks*, Dissertation from University of Oklahoma, 1964.

[25] Hill H.J. and Milburn J.D., *Effect of Clay and Water Salinity on Electrochemical Behavior of Reservoir Rocks*, Trans. AIME, Volume 207, pp. 65-72, 1956.

[26] Huckert J., *Engineering Tables* , McGraw-Hill Book Company, Inc., 1956.

[27] Issacs N.S., *Liquid Phase High Pressure Chemistry*, John Wiley and Sons, A Wiley-Interscience Publication.

[28] Jackson P.D., Smith T.D. and Stanford P.N., *Resistivity-Porosity-Particle Shape Relationships for Marine Sand*, Geophysics, Volumn 43, pp. 1250-1268, 1968.

[29] Jacobs I.S. and Lawson I.S., *An Analysis of the Pressure Dependence of the Dielectric Constant of Polar Liquids*, Journal of Chemical Physics, Volumn 20, No. 7, 1952.

[30] Johnston D.H., *Physical Properties of Shale at Temperature and Pressure*, Geophysics, Volumn 52, No. 10, October 1987, p. 1391-1401.

[31] Lienhard J., *Heat Transfer Textbook*, Prentice Hall, Inc., 1987.

[32] Lockner D.A. and Byerlee J.D., *Complex Resistivity Measurement of Confined Rock*, Journal of Geophysical Research, Volumn 90, No. B9, pp. 7837-7847, 1985.

[33] Lysne P.C., *A Model for the High Frequency Electrical Response of Wet Rocks*, Geophysics, Volume 48, No. 6, June 1983, p. 775-786.

[34] Mavko G.M. and Nur Amos, *The Effect of Nonelliptical Cracks on the Compressibility of Rocks*, Journal of Geophysical Research, September 10, 1978.

[35] Patnode H.W. and Wyllie M.R.J., *The Presence of Conductive Solids in Reservoir as a Factor in Electrical Log Interpretation*, Trans. AIME, 1959, 189, p.47.

[36] Pirson S.J., *Elements of Oil Reservoir Engineering*, McGraw-Hill Book Company, Inc., 1950.

[37] Quist A.S. and Marshall W.L., *Electrical Conductances of Aqueous Sodium Chloride Solutions from 0 to 800 and at Pressure to 4000 Bars*, Journal of Physical Chemistry, 1968, Volumn 72, pp. 684-702.

[38] Redmond J.C., *Effect of Simulated Overburden Pressure on the Resistivity, Porosity and Permeability of Selected Sandstones*, Dissertation from Pennsylvania State University, 1962.

[39] Reza T., Yuen D.J., Habashy T.M., and Kong J.A., *A Coaxial-Circular Waveguide for Dielectric Measurement*, IEEE Transactions on Geoscience and Remote Sensing, 1990.

[40] Sanyal S.K., *The Effect of Temperature on Electrical Resistivity and Capillary Pressure Behavior of Porous Media*, Dissertation from Stanford University, 1972.

[41] Shen L.C. and Kong J.A., *Applied Electromagnetism*, PWS Publishers, 1987.

[42] Srinivasan K.R. and Kay R.L., *Pressure Dependence of the Dielectric Constant of H_2O and D_2O*, Journal of Chemical Physics, Volumn 60, No. 9, pp.3645-3649, 1974.

[43] Vij J.K., *Pressure and Temperature Dependence of the Permittivity and Density of 1,1-Dimethoxy-2-Propanone*, Journal of Chemical Physics, Volumn 79, No. 12, pp. 6182-6188, 1983.

[44] Wahl E.F., *Geothermal Energy Utilization*, John Wiley & Sons, 1977.

[45] Walsh J.B. and Brace W.F., *Elasticity of Rock: A Review of Some Recent Theoretical Studies*, Rock Mechanics and Engineering Geology, Volumn 4, 1966, p 283-297.

[46] Winsauer W.O., Shearin H.M.Jr., Masson P.H., and Williams M., *Resistivity of Brine-Saturated Sands in Relation To Pore Geometry*, Bulletin of the American Association of Petroleum Geologists, Volumn 36, No. 2, pp. 253-277, 1952.

[47] Witte L. D., *Resistivities and Fluid Contents of Porous Rocks*, The Oil and Gas Journal, pp. 120-132, 1950.

[48] Wyble D.O., *Effect of Applied Pressure on the Conductivity, Porosity, and Permeability of Sandstones*, Journal of Petroleum Technology, Volumn 10, pp. 57-59, 1958.

[49] Wyble D.O., *Effect of Pressure on Conductivity, Porosity and Permeability of Oil-Bearing Sandstones*, Dissertation from Pennsylvania State University, 1958.